# VIBRATING WIRE SENSORS FOR BEAM INSTRUMENTATION

Arutunian, S.G.
Yerevan Physics Institute, Armenia

*Abstract*

Thermal sensors based on the vibrating wire principle are distinguished by high accuracy and stability. An important advantage of these sensors is that they produce a frequency signal that can be transferred large distances without disturbance. Original vibrating wire sensors and monitors for the measurement of beam transversal characteristics of charged-particle and photon beams are described. By means of these devices, measurements of an electron beam in the Yerevan synchrotron, a proton beam at PETRA (DESY), and a hard x-ray undulator beam at the APS (ANL) have been performed.

## INTRODUCTION

The operating principle of Vibrating Wire Sensors (VWS) or Vibrating Wire Monitors (VWM) is based on the measurement of the change in the frequency of a vibrating wire, which is stretched on a support, depending on the physical parameters of the wire and environment in which oscillations take place. Today the area of application of this technique is expanding and the number of vibrating wire-based instruments has increased. Strain, displacement, piezometric level, pressure, angle and moment of rotation, viscosity of the media, and ultralow thermometry under 1 K are measured by VWS [1-7]. An interesting vibrating wire field-measuring technique has been developed for determination of magnetic center of units in accelerators (see, e.g., [8-10]).

The important advantages of properly constructed vibrating wire sensors are inherent long-term stability, high precision and resolution, good reproducibility and small hysteresis. The advantage of vibrating wire sensors is also that the frequency signal is imperturbable and can be transmitted over long cables with no loss or degradation of the signal. The reliability of the sensors becomes the overriding feature in the selection of a technology. It is also is important to ascertain a low drift and minimum change in sensitivity. An important parameter of vibrating wire-based sensors is their ability to operate in hard conditions (high operational power and temperature cycling, thermal shock, thermal storage, autoclaving, fluid immersion, mechanical shock, electromagnetic and electrostatic environments [11]).

We take an electromechanical resonator with a metallic vibrating wire excited by the interaction of a current with a permanent magnetic field as a basis for the VWS of electron and proton beams. In this paper we discuss an application of such resonators for precise profile measurement of particle and photon beams. The interaction of the beam with the wire mainly causes heating of the wire. Thus we expect that the frequency of natural oscillations of the wire will provide information about its temperature. The thermal method of measurement also allows registering neutron flux.

## MAIN CHARACTERISTICS

The operating principle of vibrating wire sensors is measurement of the change in the frequency of a vibrating wire, which is stretched on a support, depending on the physical parameters of the wire and the environment in which oscillations take place. A detailed description of the vibrating wires sensors can be found in our publications (see [12] and cited references). Below we present a short description of the VWS and some aspects not discussed in previous publications.

*Sensor main components*

In Fig. 1 the sensor main components are presented. Wire (1) ends are pressed in the clips (2) and pass through the magnet field system (samarium-cobalt permanent magnets and magnet poles (3) and (4)). The magnet provides field strength on the order of 10 kG in the gap. Clips are fixed on the sensor support structure (5). Sensor is fastened on the scan feed arm by details (6) and (7).

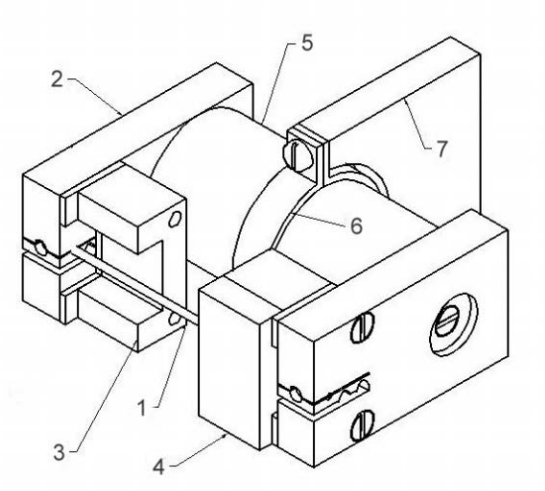


Fig. 1: Vibrating wire sensor main view.

By use of a simple positive feedback circuit, the magnetic system excites the second harmonic of the wire's natural oscillation frequency while keeping the middle of the wire exposed for detection of beam heating.

*Wire oscillation excitation*

Wire oscillations arise as a result of the interaction between the oscillating current through the wire and the applied magnetic field. When the oscillating current passes through the wire, the Lorentz force shifts the

# FUTURE ACCELERATOR CHALLENGES IN SUPPORT OF HIGH-ENERGY PHYSICS*

M. S. Zisman‡, LBNL, Berkeley, CA 94720 U.S.A.

*Abstract*

Historically, progress in high-energy physics has largely been determined by development of more capable particle accelerators. This trend continues today with the imminent commissioning of the Large Hadron Collider at CERN, and the worldwide development effort toward the International Linear Collider. Looking ahead, there are two scientific areas ripe for further exploration—the energy frontier and the precision frontier. To explore the energy frontier, two approaches toward multi-TeV beams are being studied, an electron-positron linear collider based on a novel two-beam powering system (CLIC), and a Muon Collider. Work on the precision frontier involves accelerators with very high intensity, including a Super-B Factory and a muon-based Neutrino Factory. Without question, one of the most promising approaches is the development of muon-beam accelerators. Such machines have very high scientific potential, and would substantially advance the state-of-the-art in accelerator design. The challenges of the new generation of accelerators, and how these can be accommodated in the accelerator design, are described. To reap their scientific benefits, all of these frontier accelerators will require sophisticated instrumentation to characterize the beam and control it with unprecedented precision.

## INTRODUCTION

Scientific progress in high-energy physics has traditionally depended on advances in accelerator design. This trend has taken the community from the early electrostatic accelerators to cyclotrons, to synchro-cyclotrons, to synchrotrons, and finally to both circular and linear colliders. Achieving the full performance potential from each generation of accelerators requires corresponding advances in accelerator technology, including magnets, vacuum systems, RF systems, and instrumentation.

The critical scientific role played by accelerators is due to the fact that they permit the study of high-energy physics phenomena under (more or less) controlled conditions. However, the cost of today's proposed accelerator projects is high, and this has consequences for the community. Indeed, there is a danger at present of "pricing ourselves out of the market" if we are not conscious of costs in each aspect of the design. The practical way of mitigating project costs is to share the burden and, with this in mind, international cooperation and collaboration are key to our ability to successfully launch new projects.

*This work was supported by the Office of Science, U. S. Department of Energy, under Contract No. DE-AC02-05CH11231.

‡mszisman@lbl.gov

## ACCELERATOR DELIVERABLES

Particle accelerators are designed to deliver two parameters to the HEP user—energy and luminosity. Of these, energy is by far the easier parameter to deliver, and the easier one to accommodate for the experimenters. Increased luminosity invariably presents a major challenge, not only to the accelerator builders but to the detector builders. Luminosity, $L$, is a measure of the collision rate per unit area and has dimensions of $\mathrm{cm}^{-2}\ \mathrm{s}^{-1}$. For a given event probability ("cross section"), $\sigma$, the event rate at a collider is given by $R = L\sigma$. For a collider having equal beam sizes at the collision point, luminosity is given by

$$L = \frac{N_1 N_2 f_c}{4\pi \sigma_x^* \sigma_y^*}, \qquad (1)$$

where $N_1$ and $N_2$ are the number of particles per bunch in beams 1 and 2, respectively, $f_c$ is the collision frequency, and $\sigma_x$* and $\sigma_y$* are the horizontal and vertical rms beam sizes at the collision point, respectively. It is obvious from Eq. (1) that high luminosity demands intense beams and small beam sizes at the collision point.

## PARTICLE PHYSICS QUESTIONS

In simple terms, there are two main thrusts of accelerator-based high-energy physics. The first of these, corresponding to experiments at the energy frontier, is to understand the origins of mass, that is, the mechanism that gives existing particles their widely different masses. Recent experiments [1] have shown the mass of the top quark to be comparable to that of a gold nucleus, whereas a neutrino mass (thought for a long time to be exactly zero) is likely to be only a fraction of an eV.

The second main thrust is understanding why we live in a matter-dominated universe. This is a quite fundamental question, as it basically addresses our very existence. It is believed that the Big Bang initially created equal amounts of matter and antimatter, yet these did not all annihilate. The survival of matter is related to differences in the reaction rates of particles and antiparticles, referred to as charge-conjugation–parity (CP) violation. CP violation has long been known in the quark sector [2], and two "B Factories" [3, 4] were built to study this phenomenon. Unfortunately, it turns out that CP violation in the quark sector is not enough to explain the observed baryon asymmetry in the universe. The prevalent view is that the additional CP violation needed occurs in the lepton sector. While this has never been observed, neutrinos are considered the hunting ground for finding it.

# BEAM MEASUREMENTS AT LCLS*

J. Frisch, R. Akre, F.-J. Decker, Y. Ding, D. Dowell, P. Emma, S. Gilevich, G. Hays, Ph. Hering, Z. Huang, R. Iverson, R. Johnson, C. Limborg-Deprey, H. Loos, E. Medvedko, A. Miahnahri, H.-D. Nuhn, D. Ratner, S. Smith, J. Turner, J. Welch, W. White, J. Wu, Stanford Linear Accelerator Center, Menlo Park CA 94025, U.S.A

*Abstract*

The LCLS accelerator is presently in a commissioning phase[1] and produces a 14GeV beam with normalized emittances on the order of one mm-mr, and peak current exceeding 3000 Amps. The design of the beam measurement system relies heavily on optical transition radiation profile monitors, in conjunction with transverse RF cavities, and conventional energy spectrometers. It has been found that the high peak currents and small longitudinal phase space of the beam generate strong coherent optical emission that limits the quantitative use of OTR and other prompt optical diagnostics, requiring the use of wire scanners or fluorescent screen based measurements. We present the results of beam measurements, measurements of the coherent optical effects, and future plans for the diagnostics.

## LCLS ACCELERATOR

The Linac Coherent Light Source is a SASE Free Electron Laser, designed to produce X-rays with wavelengths down to 1.5 Angstroms, using electron beam energies up to 13.6 GeV.

Table 1: Accelerator Design Specifications

| | |
|---|---|
| Energy | 4.3 to 13.6 GeV |
| Bunch Charge | 200 pC to 1 nC |
| Design emittance | ~ 1.2 mm-mr slice |
| Peak current | ~ 3.4 KA. |
| Repetition rate | 120Hz, single pulse |

An accelerator layout with beam parameters is given in figure 1.

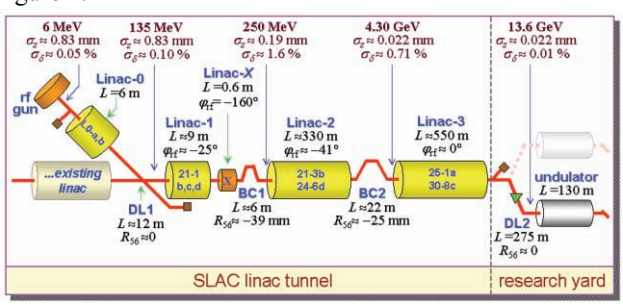


Figure 1: Accelerator layout.

Linac-2 and Linac-3 are only slightly modified from their configuration for the SLC [2]. The remainder of the machine is new, though it makes use of some old SLAC accelerator structures and magnets. As of April 2008, the beam is accelerated to the end of Linac-3 with nominal parameters, except that the repetition rate is presently limited to 30 Hz during commissioning.

## BEAM DIAGNOSTICS AND MEASUREMENTS

The LCLS design relies heavily on beam-based control and feedback, necessitating the use of a variety of beam measurement devices:

- Position: Stripline BPMs
- Charge: BPMs, Toroids, Faraday Cups
- Beam Loss: Ion chambers and PMTs
- Profile: Wire Scanners, Optical Transition Radiation monitors, and fluorescent screens
- Emittance: Multiple profile monitors, or Quadrupole magnet gradient scans on a single profile monitor.
- Longitudinal Measurements: Spectrometers, Millimeter wave bunch length monitors, Transverse RF deflection cavities.

### *Beam Position Monitors*

The LCLS injector, and a few locations along the Linac use self-calibrating strip-line BPMS based on digital down conversion: figure 2.

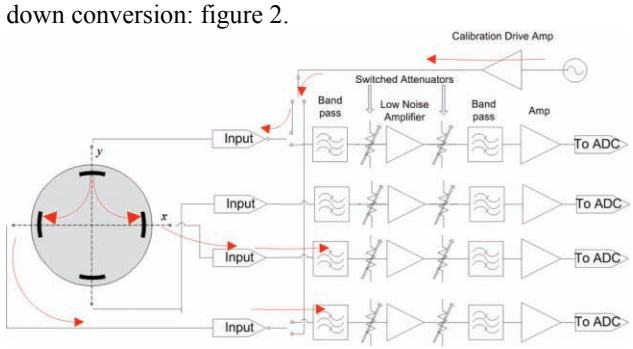


Figure 2: BPM Electronics

The BPMS operate at a center frequency of 140MHz, with a 7 MHz bandwidth. On every pulse, a tone burst is injected onto one strip, and the coupling to the perpendicular strips is measured. This corrects for gain changes in the readout channels and cables. [3]

The BPM noise is measured by performing a linear regression between the BPM under test, and the other BPMS in the accelerator, with the residual indicating the position noise, figure 3.

*Work supported by DOE Contract DE-AC02-76SF00515

# LHC MACHINE PROTECTION

B. Dehning, CERN, Geneva, Switzerland

*Abstract*

The LHC equipment is protected by passive and active components against beam-induced destruction. For the fast losses a passive system consisting of collimators, absorbers and masks is used. For the other losses an active system consists of beam loss monitors, a beam interlock system and the beam dump. The LHC protection requirements are different than those of other accelerators, mainly due to its energy, its stored beam intensity, and its dimension. At the LHC top energy the beam intensity is about 3 orders of magnitude above the destruction limit of the superconducting magnet coils and 11 orders above their fast loss quench limit. These extreme conditions require a very reliable damage protection and quench prevention with a high mean time between failures. The numerous amounts of loss locations require an appropriate amount of detectors. In such a fail safe system the false dump probability has to be kept low to keep a high operation efficiency. A balance was found between a reliable protection and operational efficiency. The main protection systems and beam instrumentation aspects of the measurement systems will be discussed.

## DESTRUCTION POTENTIAL

The destruction potential of the LHC is illustrated by test measurements done in the SPS. The beam prepared for injection into the LHC has been directed onto a stack of copper and steel plates (Fig. 1). The beam, with a size

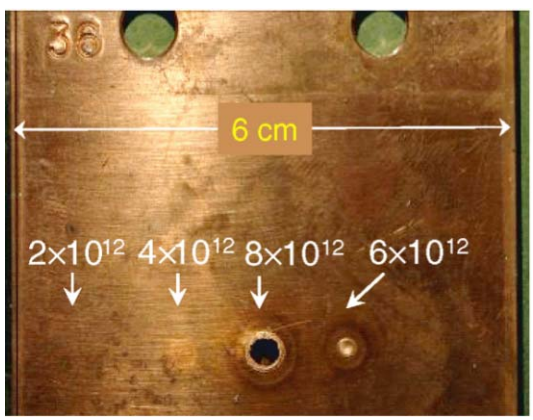


Figure 1: Destruction test of a Cu target in the SPS with an LHC beam.

of $\sigma_x$=1.1, $\sigma_y$=0.6 mm and intensities of several $10^{12}$ protons at 450 GeV, clearly damaged the copper plates at a penetration depth where the maximum energy is deposited. The steel plates were not damaged [1]. The safe intensity of 2 $10^{12}$ represents only 0.6 % of the total intensity of 3 $10^{14}$ at the LHC injection energy.

To illustrate the destruction potential of the LHC beam at top energy of 7 TeV, a simulation of the material phase transition in the longitudinal penetration channel is shown in Fig. 2.

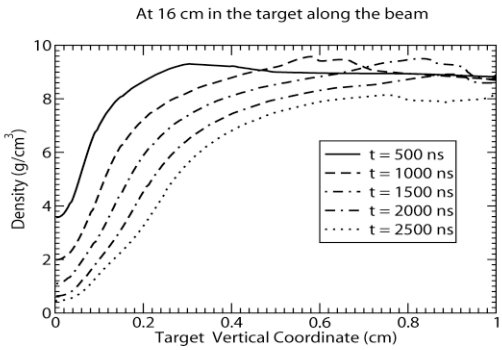


Figure 2: Density change of a Cu target material during the impact of 100 LHC bunches (bunch train duration 2500ns) with an intensity of 1.1 $10^{11}$ proton per bunch at 7 TeV.

The energy deposition leads to a temperature increase, followed by a pressure increase, which causes a shockwave leading to a reduction of the density. The following bunches would interact with less material where the density is reduced and would penetrate even further. It is expected that the whole LHC beam would penetrate over 10 m through the material after impacting [2].

Beam induced destruction of equipment is one reason an accelerator might be rendered non-operational. Beam induced heating at the superconducting coils of the LHC magnets will cause a loss of their low resistance. In case of a failure, the tail of the beam will impact at the inner wall of the vacuum chamber and a secondary particle shower will deposit its energy in the vacuum chamber and in the surrounding coil (see Fig. 3). The lines of constant energy density show a decrease of the energy density in the radial direction. The largest temperature increase is not caused by energy deposition near the vacuum chamber, because a He cooling channel between the vacuum chamber and the coil transports heat to the heat bath region for steady state losses (> 1 s). Instead, the quench location is near the border between the inner and outer coils, where the heat flow is minimal (see Fig. 3, bottom) [3].

## THE PROTECTION SYSTEM

Figure 4 shows a classification of the beam losses according to their duration. For the very fast losses (< 4 turns, 356 us) only passive components can protect the equipment. At LHC over 100 collimators and absorbers

# HARD X-RAY SYNCHROTRON RADIATION MEASUREMENTS AT THE APS WITH VIBRATING WIRE MONITORS*

G. Decker[1], R. Dejus[1], S.G. Arutunian[2], M.R. Mailian[2], I.E. Vasiniuk[2]
[1] Argonne National Laboratory, Argonne, IL 60439
[2] Yerevan Physics Institute, Alikhanian Br. Str. 2, 375036, Armenia

*Abstract*

A 5-wire vibrating wire monitor (VWM005) was developed and tested at the Advanced Photon Source (APS). The sensor was mounted on the outboard side of a bending-magnet synchrotron radiation terminating flange in sector 37 of the APS storage ring. The parallel wires were separated vertically by 0.5 mm; however, due to the possibility of rotation about a horizontal axis, the effective distance between the wires was reduced by a significant factor. To increase the response speed, the sensor was installed in air, resulting in a step response time of less than one second. Due to the extreme sensitivity of the detector, the very hard x-ray component of synchrotron radiation was successfully measured after its passage through the terminating flange.

## BACKGROUND

At the APS, insertion device photon beam position monitoring is integrated into DC orbit correction algorithms, providing submicroradian levels of pointing stability over periods greater than 24 hours. Existing photon beam position monitors (BPMs) make use of ultraviolet (UV) and soft x-ray photoemission from metallized diamond blades arranged in sets of four and positioned edge-on at the periphery of the photon beam. These monitors suffer from a number of insertion device gap-dependent systematic errors associated with unavoidable soft background radiation. This radiation is associated with strong steering correctors located immediately upstream and downstream from the undulator source; they are part of the so-called Decker distortion scheme for reducing stray radiation overall [1].

In an effort to further improve upon photon beam position monitoring, an effort was initiated in 2005 to develop a BPM that is completely insensitive to the UV and soft x-ray components of undulator beams. One active area of research is the development of PIN diodes arranged to sense copper x-ray fluorescence in the backward direction [2-4]. The present work is the culmination of a number of informal meetings that took place at DIPAC 2005, and is in fact a hybrid of Arutunian et al.'s vibrating wire monitor (VWM) concept [5] and Scheidt's work with very hard x-rays at ESRF [6].

First experiments with the VWM at the APS were conducted in vacuum with an undulator beam in early 2007 [7] using the same facility where the PIN diode measurements were made. The main conclusions from that work were that the VWM is sensitive to extremely low levels of x-ray flux, but the detector's time response is quite slow since the primary means of achieving thermal equilibrium in vacuum is through radiation. Nevertheless, the measurments and subsequent analysis have provided an interesting quantitative validation of the theory of undulator radiation. Shown in Fig. 1 are data collected for the two-wire detector installed in vacuum at APS beamline 19-ID during a vertical angle scan of the undulator source, which was a standard APS undulator A operating at a large gap of 60 mm. The principle for extracting temperature changes from individual wire acoustic resonance frequencies is described in reference [7] and in detail in reference [8], which also describes the operating principle of the device.

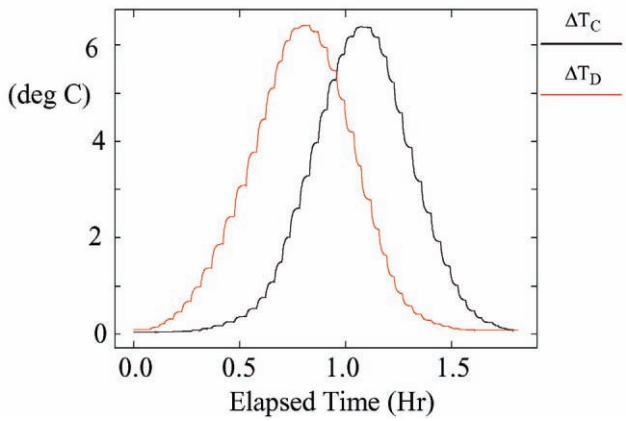


Figure 1: VWM data from undulator radiation during a vertical angle scan

The vertical angle was scanned in 5-microradian steps, pausing about three minutes after each change to reach equilibrium. As described in detail in reference [7], data analysis for this scan involved breaking the data set into 43 pieces, performing an exponential fit to each segment to extract an asymptotic temperature, executing an elaborate procedure to remove thermal drift with a linear drift model (0.01 degrees C / hour), and finally a performing normalization to stored beam current. The resulting profiles were seen to be very well approximated by Gaussians.

That the profile of an undulator beam should so closely match a Gaussian was somewhat surprising, given the known rather exotic profiles for individual undulator harmonics. To investigate this, the x-ray power density emitted from a standard APS undulator A with 60-mm gap (K = 0.023) was calculated after passing through 7 mm of beryllium [9]. This calculation included the particle beam dimensions, using a natural emittance of 2.5 nm-rad and 1% horizontal / vertical coupling. Shown

*Work supported by U.S. Department of Energy, Office of Science, Office of Basic Energy Sciences, under Contract No. DE-AC02-06CH11357.

# THE PROGRESS OF BEPCII STORAGE RING DIAGNOSTICS SYSTEM

J.S. Cao#, L. Ma, H.Z. Ma, L. Wang, Q. Ye, J.H Yue, L. Zhang, X. Y. Zhao, Y. Zhao, Z. Zhao

Institute of High Energy Physics, Chinese Academy of Sciences, Beijing 100049, China

*Abstract*

In this paper, we will present the progress of BEPCII storage rings beam diagnostics system along with the BEPCII commissioning. Tools such as Libera BPM had been used for the BPR first turn measurement and the injection residual orbit research of BER. COD_BPM can satisfy the resolution requirement for the beam-beam scan in the interaction region, and for the COD measurement, BCM (bunch current monitor) can help us on the different injection pattern. The TFB system is important to suppress the strong multi-bunch instabilities during the higher beam current running. The tune meters, the beam-loss monitors, DCCT and SLM (synchrotron light monitor) are also described in this paper.

## INTRODUCTION

As the upgrade project of Beijing Electron Positron Collider (BEPC), BEPCII is still serving the purposes of both high energy physics experiments and synchrotron radiation applications [1]. The BEPCII is a double ring electron-positron collider and a synchrotron radiation (SR) source with its outer ring, or SR ring. It can work on collision mode or dedicated synchrotron radiation mode. The design goals of the BEPCII are shown in Table 1.

Table 1: The design goals of the BEPCII

| | |
|---|---|
| Beam energy | 1-2.1 GeV |
| Optimum energy | 1.89 GeV |
| Luminosity | $1\times10^{33}$ $cm^{-2}s^{-1}$ @1.89 GeV |
| Injector Linac | Full energy inj.: 1.55-1.89 GeV<br>Positron inj. rate > 50 mA / min |
| Dedicated SR | 250 mA @ 2.5 GeV |

For the collision mode, the electron ring (BER) and positron ring (BPR) cross each other in the northern and southern interaction points (IP's) with a crossing angle. In the northern crossing region, a vertical orbit bump is used to separate the two beams, while the southern IP is used for BESIII detector. When BEPCII works in the dedicated synchrotron radiation mode (SR), the electron beam circulates in the two outer half rings. A bypass in the northern IP is designed to connect two outer half rings. In the southern crossing region, a special pair of superconducting magnet complexes, mainly including quadrupole magnets (SCQ) and bending magnets (SCB), are used for 1.5 cm β function in the y direction at the IP on colliding mode and to serve as the bridge connecting two outer half rings for SR operation, respectively. Because the construction schedule of the cryogenics system and superconducting magnets was little delayed compared to the other systems, it was decided to install conventional magnets in the interaction region (IR) as the backup scheme, so that we can provide beam to SR users as early as possible, and accumulate the beam commissioning experience on the colliding mode. The backup lattice is similar to that of the original design.

Two phases of commissioning of the BEPCII rings have been completed: collision mode commissioning, and providing beam to beamline users in the dedicated synchrotron radiation mode. Phase one commissioning started on Nov. 13, 2006 by using conventional magnets instead of SC magnets in the IR. Phase two commissioning started on Oct. 24, 2007 by using SC magnets (without the BESIII detector). In the two phases, the beam diagnostics system played important roles, such as using the Libera BPM for first-turn beam circulating and for injection residual orbit research on the BER, and transverse bunch-by-bunch feedback (TFB) system to suppress the strong multi-bunch instabilities in higher-beam-current running, and so on.

## LIBERA BPM

In the storage rings of BEPCII, a total of 16 units of Libera BPM are used. Libera control platform is located in Central Control Room. We can implement the control of Libera and data acquisition through the local-area network. BEPCII event timing system provides the trigger signal through an event receiver (EVR) module. Then we use clock splitter to synchronize data acquisition in different Liberas.

The Libera BPM played an important role during the commissioning of the first-turn and first-several-turns beam-circulating in BER and BPR (Figure 1) We only took 3 hours and one day to realize the beam accumulation in BER and BPR, respectively.

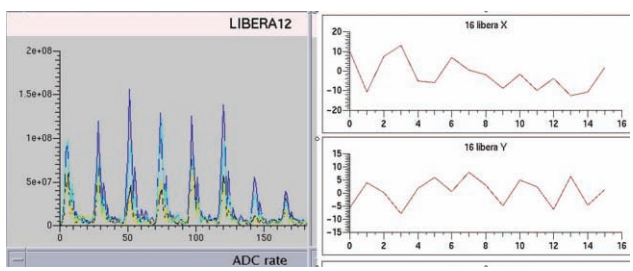


Figure 1: Libera BPM signal for first several turns of beam in the BER

Another important role Libera played is the optimization of timing delay of injection kickers and minimization of residual orbit oscillation in BER. The BEPCII includes two injection kickers and a Lambertson magnet for each

#caojs@ihep.ac.cn

# MEASUREMENTS OF THE ELECTRON CLOUD DENSITY IN THE PEP-II LOW ENERGY RING*

J. Byrd, S. De Santis, K. Sonnad, LBNL, Berkeley, CA 94720, U.S.A.
F. Caspers, T. Kroyer, CERN, Geneva, Switzerland
A. Krasnykh, M. Pivi, SLAC, Menlo Park, California.

*Abstract*

Clouds of low energy electrons in the vacuum beam pipes of accelerators of positively charged particle beams present a serious limitation for operation of these machines at high currents. Because of the size of these accelerators, it is difficult to probe the low energy electron clouds over substantial lengths of the beam pipe. We have developed a novel technique to directly measure the electron cloud density via the phase shift induced in a TE wave that is independently excited and transmitted over a section of the accelerator. We infer the absolute phase shift with relatively high accuracy from the phase modulation of the transmission due to the modulation of the electron cloud density from a gap in the positively charged beam. We have used this technique for the first time to measure the average electron cloud density over a 50 m straight section in the positron ring of the PEP-II collider at the Stanford Linear Accelerator Center. We have also measured the variation of the density by using low field solenoid magnets to control the electrons.

## INTRODUCTION

The accumulation of low-energy background electrons in regions of the beampipe of high-energy accelerators of positively charged beams presents one of the most serious challenges to increasing currents in these machines. Depending on bunch repetition rate, beam current and other machine conditions, electrons extracted from the beampipe walls, usually by synchrotron radiation, can be transversally accelerated by the circulating beam and extract even more electrons when they strike the beampipe again. This resonant mechanism leads to a buildup of these electrons, which can negatively affect the accelerator's operation in a variety of ways [1].

Because of its importance for a number of present and future high profile projects, such as the Large Hadron Collider and the International Linear Collider, the electron cloud dynamics, its effects on the beam and their cures have been the object of numerous studies in the past few years. From an experimental point of view, electron cloud effects have been observed in various high intensity synchrotrons and storage rings [2-4].

*Work supported by the U.S. Department of Energy under Contract Nos. DE-AC0-05CH11231 and DE-AC03-76SF00515

The methods used consist in the analysis of the beam's dynamic behaviour,, which can necessarily give only an averaged measurement of the electron cloud density (ECD) around the machine, and local detectors [5], which only measure the energy spectrum of electrons near the beampipe wall at a specific location.

In this paper we present a novel method featuring several positive characteristics, namely the possibility of being applied anywhere a pair of beam position monitors (BPM) are available, without the necessity of any dedicated hardware nor installation, and the ability of probing the electron cloud density directly along the beam path and not only in the vicinity of the beampipe walls.

The method consists in propagating an electromagnetic wave along the beampipe, between two sets of BPM's delimiting the region that one wants to measure.

The propagating wave does not interact with the ultrarelativistic beam, but is affected by the low-energy electron densities it encounters. This interaction essentially translates into a phase delay that can be theoretically evaluated, as shown in the next paragraph.

Besides this basic interaction mechanism it is also possible to obtain a resonant interaction in regions where a local magnetic field is of such strength as to define a cyclotron frequency equal to the frequency of the propagating wave. The theoretical treatment of this case is still object of work. We present nonetheless some preliminary results, with simulations and experimental measurements.

## THEORETICAL EVALUATION OF THE ELECTRON CLOUD EFFECTS ON MICROWAVE PROPAGATION THROUGH THE BEAM PIPE

The derivation of the wave dispersion relationship for propagation of an electromagnetic wave through an electron plasma has been described in [6] and is limited to first order perturbations, so that the model does not anticipate any amplitude variation of the transmitted wave. The phase shift of a wave of angular frequency $\omega$ caused by a homogeneous density of cold electrons per unit propagation length is given by:

$$\Delta\varphi / L = \frac{\omega_p^2}{2c\sqrt{\omega^2 - \omega_c^2}} \qquad (1)$$

where $\omega_c$ is the beampipe cut-off frequency and $\omega_p$ is $2\pi$ times the plasma frequency $f_p$, which in turn is

# THE BEAM DIAGNOSTIC INSTRUMENTATION OF PETRA III

K. Balewski, A. Brenger, H.-T. Duhme, V. Gharibyan, J. Klute, K. Knaack, I. Krouptchenkov, G. Kube, T. Lensch, D. Lipka, J. Liebing, Re. Neumann, Ru. Neumann, G. Priebe, F. Schmidt-Foehre, H.-Ch. Schroeder, R. Susen, S. Vilcins-Czvitkovits, M. Werner, Ch. Wiebers, K. Wittenburg
Deutsches Elektronen Synchrotron DESY, Hamburg, Germany.

*Abstract*

The former electron and proton preaccelerator PETRA at DESY is currently reconstructed and will be converted into a high brilliant storage-ring-based X-ray source called PETRA III [1]. Commissioning of the machine is scheduled for January 2009. PETRA III will operate at 6 GeV electrons or positrons with 100 mA stored current and a design emittance of 1 nm rad. Top-up operation is planned right from the beginning to reduce changes in heat-load and thermal drifts to a minimum,. Suitable beam diagnostic instrumentation and machine protection systems have to be established to guarantee the low emittance, sub-micron beam stability and save machine operation. To ensure a very high availability of the beam in top-up mode, injector and pre-accelerator diagnostic systems are refurbished as well. This paper presents a complete overview of the instrumentation and their latest developments to achieve these requirements.

## INTRODUCTION

PETRA III will be a new high-brilliance synchrotron radiation source at DESY. The 6 GeV storage ring is on track to deliver the most brilliant storage-ring-based X-rays to users in 2009. The construction activities started in July 2007 when HERA went out of operation after 15 years of delivering high energy physics data. The 2.3 km long accelerator is completely redesigned, including the total rebuilding of one-eights of the storage ring where 14 undulators (incl. 5 canted) in 9 straight sections were installed. A new 300 m long experimental hall covering this octant with 14 independent beamlines (+ one diagnostic beam line) was recently build. In order to provide vibration-free conditions for the experiments the experimental hall rest on 99 piles of 1 m diameter that reach 20 m deep into the ground and a massive floor which consists of a 1 m thick monolithic slab of steel fiber enforced concrete. The remaining 7/8 of the storage ring are currently refurbished. Two damping wiggler sections were installed to achieve the designed low emittance of 1 nm rad. The vacuum system together with the beam position monitors (BPMs) was completely redesigned. PETRA III will run with a beam current of 100 mA (upgrade to 200 mA foreseen). Typically up to 100% of the ring circumference is filled with bunches of 8 ns distance (optional 2 ns) of nearly identical charge ($N = 5 \cdot 10^9$ $e^{+,-}$/bunch ± 10%) but other bunch patterns are possible. The bunch length will be 100 ps immediately after injection and 40 ps for stored beam.

In the following the beam diagnostic instrumentation of PETRA III will be described in detail.

## BEAM POSITION MONITORS (BPMS)

PETRA III will be equipped seven different pickup types; their properties are summarized in Table 1. A total of 227 BPMs is foreseen, one BPM per standard FODO-cell and additional BPMs at the locations of insertion devices. The BPM-system has to serve for two major tasks resulting in different operational modes and requirements:

1) Machine commissioning and development: Single turn, single pass capability to acquire beam positions is required for:

-of the non-stored first turn and

-of each of consecutive turns

In these turn-by-turn operation modes the resolution requirement is relaxed (50...100 μm).

2) Orbit feedback and observation: In standard user operation the beam orbit of the stored beam has to be kept constant with respect to the reference (golden) orbit. All BPMs have to be squeezed to their maximum performance in terms of resolution (1/10 of the 1σ beam width) and reproducibility. To achieve this, the bandwidth of the BPM-readout can be reduced to 300 Hz and averaged position measurements of many turns will be acquired. In addition the BPM system has to provide position data with a frequency of about 130 kHz (turn by turn) to feed the fast orbit feedback system. Even at that bandwidth the resolution of a BPM must not exceed 50 μm.

All tasks are foreseen to be fulfilled with the LIBERA Brilliance BPM electronics from Instrumentation Technologies. A number of test measurements were performed in advance [2] to ensure, that the required specifications [3] will be covered by LIBERA. It was demonstrated that already the LIBERA Electron meets the required specifications and the new LIBERA Brilliance exceeds them. However, three parameters were discovered to be critical, namely 1) the temperature drift of LIBERA, 2) the bunch pattern dependence of the position readout and 3) the maximum input voltage of the channels:

1) A dependence on the bunch pattern was observed with LIBERA Electron, but LIBERA Brilliance should eliminate this behaviour. If there will be still a considerable dependency for extreme bunch patterns, it is planned to generate different “golden orbits” for certain fillings.

2) The temperature drift of 0.2 μm/°C allows operating LIBERA only in air-conditioned surroundings. Therefore all racks will be concentrated inside temperature

# LASER-BASED BEAM DIAGNOSTICS*

G. A. Blair, Royal Holloway Univ. of London, Egham, Surrey TW20 0EX,UK.

*Abstract*

Lasers are increasingly being employed in particle beam diagnostics. Laser-based techniques are attractive because they are essentially non-invasive to the beam under test and can not be destroyed by it. They also have the potential to be extremely fast. Uses include transverse beam profile measurement at electron machines using the Compton effect and at proton machines using laser-ionization of H- beams. An introduction is provided to Gaussian beam propagation and how this affects the laser properties and final focus optics needed for the various applications. Recent applications and results from ongoing research projects will be reviewed, with particular emphasis on the "laser-wire" systems recently employed at the PETRA and ATF machines. Future possibilities will be discussed, including higher order laser modes and interferometric techniques.

## INTRODUCTION

Future electron machines will need accurate determination and monitoring of their transverse phase space in order to meet their challenging performance specifications. A detailed analysis of the issues and challenges involved in such measurements are presented in Ref. [1], with particular reference to the International Linear Collider (ILC) [2]; a brief summary of this work is presented below in order to motivate the challenges of the laser and optics prestented later.

The Laser-Wire (LW) is a key beam diagnostics, which is useful for beam profiles ranging from several tens of microns, down to the micron scale. Smaller beam profiles have been measured using laser interferometric techniques [3, 4] whereas traditional solid wires or screens can be used for larger profiles (although they are disruptive to the electron beams). Very challenging, low f-number, laser optics are necessary for the LW in order to achieve the required small laser spot-sizes and the subsequent performance is evaluated numerically and described in below. The laser systems necessary to power the LW are also very challenging and the necessary specifications are next derived and discussed.

## TRANSVERSE EMITTANCE MEASUREMENT

The International Linear Collider (ILC) has demanding emittance goals that will need to be measured accurately in order to maximise the machine performance; the parameters of the ILC [2] are presented in Tab. 1, which provides the context for the requirements on measurement beam spot sizes and scanning speeds, discussed below.

Table 1: Nominal ILC Parameters

| | | |
|---|---|---|
| Beam energy | $E$ | 250(500) GeV |
| Norm. horiz. emittance | $\gamma\epsilon_x$ | $10^{-5}$m rad |
| Norm. vert. emittance | $\gamma\epsilon_y$ | $4 \cdot 10^{-8}$ m rad |
| Train repetition rate | $f$ | 5 Hz |
| Num. bunches per train | $N_{\rm train}$ | 2625 |
| Inter-bunch spacing (ns) | | 369 |
| Bunch length | $L_b$ | 300 $\mu$m |
| Num. electrons per bunch | $N_e$ | $2 \times 10^{10}$ |

### *Beam Phase Space*

The phase-space of a general Gaussian particle beam can be described by four-dimensional (4d) matrix:

$$\sigma = \begin{bmatrix} \langle x^2 \rangle & \langle xx' \rangle & \langle xy \rangle & \langle xy' \rangle \\ \langle xx' \rangle & \langle x'^2 \rangle & \langle x'y \rangle & \langle x'y' \rangle \\ \langle xy \rangle & \langle x'y \rangle & \langle y^2 \rangle & \langle yy' \rangle \\ \langle xy' \rangle & \langle x'y' \rangle & \langle yy' \rangle & \langle y'^2 \rangle \end{bmatrix} \quad (1)$$

The standard approach to reconstructing the 4d coupled beam matrix with the least-squares fit method is presented in Ref [5]. At a scanner location in the beam-line it is possible to measure three values, $\langle x^2 \rangle$ , $\langle y^2 \rangle$ and $\langle xy \rangle$, with the help of a horizontal ($x$), a vertical ($y$), and a tilted ($u$) wire scanner, as illustrated in Fig. 1, where the tilt-scanning angle, $\phi$, is also defined.

The optimal value for $\phi$ is given by

$$\phi_0 = \tan^{-1}\left(\frac{\sigma_x}{\sigma_y}\right) . \quad (2)$$

and typical values of interest to the ILC beam delivery system (BDS) are presented in Tab. 2.

The ten independent entries of Eq. 1 can be obtained either by changing the optics in a controlled manner at the wire location [6, 5, 7] or by locating the wires at different positions in the beam-line. The latter technique will be relevant for routine fast-scanning operation at the ILC. Here it will be assumed that six laser-wire scanning stations are located at optimal locations in the BDS and that each laser-wire station measures $x$,$y$ and $u$ with the same relative measurement error. The emittance can then be inferred by inverting the relations between the transverse spot

* Work supported by the UK Science and Technology Facilities Council and by the Commission of European Communities under the 6th Framework Programme Structuring the European Research Area, contract number RIDS-01189.

# Electro-optic techniques in electron beam diagnostics

J. van Tilborg*, Cs. Tóth, N. H. Matlis, G. R. Plateau, and W. P. Leemans
Lawrence Berkeley National Laboratory, Berkeley, California

*Abstract*

Electron accelerators such as laser wakefield accelerators, linear accelerators driving free electron lasers, or femto-sliced synchrotrons, are capable of producing femtosecond-long electron bunches. Single-shot characterization of the temporal charge profile is crucial for operation, optimization, and application of such accelerators. A variety of electro-optic sampling (EOS) techniques exists for the temporal analysis. In EOS, the field profile from the electron bunch (or the field profile from its coherent radiation) will be transferred onto a laser pulse co-propagating through an electro-optic crystal. This paper will address the most common EOS schemes and will list their advantages and limitations. Strong points that all techniques share are the ultra-short time resolution (tens of femtoseconds) and the single-shot capabilities. Besides introducing the theory behind EOS, data from various research groups is presented for each technique.

## INTRODUCTION

Electron accelerators are playing a major role in today's scientific landscape. Compact relativistic electron bunches, containing $> 10^9$ electrons, with a transverse size of several microns and a temporal duration of 10's to 100's of femtoseconds, can be utilized for numerous applications. On one hand one can think of experiments where the electrons are utilized directly (for example: colliders, electron diffraction, and magnetic switching). On the other hand, these compact bunches can produce intense electromagnetic radiation such as X-rays, gamma rays, ultraviolet photons, and terahertz (THz) radiation, among others (think for example of synchrotron radiation or free electron lasers). For all these applications, the quality of the electron bunch is a critical parameter. One way to assign a parameter for bunch quality is through the introduction of a beam brightness, defined as

$$\text{Brightness} = \frac{\text{Charge} \cdot \text{E}_{\text{kin}}}{\text{Duration} \cdot (\Delta\text{E}_{\text{kin}}/\text{E}_{\text{kin}}) \cdot \text{Emittance}}, \quad (1)$$

where $\text{E}_{\text{kin}}$ is the electron kinetic energy with spread $\Delta\text{E}_{\text{kin}}$, and where the emittance represents the transverse emittance.

Each of the parameters listed in Eq. (1) needs to be measured and controlled for optimized accelerator performance. The work presented in this paper will address characterization of the temporal bunch duration, with the emphasis on bunches of ultra-short (femtosecond) duration.

* JvanTilborg@lbl.gov

## *Coherent radiation from electron bunches*

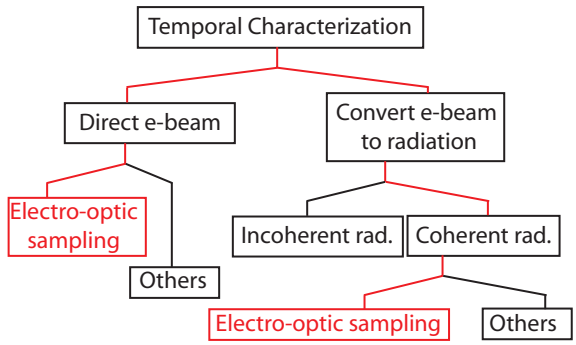


Figure 1: The technique of electro-optic sampling (EOS) can be applied to either the direct electron beam, or on the coherent radiation emission (typically at THz frequencies) that is produced by the electron bunch.

The temporal charge profile of an electron bunch can be labeled as $Q(t)$. The Fourier transformation of this profile is given by $Q(\omega) = \int dt Q(t) \exp(-\imath\omega t)$, where $\omega = 2\pi\nu$, with $\nu$ the frequency and $\omega$ the angular frequency. The spectral profile $Q(\omega)$ is complex (real and imaginary parts) and can be expressed as

$$Q(\omega) = |Q(\omega)|e^{\imath\phi(\omega)}, \quad (2)$$

where $|Q(\omega)|$ is the absolute spectrum and $\phi(\omega)$ the spectral phase. Note that only through measurement of both $|Q(\omega)|$ and $\phi(\omega)$ can the temporal profile $Q(t)$ be fully reconstructed.

As illustrated in Fig. 1, there are two paths to characterize the temporal duration of an electron bunch. The first path focuses on measurement of the field profile of the bunch itself (labeled as "Direct e-beam"), while the other path focuses on the emission of electro-magnetic radiation by the electron bunch. The mechanism for radiation emission can be transition radiation, diffraction radiation, Cherenkov radiation, Smith-Purcell radiation, or synchrotron radiation, among others. Since properties of the electron bunch duration are present in the emitted electromagnetic pulse, analysis of the radiation can lead to temporal bunch characterization.

The radiation can be categorized, see Fig. 1, as incoherent radiation (at wavelengths shorter than the bunch length) and coherent radiation (at wavelengths longer than the bunch length). It was demonstrated by Catravas *et al.* [1, 2] that through fluctuation interferometry of the incoherent radiation one can estimate the pulse duration. Also, a (sub)picosecond streak camera can be used to detect the pulse duration of the incoherent light [3]. Most

# RADIATION DAMAGE IN DETECTORS AND ELECTRONICS

Ronald Lipton, Fermilab, Batavia, IL 60510, U.S.A.

*Abstract*

Coping with radiation-related effects is a constant challenge to the detectors and electronics deployed at high intensity and luminosity accelerators. Work associated with the LHC R&D collaborations has extended the range of understanding of these effects to unprecedented integrated dose levels. At the same time the availability of deep submicron technology and a variety of process variations available in IC production have redefined the tools available to build electronics to accommodate irradiation. This paper will briefly review our current understanding of the mechanisms of radiation damage and techniques to extend the lifetimes of detectors and electronics.

## RADIATION EFFECTS IN SILICON AND $SIO_2$

I will concentrate here on the standard electronic materials – silicon and its oxide. We can divide the world of radiation damage into electromagnetic and bulk damage components. Ionizing radiation, such as x-rays, gammas, and electrons, create free charge in materials, which affects properties and performance. Hadrons (neutrons, pions, protons) can also produce "bulk" damage – damage to the silicon crystal lattice by displacing atoms from their usual sites. Electronics, because of the thin sensitive layer, tend to be most sensitive to ionization and the associated accumulation of charge in the material. Detectors are sensitive to both, with the most important damage often coming from bulk effects.

## BULK DAMAGE – EFFECTS ON DETECTORS

Particle Physics detectors are unusual structures in the microelectronics world. They are fabricated with lightly doped, float zone, silicon, they use rather thick structures to collect a large signal, and they have a regular array of electrodes.

### *Displacement Damage in Silicon*

Hadrons can interact and cause significant damage to the silicon crystal lattice. The amount and type of damage depends on the particle type and energy. The damage is usually quantified by the amount of Non-Ionizing Energy Loss (NIEL – KeV $cm^2/g$) or displacement damage (MeV-mb). For convenience damage is usually scaled to the NIEL of 1 MeV neutrons. However the pattern of energy loss depends on the type of particle and the pattern of damage clusters left by the particle.

Atoms scattered by inceident hadrons leave both vacated lattice sites (vacancies) and "free" atoms (interstitials) known as Frenkel pairs. The pattern of energy deposit is important – low energy transfers will leave sparse "point defects." Higher energy transfers can leave clusters of defects. Frenkel pairs in these clusters have a higher probability for recombination. The defects can have energies inside the bandgap, and act as additional donors or acceptors with energy levels different than the usual dopants. They can also act as generation centers for leakage currents. Other defects can act as traps for charge carriers and affect the charge collection efficiency of detectors. Vacancies and interstitials can also interact with the impurities in the silicon, and either be activated or passivated. Finally, they can recombine to anneal away some of the initial bulk damage.

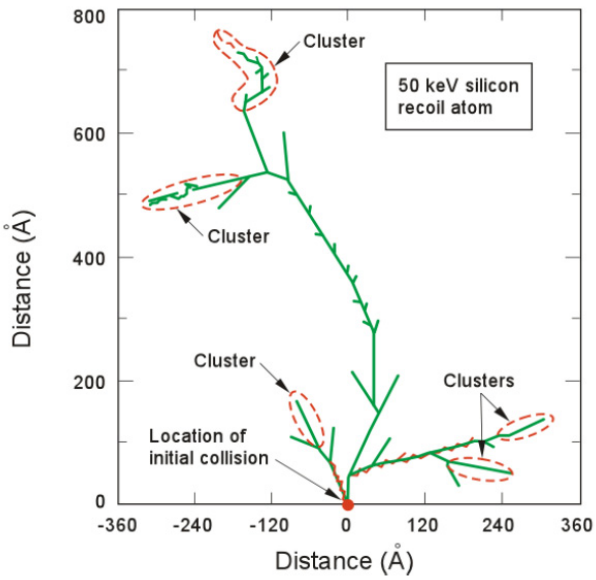


Figure 1. Simulation of damage caused by a 50 KeV silicon recoil nucleus [1].

The simplest effect, caused most efficiently by midgap states, is an increase in overall leakage current. This is a almost universal effect, and does not seem to depend on the details of doping, impurities, or processing. It is parameterized by:

$$I_{\det} = I_0 + \alpha \times flux \times Vol \qquad (1)$$
$$\alpha = 2 - 3 \times 10^{17} A/cm^2$$

There is a strong annealing effect in leakage current (Figure 2). The overall annealing time has several

# PERFORMANCE OF FPGA-BASED DATA ACQUISITION FOR THE APS BROADBAND BEAM POSITION MONITOR SYSTEM*

H. Bui, G. Decker, R. Lill, A. Pietryla, W. E. Norum
Argonne National Laboratory, Argonne, IL 60439 USA

*Abstract*

The Advanced Photon Source (APS) monopulse beam position monitor (BPM) system, designed to measure single- and multi-turn beam positions, is one of three BPM systems currently in use to measure and control both AC and DC orbit motions. Recently, one sector of the monopulse BPM system was upgraded by replacing its 1992-era 12-bit signal conditioning and digitizing unit (SCDU) with a field-programmable gate array (FPGA)-based system for signal processing. The system consists of a repackaging of the broadband rf receiver modules together with a VME Extensions for Instrumentation (VXI) form factor housing eight 14-bit digitizers and one FGPA. The system will be described in detail, including an overview of its new functionality, and performance will be discussed. Of particular interest is the noise floor, which will be contrasted with the previous system and with other systems in use at the APS.

## INTRODUCTION

The Advanced Photon Source broadband monopulse BPM system is designed to measure single- and multi-turn beam position used in a feedback system to control both AC and DC orbit motion. Presently, a VXI-based signal conditioning and digitizing unit (SCDU) is used for data acquisition. A monopulse rf receiver, located inside the SCDU, receives 10-MHz band-limited sum and difference signals from an in-tunnel filter-comparator and outputs beam intensity and normalized position [1]. Both signals are digitized via 12-bit analog-to-digital converters (ADCs), operating at the 271-kHz ring revolution frequency, and values are stored in registers. The Memory Scanner module, residing in the same VXI crate, reads the output registers and provides a programmable boxcar average. It also provides a high-speed fiber-optic port to stream data to the feedback system. The system has been in operation for more than ten years. Compared to today's technology, the SCDU is dated, and needs a technology upgrade. The planned upgrade was to remove the monopulse receiver from the SCDU for reuse, and replace the SCDU with an FPGA-based VXI data acquisition and processing module [2]. The new BPM Signal Processor (BSP100) contains eight ADCs, an embedded IOC, and a single Altera Stratix® II FPGA. It can acquire and process data for four monopulse receiver units. This paper describes the new system's functionalities and test results.

*Work supported by U.S. Department of Energy, Office of Science, Office of Basic Energy Sciences, under Contract No. DE-AC02-06CH11357.

## SYSTEM OVERVIEW

The new monopulse BPM system (shown in Figure 1) consists of five subcomponents:

- In-tunnel hardware (capacitive button pickups, matching networks, filter comparator, Heliax® cables)
- Receiver chassis
- Power supply chassis
- Fan unit
- BPM signal processor (BSP100)

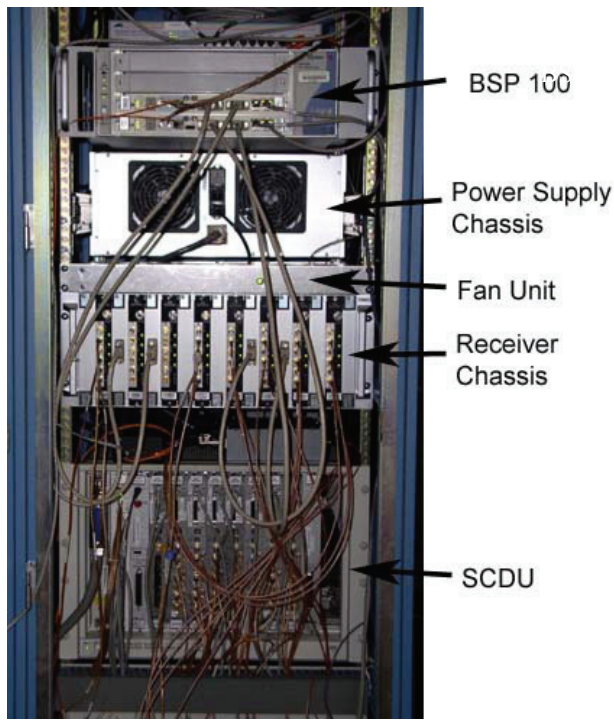


Figure 1: New monopulse BPM system installed at Sector 38.

The in-tunnel portion of the new monopulse BPM system, including capacitive button pickups, matching networks [3], filter comparator, and Heliax® cables, remains unchanged.

The monopulse receiver was removed from the SCDU and packaged together with an interface circuit board, mounted on a custom-designed heat-sink aluminum block, that can be plugged into a receiver chassis. The interface circuit board not only provides regulated power and filtering and I/O signal conditioning to the monopulse receiver, but also is capable of generating a 21-dBm,

# NEW METHOD TO MONITOR THE TRANSVERSE DISTRIBUTION OF CURRENT IN PARTICLE BEAMS

M. J. Hagmann, NewPath Research L.L.C., P. O. Box 3863, Salt Lake City, UT 84110, U.S.A.

*Abstract*

A group of sinusoidally-wound coaxial toroidal coils can be used to determine the transverse distribution of a time-dependent current through their common aperture. The current is expressed in a basis of chapeau (pulse) functions over an array of pixels, and matrix methods are used to calculate the current in each pixel from the voltages induced on the coils. Optimum configurations of pixels are used, for which the condition number of the matrix is bounded by the number of pixels. For example, with 50 pixels the fractional errors in the currents are approximately 50 times the fractional errors in the measured voltages in addition to imperfections in the fabrication and placement of the coils. Numerical tests were made by specifying the currents, calculating the induced voltages, adding Gaussian noise to model measurement errors, and then using the algorithms to calculate the currents. These simulations confirm that the condition number is bounded by the number of pixels.

## INTRODUCTION

Others have used a variety of different techniques to monitor the transverse distribution of the beam current in accelerators, including secondary emission monitors, wire scanners, multi-wire chambers, gas curtains or jets, residual gas monitors, scintillator screens, scrapers and measurement targets, synchrotron radiation, and Laser-Compton scattering [1], as well as optical transition radiation [2] and the deflection of a probe beam of electrons [3].

A Rogowski Coil is a non-ferrous current probe formed by bending a uniformly wound helical coil to follow a closed curve having arbitrary shape [4-6]. When a time-dependent current passes through the aperture that is enclosed by the bent helix a voltage is induced on the coil which is independent of the location of the current. However, currents that are located outside of the aperture do not induce a voltage on the coil. Deviations from a uniform winding are carefully avoided because they cause the induced voltage to depend on the location of the current within the aperture, but it will be shown that a group of coils having a specific type of nonuniformity may be used to accurately determine the transverse distribution of the current.

## ANALYSIS

Figure 1 is a diagram used for deriving expressions for the open-circuit voltage induced on a non-ferrous toroidal coil that may have a nonuniform winding. The toroid has a mean radius R, and the cross-sectional area of the tube of the toroid is A. Consider the induction in an incremental winding of length Rdθ that is centered at $(R,\theta)$ or equivalently $(X_1,Y_1)$, which is caused by a filament with current $I = I_{10}e^{j\omega t}$ that intersects the X,Y plane at point $P(X_2,Y_2)$. The dashed line $L_1$ is directed normal to the increment of winding. Dashed line $L_2$ is parallel to the magnetic field, and dashed line $L_3$ is parallel to the X-axis.

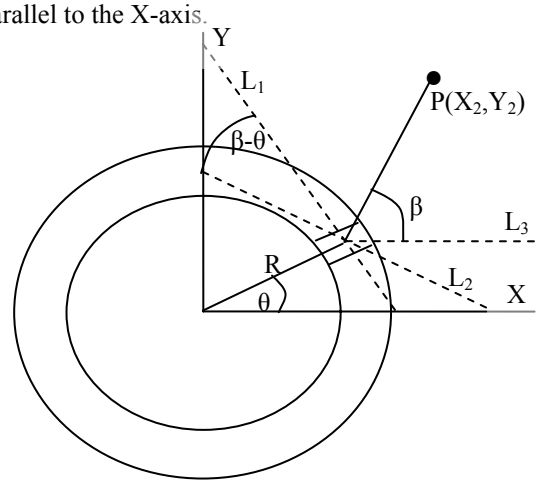


Figure 1: Diagram for analysis.

Let N'(θ) be the number of turns per unit length of the coil, as measured on a circle with radius R. For example, with a toroidal coil having a uniform winding, $N' = N_0' = N_T/2\pi R$, where $N_T$ is the total number of turns. The number of turns in an increment of the winding is $dN = N'(\theta)\, R\, d\theta$. Thus, if the height and width of the tube are much less than R, the open-circuit voltage on the entire winding is given by

$$V_{OC} = -\int_0^{2\pi} \frac{j\omega\mu_0 N'(\theta) RAI \cos(\beta-\theta)\, d\theta}{2\pi\sqrt{(X_2-X_1)^2+(Y_2-Y_1)^2}} \quad (1)$$

Using trigonometry to obtain an expression for $\cos(\beta - \theta)$, Eq. (1) simplifies to give the following:

$$V_{OC} = \frac{j\omega\mu_0 AI}{2\pi}\int_0^{2\pi} \frac{N'(\theta)\left[1-\frac{X_2}{R}\cos\theta-\frac{Y_2}{R}\sin\theta\right]}{\left[\left(\frac{X_2}{R}-\cos\theta\right)^2+\left(\frac{Y_2}{R}-\sin\theta\right)^2\right]} d\theta \quad (2)$$

The expressions for N' are chosen from the following set, which constitutes the basis for a Fourier series:

$$N'(\theta) \in \left\langle N_0', \sum_{J=1}^{\infty} N_{JC}'\cos(J\theta), \sum_{J=1}^{\infty} N_{JS}'\sin(J\theta) \right\rangle \quad (3)$$

where the $N_{JC}'$ and $N_{JS}'$ are coefficients as is $N_0'$. By substituting the set in Eq. (3) into Eq. (2), and evaluating the integral, the open-circuit voltage that is induced on each coil is given by the corresponding term of the

# NEW METHOD TO MONITOR THE CURRENT AND POSITION OF ONE OR TWO PARTICLE BEAMS

M. J. Hagmann, NewPath Research L.L.C., P. O. Box 3863, Salt Lake City, UT 84110, U.S.A.

*Abstract*

A group of sinusoidally-wound coaxial toroidal coils can be used to determine the magnitudes, phases, and locations of one or two time-dependent currents through their common aperture. A single current filament requires one uniformly-wound coil and two others having turn densities proportional to the sine and cosine of the azimuthal coordinate. Three simple algebraic equations give the magnitude, phase, and location of the current in terms of the voltages induced on the three coils, and there is no ill-conditioning. Two current filaments require two additional toroids with turn densities proportional to the sine and cosine of two times the azimuthal coordinate, and the solution is obtained using the method of steepest descent. Solutions for more than two currents become numerically unstable. Numerical tests were made by specifying the magnitudes, phases, and locations of the currents, calculating the induced voltages, adding Gaussian noise to model measurement errors, and then using the algorithms to calculate the currents and their locations. These simulations confirm that this method may be used with one or two currents

## INTRODUCTION

Others have used a variety of different techniques to monitor the location of a single beam in an accelerator, including arrays of capacitive pickups, resistive wall gap monitors, electrostatic monitors, split-plate monitors, split-cylinder monitors, button monitors, longitudinal transmission lines, resonant cavities, and reentrant cavities [1]. Other techniques include secondary emission monitors, wire scanners, multi-wire chambers, gas curtains or jets, residual gas monitors, scintillator screens, scrapers and measurement targets, and synchrotron radiation [2], as well as the deflection of a probe beam of electrons [3]. Three groups have described work that is directly related to this paper. Two used four identical coils to determine the current and its location [4,5]. Murgatroyd and Woodland [6] made a short note that two coils with turn densities varying as sin(θ) and cos(θ) could measure the location of a single current, but they gave no analysis or experimental results and these authors could not be reached.

A Rogowski Coil is a non-ferrous current probe formed by bending a uniformly wound helical coil to follow a closed curve having arbitrary shape [7-9]. When a time-dependent current passes through the aperture that is enclosed by the bent helix a voltage is induced on the coil which is independent of the location of the current. However, currents that are located outside of the aperture do not induce a voltage on the coil. Deviations from a uniform winding are carefully avoided because they cause the induced voltage to depend on the location of the current within the aperture, but it will be shown that a group of coils having a specific type of nonuniformity may be used to accurately determine the current and its location.

## ANALYSIS

Figure 1 is a diagram used for deriving expressions for the open-circuit voltage induced on a non-ferrous toroidal coil that may have a nonuniform winding. The toroid has a mean radius R, and the cross-sectional area of the tube of the toroid is A. Consider the induction in an incremental winding of length Rdθ that is centered at (R,θ) or equivalently $(X_1,Y_1)$, which is caused by a filament with current $I = I_{10}e^{j\omega t}$ that intersects the X,Y plane at point $P(X_2,Y_2)$. The dashed line $L_1$ is directed normal to the increment of winding. Dashed line $L_2$ is parallel to the magnetic field, and dashed line $L_3$ is parallel to the X-axis.

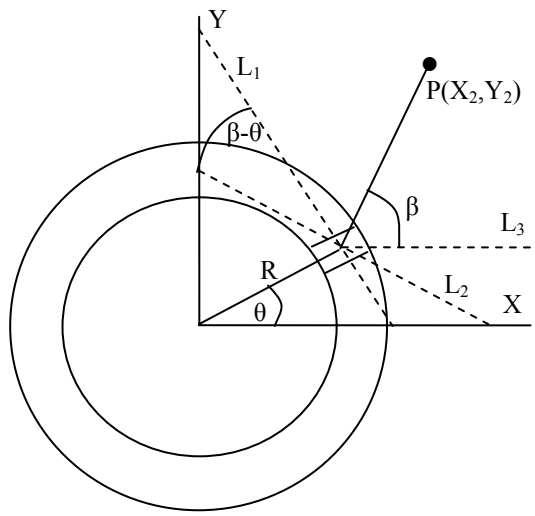


Figure 1: Diagram for analysis.

Let N'(θ) be the number of turns per unit length of the coil, as measured on a circle with radius R. For example, with a toroidal coil having a uniform winding, $N' = N_0' = N_T/2\pi R$, where $N_T$ is the total number of turns. The number of turns in an increment of the winding is $dN = N'(\theta)\, R\, d\theta$. Thus, if the height and width of the tube are much less than R, the open-circuit voltage on the entire winding is given by

$$V_{OC} = -\int_0^{2\pi} \frac{j\omega\mu_0 N'(\theta) RAI \cos(\beta-\theta)\, d\theta}{2\pi\sqrt{(X_2-X_1)^2+(Y_2-Y_1)^2}} \quad (1)$$

Using trigonometry to obtain an expression for cos(β - θ), Eq. (1) simplifies to give the following:

# INJECTION OF DIRECT-SEQUENCE SPREAD SPECTRUM PILOT TONES INTO BEAMLINE COMPONENTS AS A MEANS OF DOWNCONVERTER STABILIZATION AND REAL-TIME RECEIVER CALIBRATION*

J. Musson†, T. Allison, Thomas Jefferson National Accelerator Facility, Newport News, VA, 23606
Christopher Hewitt, Christopher Newport University, Newport News, VA, 23606

*Abstract*

Beamline components used for diagnostic elements often rely on thermal stabilization, continual physical maintenance (ie. tuning), and frequent beam-based calibrations to maintain specified performance. Direct-sequence spread spectrum (DSSS) pilot tones injected into a particular element and combined with the beam-derived signal can subsequently be separated and used to assess performance degradation. In addition, the DSSS tone can be used as a real-time calibration signal, without interference to the intended diagnostic signal. This paper demonstrates such a technique in the design of a Beam Current Monitor downconverter system, as an intended upgrade to the CEBAF Beam Loss Accounting system. A brief spread-spectrum primer is included, as well as a description of appropriate spreading codes and their generation.

## INTRODUCTION

The Continuous Electron Beam Accelerator Facility (CEBAF) employs a system of passive 1497 MHz TM010 cavities as the basis for a beam current loss accounting system (BCM/BLA) for machine protection [1]. The 1497 MHz RF signal is downconverted, and routed to a VME-based IF receiver system capable of resolving hundreds of nanoamps of instantaneous beam loss [2,3]. In addition, a 1% absolute accuracy provides accelerator operators and experimenters with a convenient means of continuous, non-invasive beam current measurement. The present system has two limitations. Firstly, confidence tests of the cavity performance can only be preformed off-line, i.e. when the beam is not present. Secondly, the RF-to-IF downconverters, located in the beam enclosure, are no longer available and will require replacement for the 12 GeV CEBAF upgrade. A new system is desired, which is capable of continuous performance assessment, able to stay within calibration limits for long periods of time, and requires minimal operator or system expert intervention. The proposed design employs a CW pilot tone, orthogonal to the electron beam signal, as a means to evaluate proper performance in real time, as well as introduce a calibration reference for long-term stability.

## DIRECT-SEQUENCE SPREAD SPECTRUM (DSSS)

The problem of intentional co-channel interference (ie. "jamming") has long been an issue with RADAR and tactical communications systems. An effective countermeasure involves spreading the carrier energy over an extreme bandwidth, often hiding beneath the thermal noise floor. If the mechanism with which the spreading is known, carrier reconstruction can be performed at the receiver using cross-correlation techniques [4].

The basis for DSSS involves multiplying the carrier with a pseudo-random bit sequence, which although looks like noise to other receiving stations, is actually a correlated, repeating sequence which has the effect of encrypting the carrier energy.

### *Spreading Codes*

Mathematically, a spreading code serves to map the low-dimensional CW carrier tone to one having a high degree of dimensionality. Furthermore, each of the dimensions should consist of orthogonal signals, which form the new basis. Then, the D equiprobable and equienergy orthogonal signals within an n-dimensional space can be re-represented in the new signal space by considering an orthonormal basis, $\varphi_k(t)$, which is defined by [5]:

$$\phi_k(t);\ 1 \leqslant k \leqslant n$$

$$\int_0^T \phi_l(t)\phi_m(t)\,dt = \delta_{lm} = \begin{cases} 1 & l = m \\ 0 & l \neq m \end{cases} \quad .$$

Then, the new signal representation is:

$$S_i(t) = \sum_{k=1}^{n} S_{ik}\phi_k(t) \qquad 1 \leqslant i \leqslant D; \qquad 0 \leqslant t \leqslant T$$

where

$$S_{ik} = \int_0^T S_i(t)\phi_k(t)\,dt \quad .$$

The resulting average energy for each of the signals is represented by:

$$\int_0^T \overline{S_i^2(t)}\,dt = \sum_{k=1}^{n} \overline{S_i^2} = E_s; \qquad 1 \leqslant i \leqslant D$$

*Authored by Jefferson Science Associates, LLC under U.S. DOE Contract No. DE-AC05-06OR23177.
†musson@jlab.org

# THE BEPCII DCCT SYSTEM

Y. Zhao#, J.S. Cao

Institute of High Energy Physics, Chinese Academy of Sciences, Beijing 100049, China

*Abstract*

A DC Current Transformer (DCCT) as a standard diagnostic system for beam current plays an important role in BEPCII, the upgrade project of the Beijing Electron Positron Collider. Two DCCTs are operating now, separately in the electron and positron rings, to monitor the beam current, the beam injection rate, the beam loss rate and the beam lifetime. In this paper, the mechanical structure design, readout system and data processing are presented. The progress of DCCTs on each step of BEPCII commissioning, such as improving the beam lifetime and reducing the background noise, are also included.

## INTRODUCTION

DCCT systems usually consist of three parts: sensor, electronics and the DAQ & control. The sensor is always affixed on the linear tube, for it is sensitive to the parasitic magnetic field caused by RF cavity, quadrupole magnet and the power cable, and must be far from those parts. Figure 1 shows the layout of the DCCT.

In BEPCII, two DCCT sensors are fixed in each outer ring, symmetrically around the south interaction points. The two sensors are individually used for the electron ring and positron ring when BEPCII operates in the collision mode. In dedicated synchrotron radiation mode, both of them are used for the electron ring. The sensor and electronics are made by the Bergoz Instrumentation Company. DCCT is an integrative system, so it works in single bunch or multiple bunch operation.

Tabel 1 gives the main technical parameters.

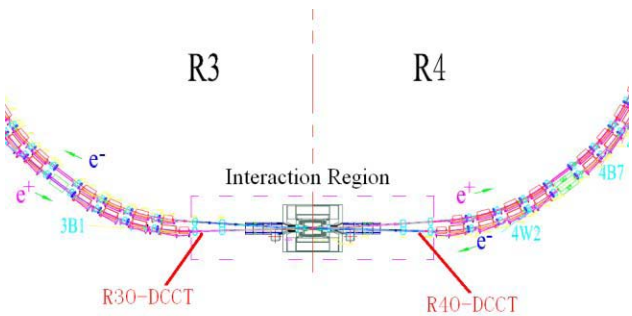


Figure 1: Layout of DCCT

Table 1: The main technical parameters of DCCT

| Parameters | Value |
|---|---|
| Dynamic range | 0.0~1.5A |
| Linearity | 0.1 % |
| Zero drift | <0.05mA |
| Remarks | shielding needed |
| Detector size | 350 mm with flange |
| Location | far from RF cavity |

## THE MECHANICS & INSTALLATION

A vacuum chamber with a ceramic gap has been used for avoiding the parasitic current caused by the chamber's electrical conductivity. Considering the 30 kHz bandwidth of the DCCT's signal, we decided to enhance the high frequency pass band to prevent the bunch frequency component from leaking from the gap when BEPCII operates in the single bunch mode. Thus the cut-off frequency could be lower than the bunch frequency but higher than the pass band of the DCCT. After calculation and simulation in the lab, the preparatory configuration of the system was confirmed. Figure 2 shows the structure and the parameters[3]. Copper foil and a layer of polyester film were used over the gap, to reduce the low-frequency signal leakage. Two magnetic shielding layers were adopted to protect the sensor from unorderly magnetic fields. The outer layer is electrostatic shielding against RF and for circulation of wall current.

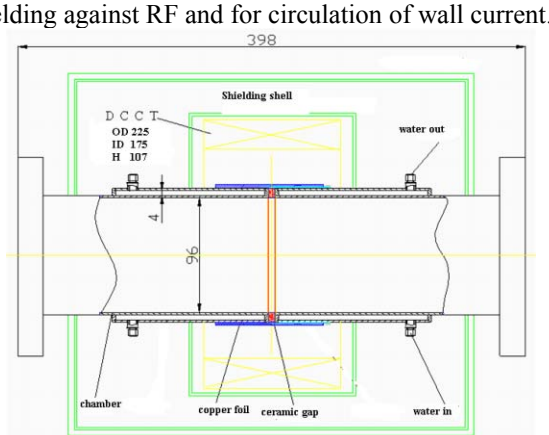


Figure 2: Structure of DCCT tube.

## THE ELECTRONICS & DAQ

The electronics and the DAQ system of DCCT are in the local stations of beam instrumentation, and consist of 2 cassettes, 2 DVMs and an IPC. The sensors in the tunnel are connected to the electronics by 120 m of cable. Figure 1 shows the structure. In the earlier design, a low pass filter had been put between electronics and DVM to decrease 50 Hz interference; it has since been removed.

#zhaoying@ihep.ac.cn

# SCINTILLATION SCREEN INVESTIGATIONS FOR HIGH CURRENT ION BEAMS AT GSI LINAC

E. Gütlich, P. Forck, R. Haseitl, P. Kowina
Gesellschaft für Schwerionenforschung GSI, Darmstadt, Germany

*Abstract*

Scintillation screens are widely used for qualitative beam profile monitoring. However, precise measurements might yield ambivalent results, especially for high beam currents. We have investigated the optical properties of various scintillating materials with different beams in the energy range 5.5 to 11.4 MeV/u delivered by the heavy ion linac at GSI. Investigations were not only focused on well-known sensitive scinitillators but also on ceramic materials with lower light yield. Their properties (yield, beam width, higher statistical moments) were compared to different quartz glasses. The image of each macropulse was recorded by a digital CCD camera and individually evaluated. For some materials, a decrease of the light yield occurs. For a focused beam, the imaged width depends on the material. Moreover, the light yield and width depend significantly on the screen temperature, which is increased by beam impact.

## DEMANDS AND SETUP

For decades, scintillation screens have been used for beam profile measurement in nearly all accelerator facilities. These screens are an essential part of a pepper-pot ermittance system used for the determination of the width of "beamlets" created by a plate with ≈100 small holes. The realization at GSI, as used for high current operation of UNILAC, is described in [1]. The angular distribution within the phase space is calculated from the intensity distribution of the beamlets. This requires an accurate measurement of the spot's light distribution. However, there had been doubts concerning the accuracy of the pepper-pot method [2], which might be related to possible image deformation by the scintillating screen.

We investigated the optical properties of 16 fluorescence materials with ∞5.5 and 11.4 MeV/u and different beam currents as delivered by UNILAC. Typical sizes for the focused beam were σ≈2mm. Sensitive scintillation screens, like YAG:Ce or ZnS:Ag were irradiated in addition with lower currents. Ceramic materials with less light yield, like BN, $ZrO_2$, $ZrO_2$ doped with Mg, pure $Al_2O_3$ and $Al_2O_3$ doped with Cr (Chromox) were investigated and compared to quartz-glass (Herasil 102) and quartz-glass doped with Ce (M382); see Table 1.

A movable target ladder, as shown in Fig.1, was equipped with 6 different screens of ∅30mm and installed in a vacuum chamber. The irradiations were performed with pressure of ≈$5x10^{-7}$ mbar. The target ladder allows beam observations without longer interruption, which ensures the same beam properties for all materials. The scintillation was observed by a digital CCD camera (AVT-Marlin) equipped with a monochrome chip of VGA resolution. A Pentax B2514ER lens system of 25 mm focal length equipped with a remote controlled iris was used for compensation of material dependent light yield. Moreover, the camera's inherent amplification was changed by the gain setting. The calculation of the light yield corrects both settings. The reproduction scale for the beam image was 10 pixel/mm. Data transmission was performed by the camera's Firewire interface to a high performance data acquisition system, [3] which enables the storage of an image from each macropulse for individual offline analysis.

Table 1: Compilation of investigated materials

| Type | Material | Supplier |
|---|---|---|
| **Crystal Scintillator** | YAG:Ce, BGO, $CdWO_4$, $CaF_2$:Eu | Saint Gobain Crystals |
| **Powder** | ZnS:Ag | HLW |
| **Ceramics** | $ZrO_2$(Z700 20 A), $ZrO_2$:Mg (Z507), BN, $Al_2O_3$ and $Al_2O_3$:Cr (Chromox) | BCE Special Ceramics |
| **Quartz-glass** | Pure: Herasil 102, Ce doped: M382 | Heraeus Quartz-glass |

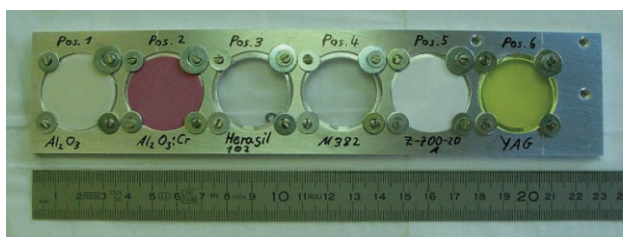


Figure 1: The target ladder equipped with ∅30mm screens is shown. The screen materials prior to irradiation are from left: pure $Al_2O_3$, $Al_2O_3$:Cr, Herasil, Quartz:Ce, $ZrO_2$ and YAG:Ce.

## TYPICAL RESULTS AND ANALYSIS

The original beam image (an example is shown in Fig. 2 top) was projected to the beam's horizontal and vertical plane. A quantitative analysis was performed with the projection. In this work we show the horizontal projection but comparable results were obtained for the vertical direction. Two examples of such projections are shown in Fig. 2 bottom. For both displayed materials the total light yield decreases during irradiation. The shape of the peak is preserved for $ZrO_2$:Mg (shown left). For $Al_2O_3$ (shown right) the shape is modified mainly around the maximum;

# COMMISSIONING OF ELECTRON BEAM DIAGNOSTICS FOR A SRF PHOTOELECTRON INJECTOR

T. Kamps*, D. Böhlick, M. Dirsat, D. Lipka, T. Quast, J. Rudolph, M. Schenk, BESSY, Berlin, Germany
A. Arnold, F. Staufenbiel, J. Teichert, Forschungszentrum Dresden, Dresden, Germany
G. Klemz, I. Will, Max Born Institut, Berlin, Germany

*Abstract*

A superconducting RF (SRF) photoelectron injector is currently under commissioning by a collaboration of BESSY, DESY, FZD and MBI. The project aims at the design and setup of a continuous-wave (CW) SRF electron injector including a diagnostics beamline for the ELBE FEL and to address R&D issues of high brightness CW injectors for future light sources such as the BESSY FEL. The layout and realization of the diagnostics beamline for the electron beam is presented including systems to monitor the momentum, charge, transverse emittance and bunchlength in various operation modes of the injector.

## MOTIVATION

Future FEL light sources such as the proposed STARS FEL [1] and the ELBE facility [2] operate with superconducting RF (SRF) for electron acceleration to enable continuous wave (CW) operation generating flexible bunch patterns.

The SRF injector project combines the advantages of photo-assisted production of short electron pulses, high acceleration field at the cathode of an RF field and CW operation of a superconducting cavity. The main challenges are the design of the superconducting cavity with a suitable cathode insertion, the risk of contamination of the cavity with cathode material, and a method to control the transverse emittance of the electron beam. The SRF gun collaboration of BESSY, DESY, FZR and MBI sets out to tackle these issues. The target of the collaboration is to setup a SRF gun [3] together with a diagnostics beamline serving as a test facility for photoelectron injectors. The task of the diagnostics beamline is to ensure safe operation of the injector, check the theoretical model for the injector by measurements and to find an optimum working point for the setup of the injector parameters.

## EXPERIMENTAL SETUP

The setup for the photoinjector consists of the SRF gun and the diagnostics beamline as depicted in Fig. 1. The electrons are generated by a pulsed laser beam impinging on the photocathode. The laser is designed to operate at 500 kHz repetition rate delivering pulses of 16 ps FWHM length with 1 $\mu$J pulse energy at 263 nm wavelength [4]. The repetition rate of the laser can be reduced for alignment and beam diagnostics measurements. This laser serves two operation modes at high bunch charge. A second laser is under development for operation of the injector at higher repetition rate (13 MHz) with a reduced bunch charge of 77 pC. The three main operation modes of the injector are summarized in Tab.1. The photocathode is made of $Cs_2Te$

| | ELBE | HC | FEL |
|---|---|---|---|
| RF frequency | | 1.3 GHz | |
| Beam energy | | 9.5 MeV | |
| Operation | | CW | |
| Drive laser | | 263 nm | |
| Photocathode | | $Cs_2Te$ | |
| Pulse length FWHM | 5 ps | 16 ps | 50 ps |
| Repetition rate | 13 MHz | 500 kHz | 1 kHz |
| Bunch charge | 77 pC | 1 nC | 2.5 nC |
| Trans. emittance | 1.5 $\mu$m | 2.5 $\mu$m | 3 $\mu$m |

Table 1: Design beam parameters of the three main operation modes: ELBE FEL, at high bunch charge (HC) and BESSY FEL (FEL).

with a quantum efficiency of better than 1 %. This cathode is placed at the entrance of a 3 1/2 cell cavity structure with a RF frequency of 1.3 GHz. The axis peak field of the accelerating mode is 50 MV/m (design value). The cavity structure is embedded in a liquid helium tank. At the exit of the SRF gun the electron beam is focused with a solenoid magnet. After that, the electrons pass the transfer section preparing the beam parameters for injection into the ELBE linac. Behind this section the diagnostics beamline is located, and the beam parameters will be measured.

## BEAM CHARACTERIZATION

In order to characterize the performance of the photoinjector, the following beam parameters need to be considered:

- The energy distribution of the beam – the kinetic energy of the electrons and the energy spread. The beam momentum will vary between a few and 9.5 MeV. The minimum momentum spread as expected from simulations will be 36 keV for the low charge operation mode.
- The total beam intensity, together with the time structure. The bunch charge can vary between a few pC

* kamps@bessy.de

# STRIPLINE DEVICES FOR FLASH AND EUROPEAN XFEL

M. Dehler, G. Behrmann, Paul Scherrer Institut, Villigen PSI, Switzerland
S. Vilcins, M. Siemens, DESY, Hamburg, Germany

*Abstract*

A prototype fast intra-bunch train feedback system is currently under development which is to be tested at FLASH. For pickups as well as kickers, stripline devices have been developed. The new pickup is based on earlier designs used in the transfer lines of the Swiss Light Source as well as in the proton cyclotron PROSCAN at PSI; in particular, the stripline electrode output coupling is intentionally mismatched in order to increase the shunt impedance seen by the beam. Two versions have been designed for a center frequency of 1.65 GHz and a loaded Q of 35. Prototypes have been fabricated and built into FLASH. The stripline kicker consists of four main elements (all in-vacuum): two stripline electrodes fabricated from extruded aluminum and two metallic ground planes, held in place by ceramic spacers. The latter reduce the mutual inductance between the electrodes and optimize the RF match for asymmetries in the RF feed. Prototypes have been built, measured in the lab, and are now in the process of being installed into FLASH.

## INTRODUCTION

As part of the Swiss contribution to the European XFEL project, the Paul Scherrer Institut is developing the prototype of an intra-bunch train. The feedback system has to correct for fast transverse orbit fluctuations within the bunch train, which are due to causes as beam loading and wake fields. Each plane, horizontal and vertical, has a dedicated system consisting of two upstream pickups for the measurement, two kickers for the correction of offsets, followed by a pair of downstream pickups used to calibrate the feedback gain. The electric signal chain consists of an analog RF front end, which down converts the pickup signals to base band, a fast, FPGA based, digital processing board with ADC and DAC mezzanines for the signal conversion, and high power broad band RF amplifiers feeding the kickers. For the European XFEL, two sets of systems are foreseen, one working after the injector region at 150 MeV and the other at the end of the main LINAC at 18 GeV (For more information on the general layout see [1]).

## KICKER

The bunch distance within the bunch train is 200 ns; this time period should be matched by the total latency of the feedback system. Within the latency budget, a maximum fill time of 10 ns is foreseen for the kickers – a choice, which a priori excludes alternative options such as air coils. This requirement would lead to a maximum design length of 3 meters for a strip line kicker. For the prototype, we plan to replace existing stripline kickers at FLASH with the new designs, thus to be compatible an even shorter overall length of 1 meter was chosen.

Table 1: Kicker Specifications

| | |
|---|---|
| Active length | 1000 mm |
| Total length | 1030 mm |
| Beam pipe diameter | 34 mm |
| Bandwidth | 50 MHz |
| Kick (P = 1W/port) | 1 keV/c |
| Input impedance (differential mode) | 50 Ω |
| Input impedance (common mode) | 61 Ω |

The required bandwidth, on the order of 2.5 MHz (coming from the 200 ns bunch spacing), is no problem given the fact that latency requirements lead to a far larger value. Table 1 gives an overview of the specifications.

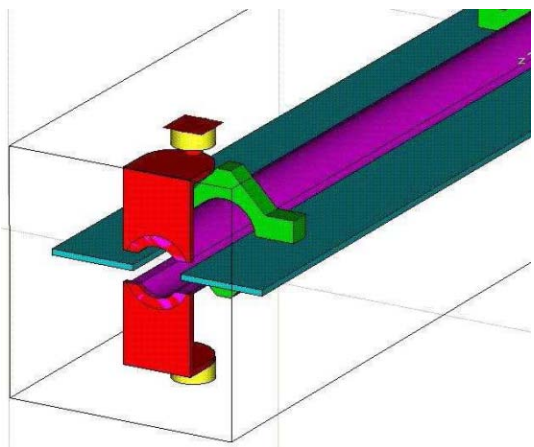

Figure 1: Front part of electrode assembly

The electrode assembly shown in figure 1 is a self supporting structure consisting of a pair of electrodes and two ground plates clamped together using ceramic spacers. The aluminum striplines are manufactured by extrusion in order to minimize twist and sag. Thus, an excellent stability and tolerance of the assembly is guaranteed.

The kicker is operated in differential mode with the electrodes at opposite polarity, the characteristic impedance seen by the amplifiers being 50 Ω. Phase and amplitude imbalances will show up as an additional common mode signal. This signal component itself is no problem for the beam itself, since it induces only a very minor longitudinal acceleration for the beam. The challenge lies in the mismatch at the input – for a standard electrode assembly without ground plates, the characteristic impedance is quite

# MEASUREMENTS AND ANALYSIS OF LONGITUDINAL HOM DRIVEN COUPLED BUNCH MODES IN PEP-II RINGS *

T. Mastorides†, C. Rivetta‡, J.D. Fox, D. Van Winkle
Stanford Linear Accelerator Center
Stanford, CA 94309, USA

*Abstract*

The growth rates of the longitudinal higher-order impedance-driven beam modes have greatly increased since the initial PEP-II design and commissioning. This increase is attributed to the addition of 6 1.2MW RF stations with 8 accelerating cavities in the HER and 2 1.2MW RF stations with 4 accelerating cavities in the LER, which allowed operations at twice the design current and almost four times the luminosity. As a result, the damping requirements for the longitudinal feedback have greatly increased since the design, and the feedback filters and control schemes have evolved during PEP-II operations.

In this paper, growth and damping rate data for the higher-order mode (HOM) driven coupled-bunch modes are presented from various PEP-II runs and are compared with historical estimates during commissioning. The effect of noise in the feedback processing channel is also studied. Both the stability and performance limits of the system are analyzed.

## LONGITUDINAL INSTABILITIES

The PEP-II rings have exhibited coupled-bunch longitudinal instabilities since commissioning. The longitudinal instabilities in PEP-II are driven by two impedance sources: cavity fundamental and cavity HOM. The LLRF systems use direct and Comb loop feedback to reduce the effective impedance of the cavity fundamental. To further damp these instabilities two additional feedback systems are used: the Low Group Delay Woofer (LGDW) and the Longitudinal Feedback (LFB).

The band limited LGDW addresses the beam motion from in-cavity low-order modes via a signal from a beam pick-up and control paths through the RF stations [1], [2]. The cavity fundamental driven beam modes have been studied and predictions for higher currents, including studies of different configurations have been presented [3], [4].

The LFB is a wideband bunch by bunch channel that addresses all modes via a digital control filter and broadband longitudinal kickers. The LFB is needed to control instabilities from the cavity HOM impedance. It is a Digital Signal Processing (DSP) based flexible programmable system that can run FIR or IIR filters. A block diagram of the LFB system is shown in Figure 1.

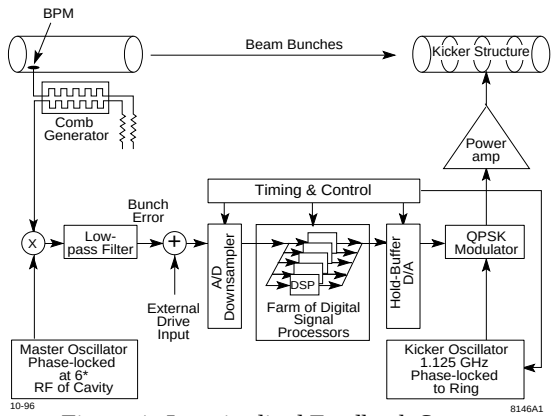


Figure 1: Longitudinal Feedback System.

This paper uses machine measurements in HER and LER to quantify the HOM driven growth rates, quantify the achieved performance of the broadband feedback, and highlight the performance limits in the systems as constructed [5].

## HOM-DRIVEN MODES: GROWTH AND DAMPING RATES

During the PEP-II design and commissioning, the impedance driving beam instabilities was estimated from cavity measurements [6]. The impedance estimates allowed calculations of the expected growth rates for the HOM driven coupled-bunch modes, as shown in Figure 2 from [7]. The growth rates were calculated during commissioning for the design parameters of 1 A and 20 cavities for the HER and 2.25 A and 4 cavities for the LER. From this

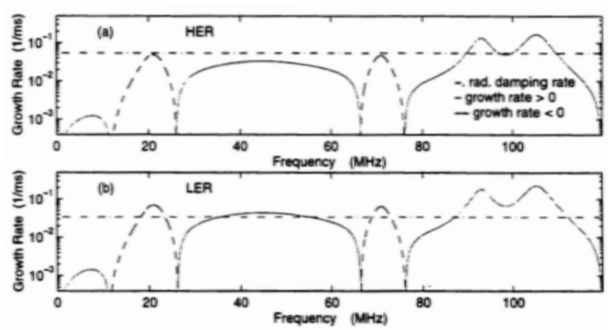


Figure 2: Growth Rate Estimates from Impedance Measurements for 1 A HER, 2.25 A LER.

figure one can see that there are two bands that excite instabilities. The strongest is a 9 MHz wide band that is aliased at around 105 MHz (mode 770) from the 238 MHz sampling and drives roughly 65 beam modes. The second band

* Work supported by the U.S. Department of Energy under contract # DE-AC02-76SF00515

† themis@slac.stanford.edu
‡ rivetta@slac.stanford.edu

# SUPPRESSION OF LONGITUDINAL COUPLED-BUNCH INSTABILITIES AT THE KEK-PF

T. Obina#, M. Tobiyama, T. Honda, M. Tadano, J. W. Flanagan, T. Mitsuhashi,
KEK, 1-1 Oho, Tsukuba, Ibaraki 305-0801, Japan
W. X. Cheng, J. D. Fox, SLAC, Menlo Park, CA, U.S.A
D. Teytelman, Dimtel Inc., San Jose, CA, U.S.A.

*Abstract*

A bunch-by-bunch feedback system has been developed to suppress longitudinal coupled-bunch instabilities at the KEK-PF. A longitudinal kicker based on a DAFNE-type overdamped cavity has been designed and installed in the ring, and a general purpose signal processor, called iGp, has been developed by the collaboration of the KEK, SLAC, and INFN-LNF. The entire feedback loop has been closed by the end of June 2007, and the feedback system has successfully suppressed the longitudinal dipole-mode instabilities up to 430 mA.

## INTRODUCTION

The Photon Factory electron storage ring at the KEK is a dedicated synchrotron radiation (SR) source with an energy of 2.5 GeV. The ring is operated in both single- and multibunch modes. In both cases, longitudinal oscillations starting from very low currents are observed. In the single-bunch operation, the phase noise of a low-level RF circuit excites synchrotron oscillations of the bunch. In the multibunch operation, several coupled-bunch modes of instabilities are observed above 50 mA. Cavity-like structures in the storage ring are suspected to be the source of the instabilities, although the sources have not been determined thus far.

Phase modulation of the RF acceleration frequency at twice the synchrotron frequency ($2f_s$) can suppress the longitudinal instabilities considerably [1]. This easy and inexpensive technique has been utilized during SR user operation for years because this method is very effective not only in suppressing the instabilities, but also for increasing the beam lifetime, approximately by a factor of 1.5. The enhancement of the beam lifetime is desirable for many users. However, phase modulation increases the energy spread of the bunch. The effect is apparently observed in some insertion device beamlines at the dispersive section of the storage ring. In these beamlines, the intensity of the input SR fluctuates depending on the status of the RF phase modulation. In order to stabilize these fluctuations, a longitudinal feedback system has been developed and a feasibility study on top-up injection, which is indispensable for the compensation of a short beam lifetime, has been carried out.

The main parameters of the PF-Ring and the bunch-by-bunch feedback system are listed in Table 1.

Table 1: Main parameters of PF-Ring.

| | | |
|---|---|---|
| RF frequency [$f_{RF}$] | 500.1 | MHz |
| Harmonic number | 312 | |
| Revolution frequency [$f_{rev}$] | 1.6029 | MHz |
| Synchrotron tune [$\nu_s$] | 0.014 | |
| Longitudinal damping rate | 0.256 | $ms^{-1}$ |
| Beam current (single/ multi) | 70 / 450 | mA |

## FEEDBACK SYSTEM

The feedback system is composed of a front-end detection unit, a signal processing unit, and a corrector unit. The block diagram of the feedback system is shown in Fig. 1.

### *Front-end Detection Circuit*

The output signals from two button-type pickup electrodes are summed by a hybrid (M/A-COM, model H-8) to cancel the transverse beam position dependence. A low-noise amplifier (LNA) is connected to a band-pass filter (BPF), which consists of three delay cables and a power combiner/splitter. The longitudinal position is detected with respect to the RF acceleration signal by synchronous detection at three times the RF frequency. The highest detection frequency is limited by the cutoff frequency of the vacuum chamber, approximately 1.8 GHz.

Though it is possible to change the RF detection phase (indicated as $\Delta\phi$ in the figure) along the bunch train, a constant phase is maintained (DC) because the difference in the synchronous phase between the head and the tail of the bunch train is not large even at 450 mA. A trombone delay adjusts the timing of the input signal and the clock of the ADC.

### *Digital Signal Processor*

A general purpose signal processor, called the iGp, has been developed by a collaboration of the KEK, SLAC, and INFN-LNF [2,3]. iGp provides real-time baseband signal processing at an RF frequency of 500 MHz for 312 bunches at the PF. The longitudinal position of each bunch is digitized by an 8-bit ADC, processed by a 16-tap finite impulse response (FIR) filter, and transmitted to a DAC after an appropriate delay is introduced. The complete signal processing is sufficiently fast compared to the revolution time of the PF-Ring. A digital filter is implemented by using a field-programmable gate array (FPGA). The FPGA also provides a number of other

#takashi.obina@kek.jp

# LOCALIZATION OF NOISE SOURCES IN THE APS STORAGE RING USING THE REAL-TIME FEEDBACK SYSTEM *

Xiang Sun# and Glenn Decker, ANL, Argonne, IL 60439, U.S.A.

*Abstract*

There are two parallel feedback systems to correct the transverse orbit at the Advanced Photon Source (APS) storage ring: a real-time feedback (RTFB) system [1] that runs at 1.5 kHz using 38 fast correctors and up to 160 beam position monitors (BPMs), and a DC feedback system that runs at 10 Hz using up to 317 correctors and over 500 BPMs. An algorithm that uses the open-loop beam motion data to spatially locate strong noise sources in the storage ring is described. The orbit data are measured with 1.5-kHz data acquisition associated with the RTFB system. This system is limited to collecting 40 time-series waveforms synchronously. If synchronous data for the whole ring could be collected, source identification would be straightforward, because a sample-by-sample orbit could be reconstructed with the inverse response matrix. Since this is not the case, a synchronization procedure was developed allowing the splicing together of spatially overlapping double-sector single-frequency trajectories. This technique is applicable to narrow-band noise sources. By multiplying the truncated pseudo-inverse response matrix of the APS storage ring by the synchronous orbit data at a fixed frequency, noise sources at a fixed frequency can be located. The experiment and calculation results are presented.

## INTRODUCTION

The real-time orbit feedback system is implemented digitally using digital signal processors (DSPs) [2,3] and consists of 21 VME crates – 1 master and 20 slaves. The 20 slave VME crates are distributed around the circumference of the 40-sector APS storage ring to manage interfaces to BPMs and correctors, and to compute orbit corrections. The master crate provides global controls to the other 20 slave crates and provides analysis tools such as "DSP scope," which works like a digital oscilloscope. The DSP scope can collect 40 channels synchronously, and each waveform has up to 4080 data points with 1.5 kHz sample rate.

While beam stability at the APS is quite good, there are a significant number of narrow-band spectral lines resulting in elevated levels of beam motion [4,5]. The problem comes from some potential spatially discrete, relatively strong sources of noise.

*Work supported by U.S. Department of Energy, Office of Science, Office of Basic Energy Sciences, under Contract No. DE-AC02-06CH11357

#xiang@aps.anl.gov

If one considers a full response matrix mapping all possible sources to all BPMs, a time series approximating each of these noise sources can be estimated by pseudo-inverting the full matrix and multiplying the orbit data that is collected synchronously.

The method for localizing narrow-band noise sources is described below. As a test case, a fast corrector in APS sector 10 was driven with a sine wave at 18.049 Hz. Because DSP scope collects only 40 waveforms at a time, it is not possible to collect data for the entire ring simultaneously. However, a synchronization procedure has been developed that results in a fixed-frequency orbit for the whole ring. After multiplying by the pseudo-inverse response matrix, the location of the known noise source can be reconstructed. This procedure was carried out driving both horizontally and vertically. Having validated the method, the same procedure was applied to a number of examples of unknown narrow-band noise sources.

## EXPERIMENT AND CALCULATION TO LOCALIZE NOISE SOURCES

### *Measurement of the Orbit Changes*

We measured the AC orbit by using as many BPMs as possible with the DSP scope tool's double-sector BPM acquisition function with the RTFB loop open. The double-sector BPM acquisition function synchronously collects 40 BPM waveforms at 1.5 kHz. This allows waveforms from ten BPMS per sector horizontally and vertically for two sectors to be acquired. Two such data sets with an overlapping sector can be synchronized with each other by making use of a common spectral line as a type of clock, provided that the spectral line is reasonably stable. By collecting 40 overlapping double-sector data sets in this fashion, one can reconstruct two complete orbits for the 40-sector ring.

We drove the fast correctors S10A:H3 and S10A:V3 separately with a sine wave at 18.049 Hz as a known strong source. The corresponding orbit changes were inferred from 1.5-kHz DSP scope data for 375 different BPMs. This test case was used to validate our method of narrow-band source localization. After stopping the 18.049-Hz excitation, we measured the ambient orbit motion with DSP scope at a 153-Hz sample rate to localize potential narrow-band noise sources in a lower frequency band. All of these measurements were conducted open loop: neither AC nor DC orbit correction systems were active.

# ALS FPGA-BASED TRANSVERSE FEEDBACK ELECTRONICS*

J. Weber, M. Chin, LBNL, Berkeley, CA, U.S.A.

*Abstract*

The Advanced Light Source Transverse Feedback System currently consists of a refrigerator sized analog delay line system. The new system is the 2nd generation Transverse Feedback System, derived from work done for PEP-II in 2004 [1]. It uses the latest generation Virtex-5 FPGA, and has 12-bit ADCs and DACs for bunch-bunch feedback at 500MHz. In addition, this system provides networked capability for setup and diagnostics.

## INTRODUCTION

At the ALS, coupled bunch instabilities are driven by the RF cavity dipole higher order modes (HOMs) and the resistive wall impedance of the vacuum chamber [2]. The existing ALS Transverse Feedback (TFB) System adequately damps these beam oscillations, but does not provide any diagnostic information or remote control capability. Recent experiences using an ADC-FPGA-DAC architecture for bunch-by-bunch feedback systems have proven largely successful. These digital systems provide extensive diagnostic capability with deep memory capable of storing hundreds of turns of bunch data. Set points and diagnostic data can be transferred to and from the system via the control system network.

The existing TFB electronics consist of two microwave receivers for detecting horizontal and vertical moment, a system (shown as two variable attenuators) for mixing the signals from the two pickup stations, a delay, and a power amplifier for driving the kicker [2]. The electronics upgrade replaces the delay element (currently a long cable) with an FPGA-based digital system. Figure 1 shows the diagram of the upgraded electronics.

The new digital system will be based on the model of the PEP-II TFB upgrade [1]. Using the latest technology, the system is capable of feedback at the full ALS bunch rate of 500MHz. Data converters with 12-bit resolution clocked at 500MHz (effective) sample the pickups and drive the kicker outputs for bunch-by-bunch feedback. The Xilinx® Virtex™-5 LX50 FPGA provides filter, delay, data capture, and control system interface functions. This paper describes the design details of the new ALS TFB electronics.

## HARDWARE

The new TFB system electronics consist of a two board set: a commercial FPGA evaluation board connected via a high-speed connector interface to a custom in-house designed board containing the high-speed analog interfaces. The block diagram for the TFB hardware is shown in Figure 2.

* This work was supported by the U.S. Department of Energy, under Contract No. DE-AC03-76SF00098

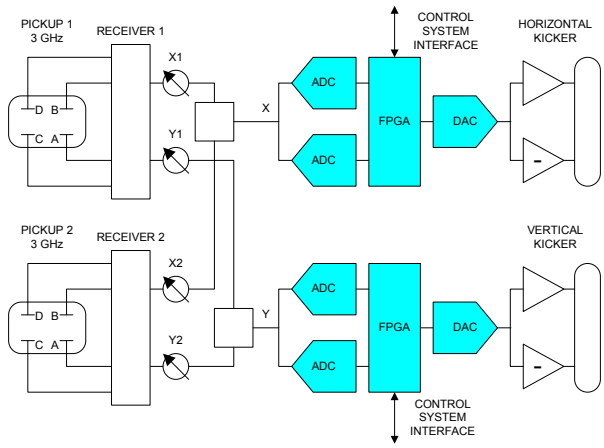


Figure 1: ALS Transverse Feedback Electronics.

The demo board chosen for this design is the Xilinx® Virtex™-5 LX Evaluation Kit from Avnet. This board contains many of the desired system components including a V5LX50 FPGA, EXP high-speed expansion connectors, 64MB DDR2 SDRAM, 16MB Flash Memory, and Ethernet PHY [3]. The FPGA contains sufficient programmable logic resources for the desired functionality and runs comfortably at the required clock speed of 250MHz. The EXP expansion connectors are controlled impedance Samtec QSE/QTE series connectors specified to run up to 750MHz for differential signals [4]. These connectors provide sufficient I/O to connect the FPGA to the high speed 12-bit data converters and other interfaces on the custom EXP daughter card. The SDRAM contains the software code to run the control system interface and the memory used for data capture diagnostics. The Flash Memory provides flexible boot options for the control system software. The Ethernet interface allows connectivity with the ALS Control System network.

The custom board is an EXP expansion daughter board that contains the high-speed data converters, clock distribution and programmable delay, and a moderate performance two-channel 16-bit DAC to set the kicker amplifier gains. Two 12-bit LTC2242-12 ADCs, sampling at $f_{RF}/2$ = 250Msps 180 degrees out of phase, sample the pickup signals on every bunch. The pickup data is transferred to the FPGA, clocked at 250MHz, which calculates the correction value to apply to the kickers on the two separate data paths. The correction data is fed through the FPGA DDR output buffers to the DAC at 500 MHz. The 12-bit MAX5886 DAC provides correction output to the kickers at 500Msps. This custom board receives the 500MHz bunch rate clock from the ALS timing system and divides and distributes it to the FPGA, DAC, and ADCs. Two MC100EP195 programmable clock delay chips can be used to fine tune the DAC and ADC clocks in 10ps increments over a 10ns range.

# STREAK-CAMERA MEASUREMENTS WITH HIGH CURRENTS IN PEP-II AND VARIABLE OPTICS IN SPEAR3*

Weixing Cheng,# Alan Fisher, and Jeff Corbett
Stanford Linear Accelerator Center, 2575 Sand Hill Road, Menlo Park, CA 94025

*Abstract*

A dual-axis, synchroscan streak camera was used to measure longitudinal bunch profiles in three storage rings at SLAC: the PEP-II low- and high-energy rings, and SPEAR3. At high currents, both PEP rings exhibit a transient synchronous-phase shift along the bunch train due to RF-cavity beam loading. Bunch length and profile asymmetry were measured along the train for a range of beam currents. To avoid the noise inherent in a dual-axis sweep, we accumulated single-axis synchroscan images while applying a 50-ns gate to the microchannel plate. To improve the extinction ratio, an upstream mirror pivoting at 1 kHz was synchronized with the 2kHz MCP gate to deflect light from other bunches off the photocathode. Bunch length was also measured on the HER as a function of beam energy. For SPEAR3 we measured bunch length as a function of single-bunch current for several lattices: achromatic, low-emittance and low momentum compaction. In the first two cases, resistive and reactive impedance components can be extracted from the longitudinal bunch profiles. In the low-alpha configurations, we observed natural bunch lengths approaching the camera resolution, requiring special care to remove instrumental effects, and saw evidence of periodic bursting.

## INTRODUCTION

The Stanford Linear Accelerator Center (SLAC) has a long history of both high-energy physics (HEP) and synchrotron radiation (SR) research with storage rings. Recently, PEP-II and SPEAR3 (Table 1) together purchased a Hamamatsu C5680 streak camera with ~2-ps resolution, digital image capture, and dual-axis synchroscan sweeping to measure bunch length, characterize impedance, and observe beam instabilities.

### *PEP-II*

The PEP-II *B* Factory completed its final run on April 7, 2008. Since the first beam in 1997, the PEP rings have run at a center-of-mass energy of 10.58 GeV, the Y(4S) resonance. Electrons at 8.97 GeV in the high-energy ring (HER) collide with 3.12-GeV positrons in the low-energy ring (LER) to produce $B\overline{B}$ pairs moving in the lab frame. For the final months of the 2008 run, the HER energy was shifted to collide at the 2S (10.02 GeV) and 3S (10.36), and then scanned up from just below the 4S to 11.2 GeV. This provided an opportunity to measure bunch length over a range of HER energies from 8.02 to 10.08 GeV.

Each PEP-II ring has a synchrotron-light monitor (SLM) observing visible dipole radiation [1]. The LER SLM collects positron emission from a dipole 30 m downstream of the interaction point (IP), while the HER SLM collects electron emission from an arc dipole. At each SLM, in-tunnel CCD cameras record beam images and interferometer fringes [2], and a visible-light transport line brings part of the beam to a focused image in an optics hutch outside the shielding wall for more sophisticated time-resolved cameras [3,4].

In the last year of PEP-II operations, the new streak camera was first installed in the LER hutch to resolve bunch-length discrepancies observed in 2004 when comparing a quick series of measurements with a borrowed streak camera to the high-frequency roll-off of the bunch spectrum [3]. The camera was then moved to the HER to track bunch length during the energy scan.

Since the beams collide at high current—typically 1.75 A in the HER and 2.6 A in the LER, for a peak luminosity of $1.0\times10^{34}$ $cm^{-2}s^{-1}$—the gradual increase in beam loading following the 100-ns abort gap in the fill pattern causes a shift in synchronous phase, so that bunches further along the train arrive earlier in the RF period. At high-currents, the transient from first to last bunch is comparable to the natural rms bunch length (~40 ps in the LER). To measure bunch length without folding in the phase shift of the entire train required dual approaches to select a narrow interval: an electronic gate of the camera's microchannel plate (MCP), and an oscillating mirror that synchronously steers the light across the entrance optics.

### *SPEAR3*

SPEAR3 is a 3-GeV storage-ring light source delivering UV to x-ray radiation into 13 beam lines (~30 branch lines) in a 500 mA, multi-bunch mode. The machine lattice was recently adjusted from achromatic (zero-dispersion) to finite-dispersion optics to reduce horizontal emittance, and tests have begun on low-momentum-compaction (low-$\alpha$) lattices for dynamical pump-probe experiments. The SLM at SPEAR3 receives unfocused

Table 1: Key PEP-II and SPEAR3 parameters.

| | PEP-II | | SPEAR3 |
|---|---|---|---|
| | HER | LER | |
| Energy (GeV) | 9 (8–10)* | 3.12 | 3 |
| $f_{RF}$ (MHz) | 476 | 476 | 476.315 |
| Harmonic No. | 3492 | 3492 | 372 |
| Bunches** | 1722 | 1722 | 280 |
| Spacing (ns) | 4.2 | 4.2 | 2.1 |

* Energy varies during the CM-energy scan.

** Typical multi-bunch fill. PEP-II fills every 2nd bucket outside a 100-ns abort gap. SPEAR3 fills every bucket, with a single bunch in a 100-ns ion clearing gap.

* Work sponsored by U.S. Department of Energy Contract DE-AC03-76SF00515 and Office of Basic Energy Sciences, Division of Chemical Sciences.

# chengwx@slac.stanford.edu

# DIFFRACTION EFFECTS IN COHERENT TRANSITION RADIATION DIAGNOSTICS FOR SUB-MM BUNCH LENGTH MEASUREMENT*

T. J. Maxwell, D. Mihalcea, Northern Illinois University, DeKalb, IL 60115, U.S.A.
P. Piot, Northern Illinois University, DeKalb, IL 60115, and Fermilab, Batavia, IL 60510, U.S.A.

*Abstract*

Electrons crossing the boundary between different media generate bursts of transition radiation. In the case of bunches of N electrons, the radiation is coherent and has an N-squared enhancement at wavelengths related to the longitudinal bunch distribution. This coherent transition radiation has therefore attracted attention as an interceptive charged particle beam diagnostic technique. Many analytical descriptions have been devised describing the spectral distribution generated by electron bunches colliding with thin metallic foils making different simplifying assumptions. For typical bunches having lengths in the sub-millimeter range, measurable spectra are generated up into the millimeter range. Analysis of this THz radiation is performed using optical equipment tens of millimeters in size. This gives rise to concern that optical diffraction effects may spread the wavefront of interest into regions larger than the optical elements and partially escape detection, generating a wavelength-dependent instrument response. In this paper we present a model implementing vector diffraction theory to analyze these effects in bunch length diagnostics based on coherent transition radiation.

## INTRODUCTION

Relativistic electrons impinging on a metallic foil emit transition radiation (TR) as they move from one medium to the next. In the case where a bunch of electrons is incident on the foil, the slight time delay in the arrival of the charges at the foil introduces a phase delay between emission of this TR. Summing contributions to the emitted electromagnetic radiation of the individual charges over the length of the bunch, one finds for the emitted radiation spectrum

$$I(\omega) = N^2 I_e(\omega) f(\omega) \qquad (1)$$

Here $N$ is the number of charges in the bunch and $I_e(\omega)$ is the power spectrum for single electron TR. We assume $N$ to be very large and leave in explicit dependence of the emitted TR spectrum on frequency. The last term $f(\omega)$ is referred to as the form factor of the bunch. For highly relativistic bunches under a one-dimensional line charge assumption, this is given roughly by

$$f(\omega) = \left| \int \rho_{long}(t) \exp(i\omega t) \right|^2 \qquad (2)$$

In principle, this $N$-squared-enhanced coherent transition radiation (CTR) provides a signal strong enough to detect for sufficient bunch charge. However, analysis of the CTR spectrum emitted by beams with typical bunch lengths $\sigma_z$ on the order of hundreds of micrometers, one must also consider the possibility of diffraction losses in any optical system used for spectral analysis due to the long coherence wavelengths. The goal of this research is to determine the response function $R(\omega)$ of such optical systems and the single-electron TR frequency dependency such that one can correct the modified equation

$$I_{Measured}(\omega) = N^2 I_e(\omega) f(\omega) R(\omega) \qquad (3)$$

to recover the mod-squared Fourier transform of the longitudinal bunch distribution $f(\omega)$ from the measured signal.

## SIMULATION

Extending previous work [1, 2] our approach is based on simulating ideal wavefront generation and propagation. Our model treats the radiation emitted at TR generation as the exact reflection of the relativistic electron's light-like electromagnetic field from the surface of the foil to generate $\vec{E}_e(\omega)$. At present the foil is treated as an ideal reflector, neglecting dielectric properties. Another approach to ensure proper treatment of the near-field electromagnetic radiation emission for low-energy electrons has been recently suggested in [3].

This source electromagnetic wave is then propagated through the optical system from one surface to the next using a fully three-dimensional vector diffraction integral as derived in [4]. While computationally expensive, this approach has demonstrated great accuracy over a wide variety of aperture size, diffraction distance, and wavelength ranges while preserving the detailed information necessary for reflections off of complex three-dimensional surfaces such as parabolic mirrors. Other methods have been suggested for accounting for these near-field phenomena via fast Fourier transform [5].

In taking this brute force approach to solving the diffraction problem, several enhancements have been added. The entire code is written in C++ and currently operates in a parallelized MPICH2 implementation. To work around the difficulty integrating over the electron's cusped source function in particular, the Cuba 1.4 [6] integration package has been added. Using Cuba's Cuhre adaptive cubature integrating routine, precision control over source integration to fix the overall energy scale of emitted TR wavefronts has been achieved and are in agreement with values predicted elsewhere [5].

Various benchmarks have been performed including comparison to other near-field ($D < \lambda \gamma^2$) TR predictions

*Work supported by US. Department of Energy, under Contract No. DE-FG02-06ER41435 with Northern Illinois University

# PROTOTYPE LASER EMITTANCE SCANNER FOR SPALLATION NEUTRON SOURCE (SNS) ACCELERATOR*

J. Pogge, Igor Nesterenko, Alexander Menshov, Dong-O Jeon, SNS Oak Ridge National Laboratory, Oak Ridge, Tennessee 37831, USA

## ABSTRACT

Taking advantage of recent successes with the Laser Wire, a new prototype is being built to use the laser wire as both a profile monitor and a slit for an emittance measuring device. This improved system takes advantage of the steering dipole magnet prior to ring injection of SNS such that only the recently stripped $H_0$ protons continue forward to the emittance device. In this way we hope to make an emittance device that is both parasitic to neutron production and is capable of accurate measurements during full-power applications.

## INTRODUCTION

As spallation neutron sources have demonstrated increasing power, it has become necessary to accurately measure the transverse phase-space distribution (emittance) of the $H_0$ beam prior to introduction into the storage ring. The high power of the proton beam and the necessity for non-destructive measurements make the use of a laser profile monitor as the emittance scanner slit especially attractive by replacing the more common and well known slit-grid (slit-harp) [1] mechanism used in lower power emittance measurements. The basic principal has been demonstrated in experiments with energies higher than 600 MeV [2,3,4]. This device will attempt to achieve results with a proton beam with energies as high as 1.4 GeV. The system is divided into two sections: the Laser Profile Monitor (LPM) and the Emittance Collection Device (ECD). The LPM is similar in capability to that of previous laser wire devices [5,6]. Specifications for this LPM are found in the following table.

Table 1. Laser Profile Monitor Specifications

| | | |
|---|---|---|
| X – Y Range | +/- 32 mm | 100nm resolution |
| Laser /H- intersection | 20 – 40 um | 3% neutralization |
| Laser Energy | 50 mJ | 10 - 20 nS pulse |
| H- Beam | 1.4 GeV | 60 Hz |

## ENGINEERING CHALLENGES

The SNS Laser Emittance Scanner design takes advantage of the first dipole steering magnet in the ring injection section to separate the $H^-$ representing 97% of the produced beam, from the recently generated $H_0$, 3% stripped by the LPM device. The primary LPM location also contains vacuum pumps, gate valves, and a key access point for moving equipment in and out of the tunnel in the HEBT section of the SNS accelerator. The design will be significantly more compact than its predecessor Laser Wire design used in 14 locations throughout the superconducting LINAC at SNS. This is primarily to allow for quick installation and removal of the LPM. The relatively low power of the separated $H_0$ allows the designers to evaluate either a scintillator camera device and a more traditional scanning harp assembly for the actual emittance collection system. This collection device will be located downstream in the LINAC dump area of the SNS accelerator approximately 11 meters from the LPM.

## IMPROVED OPTICAL DESIGN

The prototype LPM under construction at SNS (Fig. 1) uses an improved optical system to increase repeatability and accuracy of the scanning optics with a decrease in overall size.

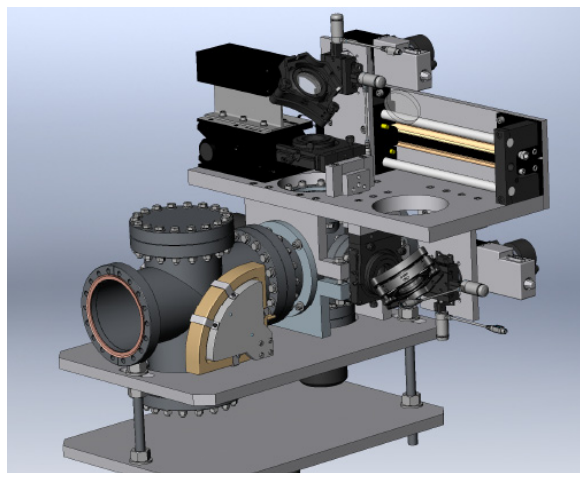

Figure 1: Improved LPM at SNS.

The new LPM also incorporates an embedded 50 mJ 1064 nm Nd:Yag pulsed laser, dramatically reducing the complexities of laser delivery to the optical scanning system. Stepper driven linear stages have been replaced with fixed angular scanning mirrors that have been precisely aligned and locked down prior to

# LANSCE-R INVESTIGATION: IMPROVING THE WIRE SCANNER MOTION CONTROL*

J. Sedillo, J. D. Gilpatrick, F. Gonzales, J. Power, LANL, Los Alamos, NM 87545, U.S.A.

*Abstract*

The LANSCE accelerator facility utlizes 110 wire scanner devices to monitor the accelerator's charged particle beam. The LANSCE facility's existing wire scanner control systems have remained relatively unchanged since the LANSCE accelerator became operational in the 1970's. The evolution of motion control technologies now permits the development of a wire scanner motion control system that improves in areas of energy efficiency, precision, speed, resolution, robustness, upgradeability, maintainability, and overall cost. The purpose of this project is to research the capabilities of today's motion control products and analyze the performance of these products when applied to a wire scanner beam profile measurement. This experiment's test bed consists of a PC running LabVIEW, a National Instruments motion controller, and a LEDA (Low Energy Demonstration Accelerator) actuator. From this experiment, feedback sensor performance and overall motion performance (with an emphasis on obtaining maximum scan speed) has been evaluated.

## INTRODUCTION

The Los Alamos Neutron Science Center (LANSCE) accelerator facility wire scanner system utilizes actuators and electronics that have existed since the accelerator's inception. The existing control system utilizes a motor drive that was developed and manufactured at LANSCE and is controlled directly by the LANSCE Operations Computers through LANSCE's Remote Instrumentation and Control Equipment (RICE) system. No feedback is employed for actuator positioning. Instead, wire scanner actuator position sensors are utilized to gauge the health of the actuator mechanics. The purpose of this study is to evaluate a previously utilized actuator, motor driver, and motion controller from the Low-Energy Demonstration Accelerator (LEDA) experiment to evaluate actuator movement performance and feedback sensor position accuracy. Furthermore, a resolver was also added so that its performance could be determined on this actuator.

## SYSTEM DESCRIPTION

In order to evaluate sensor/actuator performance, we assembled a system utilizing a LEDA (Low Energy Demonstration Accelerator) wire scanner actuator powered by a Parker GT Stepper Drive. The motion was controlled by a PCI-7344 motion controller card within a Windows-based PC running LabVIEW. The

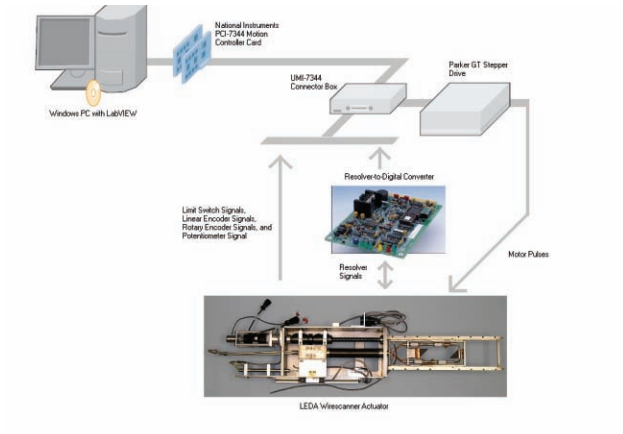


Figure 1: System Schematic

potentiometer and linear encoder maintained their original configuration of being coupled to the translational movement of the actuator. Furthermore, the rotary encoder maintained its original position as being coupled to the shaft of the stepper motor. A resolver was later added behind the rotary encoder and, like the rotary encoder, was directly coupled to the motor shaft. Details are shown in figure 2.

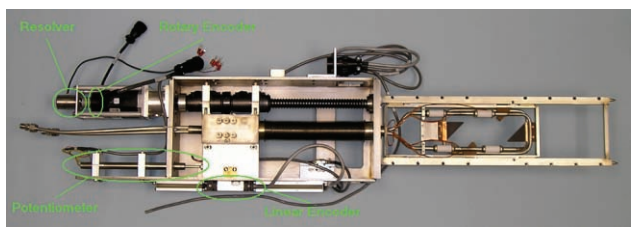


Figure 2: LEDA Wire Scanner Actuator with sensors highlighted

## POSITION SENSOR TYPES UTILIZED

### *Linear Encoder*

This sensor measures linear displacement through the use of a patterned film, two LED's, and two infrared photosensors. The pattern blocks the LED light in such a way that a quadrature signal is output from the sensor. This signal is used by the motion controller to detect sensor movement and direction. Although this sensor has a high degree of precision, the presence of semiconductor components in its manufacture increases its susceptibility to damage from ionizing radiation.

*Work supported by the United States Department of Energy.

# SPACE CHARGE WAVES AS A DIAGNOSTIC TO MEASURE TRANSVERSE BEAM SIZE OF SPACE CHARGE DOMINATED BEAMS

Jayakar C.T. Thangaraj* D.W. Feldman, R.A. Kishek, S. Bernal, M. Reiser, D. Stratakis,
R.Feldman, D. Sutter, B. Beaudoin, C.Papadopoulos, I. Haber, P.G. O'Shea
Institute For Research in Electronics and Applied Physics
University of Maryland, College Park, MD 20742

*Abstract*

Intense charged particle beams are of great interest to many wide areas of application ranging from high-energy physics, light sources and energy recovery linacs, to medical applications. The University of Maryland Electron Ring (UMER) is a scaled model to investigate the physics of such intense beams. It uses a 10 keV electron beam along with other scaled beam parameters that model the larger machines but at a lower cost. Multi turn operation of the ring (3.6 m diameter) has been achieved for highly space charge dominated beams. Such, multi-turn operation requires a non-intercepting diagnostic for measuring the transverse beam size. Localized density or velocity variations on a space-charge dominated beam travel as space charge waves along the beam. The speed at which the space charge waves separate from each other depends on the beam current, energy and g-factor. In this work, we propose a diagnostic using deliberately-induced space charge waves to measure the beam size with multi-turn operation. We present and compare experimental results with self-consistent simulation.

## INTRODUCTION

Intense beams are of significant interest in next generation linear colliders, FELs and ERLs [1, 2, 3]. Beam quality is crucial in all these applications. For example, too high an energy spreaad can create havoc to the operation of XFEL [4] . Hence, the beam has to be well diagnosed for successful operation of the machine. Fluctuations in intense beams, either as density or energy, propagate as space charge waves [5, 6]. Such space charge waves convert the density modulations in laboratory beams to energy modulations [7]. Energy modulations present in the beam gets converted back to density modulations when the beam goes through a dispersive section of an accelerator e.g. bunch compressor in LCLS [2]. Such oscillations between the energy space and density space disrupts the beam quality and hence the operation of the machine. Whenever there is a localized density or energy perturbation in an intense beam, space charge waves are launched [8]. Space charge waves are created in pairs and are classified as fast wave, when the wave travels toward the head of the beam and slow wave, when the wave travels toward the tail of the beam.

* jtobin@umd.edu, Department of Electrical and Computer Engineering, University of Maryland, College Park, USA

Previous work on space charge waves concentrated on generating such waves using various methods [9, 10, 11]. The waves separate at a speed called as the sound speed, which was found to be proportional to the beam current, on which the waves were launched. Neumann [12]demonstrated that introducing perturbation on intense beams can be very good terahertz radiation sources. In this work, we propose and demonstrate using space charge waves as a diagnostic tool [13] to measure the beam size of an intense beam. using a laser or using a induction cell,the beam can be perturbed in density or in energy thereby launching space charge waves. Once the waves start propagating, by measuring the propagating speed and the main beam current, the beam size can be estimated.

The University of Maryland Electron Ring (UMER) [14] uses a 10 keV electron beam with scaled parameters which model other bigger machines at much lower cost. Recently, multiturn operation was achieved. A technique was needed to measure the beam size without intercepting the beam. Space charge waves are a suitable diagnostics for measuring beams of intense space charge. As the speed of propagation of waves is proportional to the intensity of the beam,the more intense the beam is, the faster the waves propagate and hence easier to resolve the waves and measure the speed. The work is presented as follows: In section I, the theory of space charge waves is discussed following which the experimental setup is discussed in section II. The actual experiment and results is discussed in section III, which is followed by conclusion.

## THEORY: ONE DIMENSIONAL COLD FLUID THEORY

The linear theory of space charge waves is based on a cold-fluid model [8]. In this model, a small initial perturbation is assumed and then both momentum and continuity equations are solved. The solution shows that the perturbations propagate along the beam in the form of waves. One of them has a phase velocity greater than the beam velocity called as a fast space-charge wave, while the other one has a phase velocity smaller than the beam velocity and hence called a slow space-charge wave.

The linear continuity and momentum equations can be represented as:

$$\frac{\partial \Lambda_1}{\partial t} + v_0 \frac{\partial v_1}{\partial z} + \Lambda_0 \frac{\partial \Lambda_1}{\partial t} = 0, \qquad (1)$$

# BUNCH LENGTH MEASUREMENT AT THE FERMILAB A0 PHOTOINJECTOR USING A MARTIN-PUPLETT INTERFEROMETER*

Randy Thurman-Keup#, Raymond Patrick Fliller, Grigory Kazakevich (Fermilab, P.O. Box 500, Batavia, Illinois 60510)

*Abstract*

We present preliminary measurements of the electron bunch lengths at the Fermilab A0 Photoinjector using a Martin-Puplett interferometer on loan from DESY. The photoinjector provides a relatively wide range of bunch lengths through laser pulse width adjustment and compression of the beam using a magnetic chicane. We present comparisons of data with simulations that account for diffraction distortions in the signal and discuss future plans for improving the measurement.

## INTRODUCTION

Application of Coherent Transition Radiation (CTR) diagnostics based on correlation techniques for bunch length measurements in the sub-millimeter range was proposed more than 10 years ago and numerous articles have been devoted to the problem, [1,2,3]. The diagnostic employs Transition Radiation (TR), [4], which is coherent at wavelengths approximately equal to or exceeding the bunch length. This technique suffers from a number of issues, some of which will be discussed in this paper.

The measurements in this paper were taken at the A0 photoinjector at Fermilab during 2007. Figure 1 is a schematic of the photoinjector as it existed at that time.

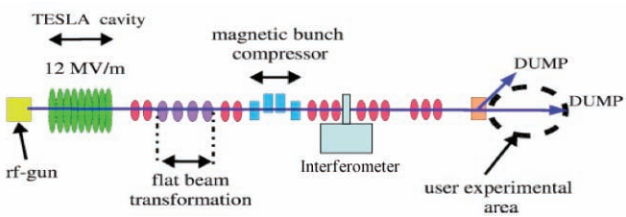


Figure 1: Schematic of the A0 photoinjector showing the main components. The interferometer is just downstream of the bunch compressor.

Beam is provided by a 1.3 GHz rf-gun with a CsTe photocathode. Typical charge is a few nC per micropulse. The micropulses are spaced by 1 μs and the overall rep rate is 1 Hz. The beam is accelerated via a TESLA 1.3 GHz SCRF cavity to energies around 16 MeV. A magnetic chicane does bunch compression of the beam just upstream of the interferometer with an expected compressed bunch length of 1-2 ps. The interferometer used for these measurements was obtained from DESY where it had also been used to make bunch length measurements. The thesis by Lars Frohlich [5] contains detailed descriptions of both the technique and the DESY measurements together with many references to previous work.

## BUNCH LENGTH INTERFEROMETRY

### *Correlation between bunch length and spectrum*

Interferometric bunch length measurements are possible because of the correlation between the bunch length and the spectral content of the CTR. This relationship is formally

$$I(\omega) = I_0(\omega) \cdot \left( N + N(N-1)\left|F(\omega)\right|^2 \right) \qquad (1)$$

where $I_0(\omega)$ is the single particle spectrum, and the complex form factor, $F(\omega)$, is the Fourier Transform of the longitudinal charge distribution

$$F(\omega) = \frac{1}{Q}\int dz\, \rho(z)\, e^{-i\omega z} \qquad (2)$$

where the transverse contributions are small, provided the observation point is close to the emission axis, and have been ignored.

Notice that the intensity is a function of only the magnitude of $F(\omega)$ and as such, in general, an exact determination of the longitudinal charge distribution cannot be obtained. However, for certain simple shapes, such as Gaussians, the approximations necessary to obtain the phase values do a fairly good job of preserving the main parameters of the bunch, such as width.

### *Reconstruction of the phase*

Determination of the phase of the complex form factor involves writing the form factor as a product of a term without complex zeros and a term that contains just the zeros.

$$F(\omega) = e^{i\varphi(\omega)} = e^{i\eta(\omega)} e^{i\xi(\omega)}$$

$$\varphi(\omega) = \eta(\omega) + \xi(\omega)$$

The phase of the first term, $\eta(\omega)$, is termed the 'minimal phase' and in fact contains most of the information for a variety of simple shapes such as Gaussians. It also happens that the minimal phase can be obtained from a Kramers-Kronig equation. The phase of the second term, however, is not obtainable from just the magnitude of the form factor and hence $\phi$ must be approximated by just $\eta$.

The imaginary part of $\eta$, $\eta_i$, is just the logarithm of the magnitude of $F$. The real part of $\eta$, $\eta_r$, is related by the Kramers-Kronig relation to the imaginary part

* Fermilab is operated by Fermi Research Alliance, LLC under Contract No. DE-AC02-07CH11359 with the United States Department of Energy.

# keup@fnal.gov

# THE ELECTRO-OPTIC SAMPLING STATIONS FOR FERMI@Elettra, A DESIGN STUDY

M. Veronese*, M. Danailov, M. Ferianis, Sincrotrone Trieste, Trieste, Italy

*Abstract*

FERMI@Elettra is a seeded FEL source, currently under construction at the Elettra Synchrotron Light Laboratory. On-line single shot and non destructive longitudinal bunch profile and bunch arrival time measurements are of great importance for this type of FEL source. These measurements will be performed by means of two Electro Optic Station (EOS) to be installed just upstream each of the two undulator chains. The paper describes the EOS stations design based on the spatial conversion scheme tested at SPPS and FLASH, and proposed for LCLS. The EOS will make use of two laser sources: a fiber laser at 780nm and the seed laser oscillator. A set of ZnTe and GaP crystal of different thicknesses will allow for flexibility in choosing high signal or high resolution configurations. The maximum resolution is expected to be of about100 fsec. The time profile mapped in a spatial laser profile will be acquired by a gated Intensified CCD.Calculations are presented for the expected EO signal and THz pulse broadening and distortion during propagation in the crystals.

## MACHINE PARAMETERS

FERMI@Elettra is an single pass seeded FEL under construction at the Sincrotrone Trieste Laboratory, based on a normal conducting Linac (50Hz repetition rate), designed to laser in the range from 100nm to 10nm. A general description of the machine is presented in the FERMI Conceptual Design Report [1]. Two main operation configurations of the machine are foreseen: the *Medium Bunch* and the *Short Bunch*. The main machine parameters at EOS location are summarized in table 1. Two identical EOS stations are foreseen one per each of the two (FEL1 and FEL2) undulator chains. The aim is to provide a high resolution single shot non destructive longitudinal profile and bunch arrival time measurement with very low time jitter. The the SPPS-DESY spatial decoding scheme [2], [3] has beem adopted since it does not require an amplifier laser system and temporal resolution of about 150fsec has been demonstrated.

Table 1: FERMI@Elettra EOS main machine parameters.

| Parameter | Medium Bunch | Short Bunch |
|---|---|---|
| Energy | 1.2 GeV | 1.2 GeV |
| Bunch Length FW | 0.9 ps | 0.17 ps |
| Charge | 1 nC | 0.5 nC |
| Beta ($\beta_x, \beta_y$) | (14m,7m) | (14m,7m) |
| Alpha ($\alpha_x, \alpha_y$) | (0.5,-0.5) | (0.5,-0.5) |
| Beam Size X ($\sigma_x$) | 110 $\mu$m | 110$\mu$m |
| Beam Size Y ($\sigma_y$) | 77 $\mu$m | 77 $\mu$m |

## LASER SOURCES

Femtosecond laser pulses from two different sources are foreseen for the spatial decoding scheme. The initial operation will be performed using a Menlosystems TC-780 fiber laser to be installed in the tunnel. The laser provides pulses at repetition rate of 78.895 MHz, with 120 fsec pulse width, and 0.8 nJ of energy per pulse. It offers noticeable performances in terms of temporal jitter with only 20fsec RMS (10Hz-1MHz) time jitter with respect to its electrical reference. This laser will allow operation from the very first days of the commissioning of FERMI in a very reliable way and is a *turn key* system.
When the ultrastable timing and synchronization distribution system will be installed we plan to use pulses from the fiber timing and synchronization distribution system (based on the MIT-DESY design). The pulses amplified by an EDFA amplifier and are used for second harmonic generation, bringing the wavelength down to 780nm. In this way we will intrinsically synchronized the ultra stable reference that will also be distributed to the users. The expected bunch arrival time jitter will then be only limited by the relative jitter between fiber links which we expect to be less than 10fsec RMS.

## SETUP

The EOS stations will be located just upstream of the modulator, the first module of the FEL undulators chain. An optical table will support both fiber laser sources, all optical components and the vacuum chamber housing the EO crystals as well as the detector. For the whole length of the optical table the vacuum chamber will be supported on the table while at both ends bellows will isolate the EOS from the rest of the machine to guarantee maximum vibration isolation. A cavity BPM will be in the immediate vicinity and will allow for position measurements with micron accuracy. The whole setup including the vacuum chamber will be isolated from the rest of the tunnel by a light tight enclosure to prevent ambient light, air turbulence and for laser related safety issues too.
The EOS layout is sketched in figure 1. The laser source selection will be provided by a remotely movable mirror. A prism compressor is foreseen to reduce the temporal duration of the pulses to below 100 fsec. A remotely controlled

* marco.veronese@elettra.trieste.it

# STATUS OF THE CTF3 SYNCHROTRON LIGHT-MONITORING-SYSTEM

C.P. Welsch[1-4], E. Bravin[1], A. Dabrowski[1], T. Lefèvre[1]
[1]*CERN, Geneva, Switzerland*
[2]*University of Heidelberg,* [3]*GSI, Darmstadt, and* [4]*MPI-K, Heidelberg, Germany*

*Abstract*

Synchrotron radiation has proven to be a flexible and effective tool for measuring a wide range of beam parameters in storage rings, in particular information about the longitudinal beam profile.

It is today an established and widely used diagnostic method providing online measurements and thus allowing for continuous optimization of the machine performance. At the CLIC Test Facility (CTF3), synchrotron radiation is routinely used at a number of diagnostic stations, in particular in the Delay Loop and the Combiner Ring. Measurements with both standard CCDs and a streak camera showed the wide range of possible applications of this method, including determination of inter-bunch spacing, charge per pulse and monitoring of the manipulation of the effective path length by an undulator.

This contribution first addresses the critical points during the design phase of long optical lines with lengths of more than 30 meters as they had to be realized at CTF3. Second, a summary of the present installations is given and results from measurements are shown.

## INTRODUCTION

CTF3 is being installed at CERN in the existing buildings of the LEP pre-injector accelerators LIL and EPA with the aim to demonstrate the technical feasibility of CLIC [1,2,3,4]. The complex starts with a 3 GHz linac that produces a pulsed electron beam with a present maximum energy of 150 MeV. The separation between individual bunches at the end of the linac is 20 cm - twice the linac RF wavelength. Moreover, the macro bunch is composed by alternated sequences 140 ns long of even and odd buckets, with the difference in phase between them being one RF wavelength.

The linac is connected by a transfer line to the Delay Loop [5] where a 1.5 GHz RF deflector deviates the odd bunch sequences to the left inside the DL and the even ones to the right, Figure 1. The DL length is 140 ns times the velocity of light c so that after this ring the odd sequence will be recombined with the incoming even sequence to fill the interleaved empty buckets. Precise adjustment of the longitudinal structure can be done with the integrated wiggler. The resulting macro bunch structure at the DL output presents 140 ns long trains of buckets separated now by 10 cm, followed by 140 ns long voids.

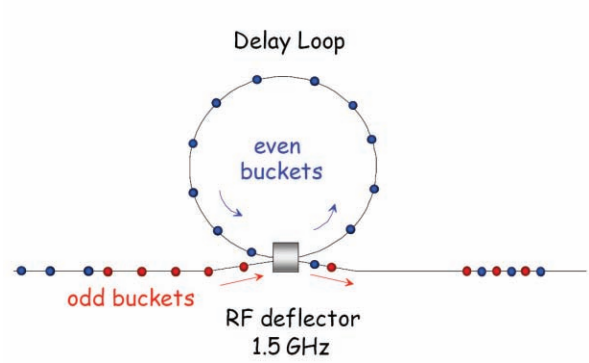


Figure 1: Schematic drawing of the injection scheme into the CTF3 Delay Loop [2].

The timing of the bunches of subsequent batches is adjusted such that they have a phase difference of 180 ° with respect to the 1.5 GHz RF of the deflector, Figure 2.

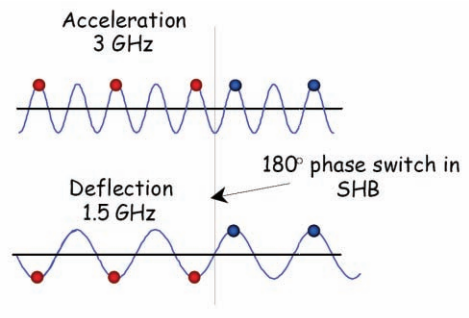


Figure 2: Illustration of required 180° phase switch between two batches of bunch trains [2].

An overview of the overall bunch combination process is shown in Figure 3. The necessary timing is controlled by the sub-harmonic bunchers working at 1.5 GHz in the injector region [6]. Every 140 ns the phase of the RF is changed by 180 degrees. This requires wide band sub-harmonic buncher structures as well as an RF power source capable of switching phase over a few bunches.

# MULTI-BUNCH BEAM SIGNAL GENERATOR FOR FEEDBACK RECEIVER DEVELOPMENT*

Jiajing Xu, John D. Fox, Daniel Van Winkle#,
Stanford Linear Accelerator Center, Menlo Park, CA 91, U.S.A.

*Abstract*

Bunched beam signals from button-style Beam-Position Monitor (BMP) electrodes can have spectral content up to 20-30 GHz and structure of narrow impulsive trains in time-domain. Multi-bunch feedback systems require receivers to process such beam signals and generate ΔX, ΔY, and ΔZ beam motion signals. To realistically test these receivers, we have developed a 4-bunch programmable impulse generator, which mimics the signals from a multi-bunch beam. Based on step-recovery diode techniques, this simulator produces modulated 100-ps impulse signals. The programmable nature of the system allows us to mimic Betatron and Synchrotron signals from 4 independent bunches with adjustable beam spacing from 1 to 8 ns. Moreover, we can observe nonlinear effects and study the noise floor and the resolution of the receiver. This paper presents the design of the system and shows typical achieved results.

## INTRODUCTION

Beam Position Monitors to measure beam transverse coordinates and longitudinal coordinate are fundamental diagnostics. The BPM detects the centroid of the beam. The oscillatory component of the coordinate is useful for the feedback systems (the average position is useful for orbit measurements). For any of these purposes, the typical signals generated at button-type or stripline beam pick-ups are impulsive and have frequency components going out to high frequencies of order 1/(bunch length). The wideband signals with so many high frequency harmonics makes the design of the coordinate circuits interesting because non-linear effects may be present from the high frequency components. Filters can help remove harmonics out of the detection band but the feed-through and attenuation in these filters can effect the coordinate measurement.

One traditional way to lab test BPM and feedback systems is via narrowband sine waves. While convenient, this does not really explore the non-linear performance and system characteristics with signal that look very much like what we see from the real BPM. For this purpose, we investigated and put together a beam simulator that we can use to test various receivers.

## METHODS

### *DIODE*

The heart of our system is a step-recovery diode that makes impulsive signals at the RF driving frequency. Also called a snap diode, a p-n junction is doped to exploit the minority carrier storage inherent in the diodes. [2] It makes use of the abrupt transition from on to off that occurs once the stored charge has been removed and produces signals with extremely fast rise-time (~100 ps).

With a periodic input, the output spectrum consists of harmonics of the input fundamental. This way, a 100-MHz input signal can be used to generate gigahertz outputs. Step-recovery diodes are often used to make circuits such as frequency comb generators. The diode is typically used with a tuned bias circuit which has roughly 10% bandwidth, so that a given diode and tuned bias circuit is useful over a 10% operating fundamental bandwidth. Using the step-recovery diode, we are able to generate a train of narrow, high amplitude pulses, shown in Figure 1. We can clearly see this sharp 100-ps impulse generated by HP-33002 in Figure 1.

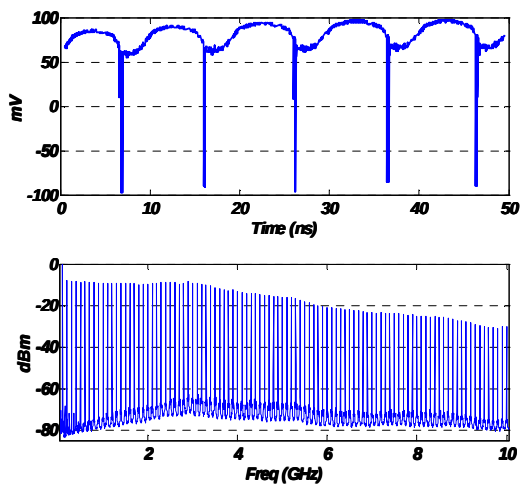


Figure 1: The impulse train generated using the 100 MHz HP-33002 snap diode in time domain (above, with 30 dB attenuation) and spectrum content (bottom, showing the 100 MHz comb)

### *The MODULATORS*

We can modulate the impulsive output signal from the diode properly to mimic different beam oscillations, i.e. phase modulation for Synchrotron oscillation and amplitude modulation for Betatron oscillation. The next step is to make a good phase modulator and amplitude modulator.

Now we will look into making a good phase modulator to replicate Synchrotron oscillation. Phase modulation can be done by using a voltage controlled phase shifter.

* Work supported by U.S. Department of Energy under contract # DE-AC02-76SF00515
# {jiajing, jdfox, dandvan}@slac.stanford.edu

# CRAB WAIST SCHEME LUMINOSITY AND BACKGROUND DIAGNOSTIC AT DAFNE

M. Boscolo, F. Bossi, B. Buonomo, G. Mazzitelli, F. Murtas, P. Raimondi, G. Sensolini
(INFN/LNF, Via E. Fermi 40 - 00044, Frascati, RM, Italy)
M. Schioppa
(Gruppo Collegato INFN, Via P. Bucci - 87036, Rende, CS, Italy )
F. Iacoangeli, P. Valente
(INFN-Roma, P.le Aldo Moro 5, Roma, Italy)
N. Arnaud, D. Breton, A. Stocchi, A. Variola, B. Viaud
(LAL, Univ Paris-Sud, CNRS/IN2P3, Orsay, France)
Paolo Branchini
(INFN Roma3, Via della Vasca Navale, 84 - 00146, Roma, Italy)

*Abstract*

Test of the crab waist scheme, undergoing at the Frascati DAFNE accelerator complex, needs a fast and accurate measurement of the luminosity, as well as a full characterization of the background conditions. Three different monitors, a Bhabha calorimeter, a Bhabha GEM tracker and a gamma bremsstrahlung proportional counter have been designed, tested and installed on the accelerator at the end of January 2008. Results from beam-test measurements, comparison with the Monte Carlo simulation and preliminary data collected during the SIDDHARTA run are presented.

## INTRODUCTION

The promising idea to enhance the luminosity with the introduction of a large Piwinski angle and low vertical beta function compensated by crab waist [1], will be a crucial point in the design of future factory collider [2], where the luminosity is the fundamental parameter. The DAFNE accelerator, located in the National Laboratory of Frascati (INFN), optimized for the high production of Φ mesons (√s=1020 MeV), has been modified during last year to test the crab waist sextupoles compensation scheme. Since fall of 2007 the machine has restarted operations, and at the beginning of February various luminosity detectors have been put in operation in order to guarantee an accurate measurement of the luminosity and of backgrounds, as well as to provide powerful and fast diagnostics tools for the luminosity improvement.

Three different processes are used to measure the luminosity at DAFNE:

- The Bhabha elastic scattering $e^+ e^- \rightarrow e^+ e^-$; it has a very clean signature (two back-to-back tracks); the available angle is limited due to the presence of the low-β quadrupoles, however, in the actual polar angle range covered by our calorimeters, $18^0$-$27^0$, the expected rate (~440 Hz at a luminosity of $10^{32}$ $cm^{-2}$ $s^{-1}$) is high enough and the backgrounds low enough to allow an online clean measurement.
- The very high rate $e^+ e^- \rightarrow e^+ e^- \gamma$ (radiative Bhabha process); it has the advantage that 95% of the signal in contained in a cone of 1.7 mrad aperture, but it suffers heavily from beam losses due to: interactions with the residual gas in the beam-pipe, Touschek effect, and particles at low angles generated close to interaction region (IR).
- The resonant decay $e^+ e^- \rightarrow \Phi \rightarrow K^+ K^-$; a rate of about 25 Hz at $10^{32}$ is expected in the SIDDHARTA experiment monitor at ~$90^o$ [3].

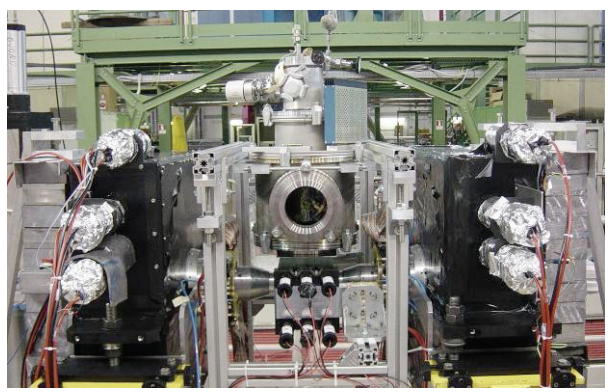

Figure 1: the SIDDHARTA preliminary setup installed at DAFNE. The Bhabhas calorimeters (black boxes) are visible on the left and right of the interaction region.

## BHABHA MONITOR

The Bhabha monitors consist of two different detectors, a 4-module sandwich calorimeter, made of lead and scintillator, and two triple GEM annular trackers.

### *Calorimeters*

Four modules of calorimeters surround the final permanent quadrupole magnets, located at a distance of 32.5 cm on both sides of the interaction region (IR), as shown in Fig. 1. They cover an acceptance of $18^o$ -$27^o$ in polar angle, and are segmented in azimuthal angle in five sectors, $30^o$ wide. The choice of not instrumenting 1/6 of the acceptance, i.e. the ±$15^o$ region, was dictated by the

# BEAM DIAGNOSTIC FOR A WIDE RANGE BEAM TEST FACILITY

B. Buonomo, G. Mazzitelli, F. Murtas, L. Quintieri.
(INFN/LNF, Via E. Fermi 40, 00044, Frascati (Roma))
P. Valente
(INFN Roma, P.le Aldo Moro 5, Roma).

*Abstract*

The DAFNE Beam Test Facility (BTF), initially optimized to produce single electrons and positrons in the 25-750 MeV energy range, can now provide beam in a wider range of intensity up to $10^{10}$ electrons/pulse. The facility has been also equipped with a system for the production of tagged photons, and the possibility of photo-production of neutrons is under study. Different diagnostic tools have been developed and are available for high-energy physics and accelerator communities for testing beam monitor devices and for all studies of particles detectors performances. The facility diagnostic devices are here presented: the main characteristics and operation are described, as well as the performances and the experience of the experimental groups collected during these years.

## INTRODUCTION

The Beam Test Facility (BTF) is part of the DAFNE collider, which includes a high current electron-positron LINAC and 510 MeV storage rings (Main Rings).

The e+/e- beam from the LINAC is stacked and damped in the accumulator ring for being subsequently extracted and injected into the Main Rings. When the injector is not delivering beam to the accumulator, the LINAC beam can be transported into the Beam Test area by a dedicated transfer line (BTF line). The main components of the line are described in the following[1].

The main parameters of the S-band LINAC (length 60 m ) are listed in the table below:

Table 1. LINAC parameters

| Particle | Electron | Positron |
|---|---|---|
| Energy | 800 MeV | 510 MeV |
| Max. Current | 500 mA/pulse | 100 mA /pulse |
| Transverse Emmittance | ≤ 1 mm mrad at 510 MeV | ≤ 10 mm mrad at 510 MeV |
| Energy spread | 1% at 510 MeV | 2.5 % at 510 MeV |
| Pulse duration | 1 or 10 ns | |
| Repetition rate | 1-50 Hz | |

Electron (positron) beams in that energy range are suitable for many purposes: high energy detector calibration, low energy calorimetry, low energy electromagnetic interaction studies, detector efficiency and aging measurements, test of beam diagnostic devices etc. Since the end of 2005 a photon tagging system has been installed and started operation with the first users.

## THE BTF TRANSFER LINE

The layout of the BTF transfer line is shown in Fig.1. The transfer line is about 21 m long, from the outlet of DHPTB101 (the pulsed dipole extracting the beam to the BTF line) to the bending magnet DHSTB002 in the BTF hall that is one of the two beam exits, and has an inner diameter of about 5 cm. All the line is kept under high vacuum ($10^{-10}$ bar) with the exception of the final part (from the DHSTB002 inlet to the 2 beam exits in the experimental hall), that is working, at present time, at $10^{-4}$ bar. The part under high vacuum ends with a Be window of 0.5 mm thick. The 10 cm air gap between the Be window and the inlet of the DHSTB002 bending allows the insertion of the silicon micro-strip chambers needed for tagged photon production.

The injector system provides beam both to the DAFNE damping ring and to the test beam area. The DHPTB101 allows to drive each of 49 pulses per second either to accumulator or to the BTF line, thus allowing a quasi-continuous operation of the facility. Indeed, even when beams are injected into the DAFNE main rings, not all the bunches are used for machine filling, so that beam can still be delivered to the BTF, but with a lower repetition rate [2]. Obviously, in this operation scheme the pulse duration and the primary beam energy must be the same of DAFNE. This is not a strong limitation, since the facility is mainly operated in single particle mode (electrons/positrons), which is the ideal configuration for detectors calibration and testing. Once per second, one of the 50 LINAC pulses is bent by 6 degrees to the spectrometer line by another pulsed dipole magnet (DHSTP001), in order to measure the LINAC beam momentum with an accuracy of ≈ 0.1%.

The intensity and the spot of the beam inside the BTF line can be measured by a beam current monitor (BCM1 beam charge to charge output ratio 50:1) and a fluorescent screen of beryllium-oxide type (FLAG01).

The intensity of the beam can be tuned by means of a vertical collimator (SLTB01), located upstream respect to FLAG01 in the BTF transfer line. In the high multiplicity ($10^{7}$ up to $10^{10}$ particles/bunches) range, the diagnostic elements of the line are completed by another beam charge monitor BCM2 (high sensivity, beam charge to output charge ratio 5:1) and two fluorescent screens FLAG02 (beryllium oxide), FLAG03(YAG:CE) mounted at the two exits of the line. In the following, the number of particles per bunch is also referred as “multiplicity of the beam”.

# A GATED BEAM-POSITION MONITOR AND ITS APPLICATION TO BEAM DYNAMICS MEASUREMENTS AT KEKB

T. Ieiri, H. Fukuma, Y. Funakoshi, K. Ohmi and M. Tobiyama, KEK, Ibaraki, Japan

*Abstract*

KEKB has transformed to an effective head-on collision by using of crab cavities from a crossing collision and gained a higher specific luminosity. A gated beam-position monitor, being capable of measuring the beam phase as well as the transverse position of a specific bunch in a bunch train, has been developed and is used to measure a beam-beam kick. The monitor estimated the effective horizontal beam size at the interaction point from a linear part of a beam-beam kick and demonstrated the effect of the crab cavities. The estimated horizontal beam size agreed with calculated size considering the dynamic beam-beam effect. Moreover, the monitor detected a displacement of the horizontal beam position along a bunch train under the crabbing collision.

## INTRODUCTION

KEKB [1] is a multi-bunch, high-current, electron/positron collider for *B* meson physics. The collider consists of two storage rings: the Low Energy Ring (LER) for a 3.5-GeV positron beam and the High Energy Ring (HER) for 8-GeV electrons. Both rings store more than 1500 bunches, where the harmonic number is 5120 with an RF frequency of 509 MHz. Bunches are stored in two rings with a 3-bucket (6 ns) or 4-bucket (8 ns) spacing, forming a single bunch train followed by empty buckets that occupies about 5 percents of the circumference. Additional bunches, called pilot bunches, are placed just after the train, at different location in each ring so that they do not collide with each other.

The two beams collide at one interaction point (IP) with a horizontal crossing angle of 22 mrad. Crab cavities installed in 2007 can horizontally tilt a bunch without changing a central orbit using a dipole-mode kick operating at the RF frequency [2]. The crab cavities achieved an effective head-on collision at the IP. The crabbing collisions are successfully performed for the first time and increased a specific luminosity [3]. Since only one crab cavity per ring is installed, the effect of the crab kick could be observed in the whole ring.

The beam-beam effects are important issues from the viewpoint of beam dynamics, including the collision tunings to raise the luminosity. Since the beam-beam force depends on bunch-by-bunch parameters, a bunch-by-bunch measurement is required to study the beam-beam effect. Although a streak camera and an oscilloscope are useful tools to observe a bunch structure, it is not easy to handle them in the usual operations. Moreover, a direct measurement of the beams at the IP is difficult in the actual configurations. On the other hand, a gated beam-position monitor, being capable of measuring the beam phase as well as the transverse position of a specific bunch in a bunch train, is a simple tool to measure a beam-beam kick. The beam-beam kick can be measured by comparing a beam position between colliding and non-colliding bunches. Although a part of a gated beam-position monitor has already been reported [4], this note represents revised performances and new applications to beam dynamics measurements under the crabbing collision.

## GATED BEAM-POSITION MONITOR

A gated beam-position monitor (GBPM), a fast switch selecting a specific bunch is attached with a turn-by-turn BPM, can measure the beam position of individual bunches. One application of a GBPM is to measure the beam-beam effect by comparing the beam parameters of a colliding bunch with those of the non-colliding pilot bunch. The signal processing is performed within a revolution period. This gated measurement has the following features:

- The position measurement is not affected by the global orbit correction.
- Imbalance in gains of the detector is cancelled out due to subtraction.
- However, the measurement is not simultaneous.
- An error would be enhanced, when the intensity between bunches to be measured is largely unbalanced.

Figure 1 shows the schematic diagram for a GBPM. Button type electrodes are mounted with a cylindrical vacuum pipe with a diameter of 64 mm to pick up a beam pulse. The optics parameters at the location of the pick-ups are listed in Table 1. The system can select an electron or a positron bunch and employs a common detector. A low-pass filter of a Bessel type with a cut-off frequency of 1.5 GHz is attached to a gate module so that high frequency components of a button signal would be eliminated. A gate selects a specific bunch in a bunch train with a pulse width of 8 ns, where a commercially available switch (Hittite-HMC234C8) is used. Owing to the IQ (In-phase and Quadrature phase) detection at the acceleration frequency of 509 MHz, the monitor can detect a longitudinal position or the beam phase of a bunch as well as the transverse beam positions [5]. Two orthogonal signals are put into 8-channel ADCs with a resolution of 12 bits. A peak of a detected pulse with 20 ns width is sampled in the ADCs at a rate of the revolution frequency of 100 kHz. The sampled data are stored turn by turn in a memory.

An on/off isolation of the gate module was tested in a bench. An isolation of more than 50 dB at 2 GHz is achieved, where two series of the switches are used to raise the isolation. The isolation of the system was also measured using real bunches placed with a spacing of 8

# MODIFIED DIGITAL FILTERING MAKES POSSIBLE "TRUE & PURE" TURN-BY-TURN MEASUREMENTS

A. Kosicek, V. Poucki, T. Karcnik, Instrumentation Technologies, Solkan, Slovenia
B. K. Scheidt, ESRF, Grenoble, France

*Abstract*

Libera, the beam position processor, features the so-called TbT (Turn-by-Turn) data output, the data rate being exactly the revolution frequency of the accelerator. This data is essential for commissioning of the accelerator as well as for various machine physics studies. However, due to the "natural" properties of correctly structured filters (respecting the Nyquist theorem), the smearing between adjacent TbT samples is not negligible. The purpose of the modified filters in DDC (Digital Down Converter) block is to efficiently reduce smearing between adjacent TbT samples, especially with partial fill patterns. The usage of Modified DDC filters provides excellent results for the studies based on TbT measurements, with the benefit of "true & pure" TbT results (no smearing). The method, its implementation and first results are discussed in this paper.

## INTRODUCTION

The smearing of TbT beam position data can be problematic for the precise measurements of certain accelerator characteristics (i.e. lattice parameters, such as the local Beta-function values and phase-advance). The basic principle of such measurements is to first apply a single-turn, flat & uniform kick to the whole beam, and then to measure, with all the TbT BPMs in the accelerator ring, the resulting Betatron oscillations of the beam for a large number of turns after the kick. At the ESRF Storage Ring such measurements are done on a beam that fills 33 % of the Ring. The advantages of such fill pattern are:

a) The individual turns are clearly separated from each other, and

b) the application of pure single turn flat kick is practically possible.

With regards to these kicker specifications, for the ESRF it means a flat field of 1 μs and rise- and fall- times (to less then a few % of the flat field strength) of less than 0.9 μs [1]. To maintain these advantages it was important that the smearing, introduced by the standard, relatively narrow DDC filters inside the Libera BPMs, was addressed. The elaboration and implementation of adapted DDC filters was done at Instrumentation Technologies. Tests on real beam were subsequently carried out at the ESRF on 8 individual Libera BPMs in the Ring [2].

## SIGNAL PROCESSING

The signal processing chain on Libera Brilliance is composed of analog signal processing, digitalization on fast ADCs (Analog to Digital Converters) and the digital signal processing, see Figure 1. Within the digital part, digital bandpass filtering is first applied, the signal afterwards being brought to DC by mixing. Then, the TbT data bandwidth is obtained by means of lowpass moving average filters. Finally, the TbT data rate is obtained with proper decimation.

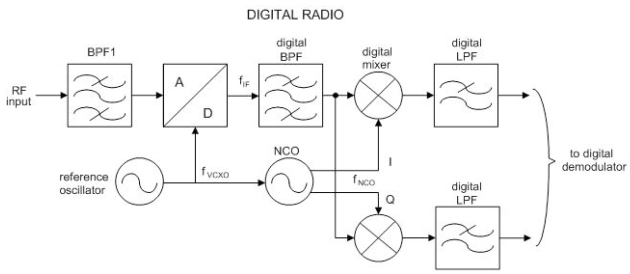


**Figure 1: Signal Processing on Libera**

Further signal processing to lower data rates for continuous data streams (serving fast feedback and monitoring) is not discussed in this article. Complete processing is implemented onboard a Virtex II Pro FPGA chip. Two main changes to the digital signal processing chain were introduced: wider bandpass digital filters and a narrower subsequent data acquisition window.

### *Digital Filters*

The data coming into digital filtering has the bandwidth of approx 12 MHz, determined by bandpass SAW filters within the analog signal processing. The filters and procedures used for standard digital filtering are constructed by the book, as required by theory. To prevent unwanted aliasing, the 3dB bandwidth of the filters is always well below half of the output sampling rate. For the ESRF case, with TbT frequency of 355 kHz, the bandwidth of the TbT data reaches less than 150 kHz with standard filters. As it is known from the theory, the narrower the filters, the longer is the time response of the output data (i.e. 'ringing' of the filter response). It was therefore a logical choice to make the filters wider. The modified IIR bandpass filters (BPF1 on Figure 1) have been widened to approximately 3 times the TbT data rate.

### *Acquisition Window*

The acquisition window of the standard moving average filters covers the whole TbT period, in the ESRF case this is 304 ADC samples or 2.81 μs. This is in principle correct since the useful signal is in principle distributed over the whole TbT period. But when the accelerator is filled with certain partial fills, the real signal will be distributed only on a certain sector of the TbT period, and the rest of the acquired data will consist mainly of noise. There is no sense to process the noise in

# STRIPLINE BEAM POSITION MONITORS FOR LCLS*

E. Medvedko, R. Johnson, S. Smith, R. Akre, D. Anderson, J. Olsen, T. Straumann, A .Young
Stanford Linear Accelerator Center, Menlo Park, CA, 94025

*Abstract*

The Linac Coherent Light Source (LCLS) must deliver a high quality electron beam to an undulator for production of coherent X-ray radiation. High resolution beam position monitoring is required to accomplish this task. Critical specifications are a dynamic range of 0.08-8.0 nC with 5 micron resolution at 200 pC in a stripline pickup of 1 inch diameter. Processor electronics were designed, based on band-pass filtering the signals followed by direct digitization of the resulting pulse train. The processor consists of Analog Front-End (AFE) and Analog-to-Digital Converter (ADC) boards, packed into 19-in rack mount chassis, 1U high. The AFE board has a very low input noise, approximately 3 micro V rms in a 7 MHz bandwidth centered at either of two frequencies, 140 or 200 MHz, depending on the length of the stripline BPM used. The maximum gain is 34 dB with programmable attenuation of up to 46 dB in 1 dB steps. An on-board pulser sends a short calibration tone burst to the striplines to perform calibration between beam pulses. The ADC board has four 16-bit digitizers with a sampling frequency of 120 MHz. For the LCLS injector 22 prototypes of the processors were built and installed in 2007. Measured resolution at 200 pC is typically 3-5 microns. A production run of 53 improved processors are currently being installed and commissioned.

## OVERVIEW

A beam position monitor consists of four stripline electrodes connected with low loss cables to a BPM Processor (Fig. 1). The BPM processor chassis consists of the Analog Front-End, ADC, and clock boards in a 19" rack-mounted chassis. A processor on the ADC board talks with the VME IOC (Input-Output Controller). The digitizer and the data acquisition system are described in references [1] and [2].

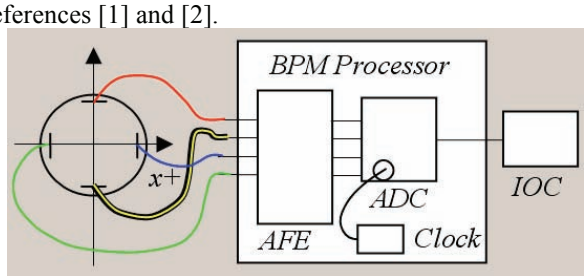


Figure 1: BPM system block diagram.

Twenty-two prototypes and 16 new production chassis are distributed along the Linac injector. Forty-three new BPM Processor chassis will be installed on LCLS this summer.

*Work supported by U.S. Department of Energy contract DE-AC02-76SF00515

### *Requirements*

There are two critical requirements – dynamic range and resolution at 200 pC beam charge.

Table 1: Requirements for the LCLS BPM system

| Parameter | Value | Comments |
|---|---|---|
| Dynamic Range | 0.08 – 8 nC | 40 dB |
| Resolution @ 0.2 nC | 5 μm | |
| Stability | 5 μm per hour | |

## ANALOG FRONTEND

Modern technology provides a variety of high dynamic-range, low noise RF amplifiers and low insertion loss filters applicable for the precision analog front-end design. Three RF amplifiers and three band-pass filters provide low noise amplification with gain programmable by two digital attenuators per channel, providing a total dynamic range control of 46 dB (Fig. 2).

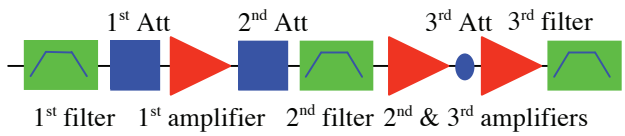


Figure 2: One channel of the Analog Front-End

Two rather different lengths of stripline pickups are used in LCLS: the typical linac BPM strips are 10 cm long, while the striplines intended to provide higher resolution for the linac-to-undulator section have 50 cm long striplines. Due to the difference in frequency response of the two type of striplines we construct BPM processors at two different frequencies, 140 MHz and 200 MHz. Bandpass filters define a bandwidth of 7 MHz at the operating frequency, either 140 MHz or 200 MHz.

Taking the component parameters from Table 2 we calculate an input-referred noise of 3 microvolts rms.

Table 2: Insertion loss (IL), Noise Figure (NF), Gain, IP3.

| | IL, dB | NF, dB | Gain, dB | IP3, dBm |
|---|---|---|---|---|
| 1st filter | 2.5 | | | |
| 1st att | 0.5 | | | |
| 1st amplifier | | 2.8 | 20.4 | 39 |
| 2nd att | 0.5 | | | |
| 2nd filter | 5 | | | |
| 2nd amplifier | | 3.3 | 14.9 | 40 |
| 3rd att | 6 | | | |
| 3rd amplifier | | 3.3 | 14.9 | 40 |
| other | 1.4 | | | |

# MEASUREMENTS ON LIBERA ELECTRON AND LIBERA BRILLIANCE BPM ELECTRONICS

A. Olmos, F. Pérez, ALBA-CELLS, Bellaterra, Barcelona, Spain

*Abstract*

ALBA synchrotron light source is a 3rd generation machine being constructed by the CELLS consortium near Barcelona, Spain. Orbit correction system will be based on the Libera Brilliance electronics and its goal will be the stabilization of the beam at the submicron level. Important parameters to reach such corrections have been measured and are reported in this document, like electronics resolution, beam current dependence, latency (among others). Comparison of the two different Libera products offered by the company (Libera Electron and Libera Brilliance) is also reported in order to analyze the benefits of choosing Libera Brilliance.

## INTRODUCTION

Synchrotron machines constructed nowadays require beam position stability in the order of hundreds of nanometres. Such stabilities can only be accomplished with a dedicated system, usually known as Fast Orbit Feedback System (FOFB). The FOFB system is in charge of the following:

- Measurement the beam position drifts around the machine.
- Transmission of all the position measurements to the computational unit/s.
- Calculation of the correction values and actuation on the beam through corrector magnets.

ALBA will use the Libera Brilliance electronics, developed by Instrumentation Technologies company, to perform the measurements and the transmission of the beam position [1]. Brilliance are an upgraded version of the already existing Libera Electron units. A vast laboratory test has been done on each of the units in order to check their specs and prove the Brilliance improvements vs. the Electron.

## LABORATORY MEASUREMENTS

Here are reported some of the results obtained during the Site Acceptance Test [2] (SAT) of the electronics. Until now, a total of 31 Electron units and 66 Brilliance ones have been tested.

### *Laboratory Setup*

Units were tested one by one using the test setup showed in Figure 1. A remote industrial PC sets the Libera parameters and retrieves the data through a Matlab based GUI [3] (both slow rate and fast rate data). An RF generator simulates the electron beam, while two function generators are used to generate the needed clock signals and events. A small modification of that setup allows us to perform latency measurements using the Libera interlock output.

We report here the measurements done on the Brilliance units. Electron units results are showed on the comparison chapter.

### *Electronics Resolution*

Vertical RMS resolution of 8 Libera units is showed on Figure 2. As seen, the needed sub-micron resolution is achieved on the electronics down to ~5.5mA beam current (-45dBm Libera input), on a 10kHz measurement rate.

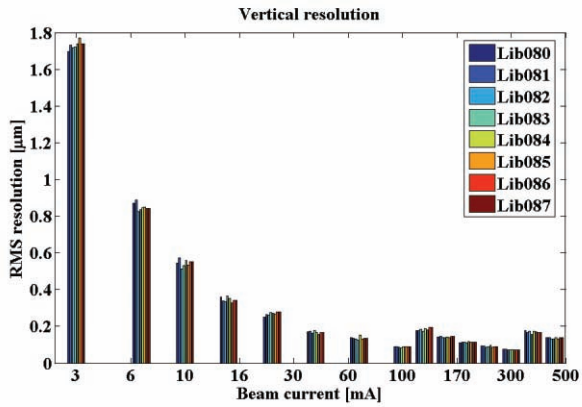


Figure 2: Vertical resolution of 8 Liberas @ 10kHz rate

Resolution is improved a factor 10 for slower rates, i.e. at 10Hz rate for control systems acquisitions.

### *Beam Current Dependence*

Beam Current Dependence (BCD) of the position readings on the stored beam has been improved on the Libera Brilliance electronics (Figure 3).

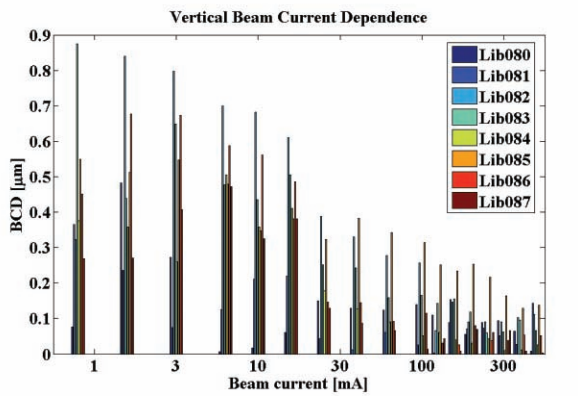


Figure 3: Vertical BCD of 8 Liberas @ 10kHz rate

Position measurement dependence, or independence, remains below 1µm even at very low beam currents. Once ALBA will be running on Top-Up mode, the BPM

# COMPARISONS OF SELECTED COTS AND CUSTOM HARDWARE FOR BEAM POSITION AND PHASE MEASUREMENTS FOR LANSCE*

J. F. Power, J.D. Gilpatrick and D. Martinez, LANL, Los Alamos, NM 87545, U.S.A.

*Abstract*

Beam Position and Phase Monitors (BPPMs) planned for the LANSCE diagnostics refurbishment will be required to measure beam position and phase of the 201.25-MHz bunched beam in the proton linac. One method to do this is direct down conversion to in-phase and quadrature-phase data of the BPPM signals using either commercial digitizers or custom designed hardware. We are evaluating selected hardware for systems with emphasis on commercial-off-the-shelf COTS hardware to the extent practical. Approximate system requirements include a beam current range of 27 db, position resolution of 0.25% of beam aperture and relative phase measurement with 0.25 degree resolution at 201.25 MHz [1]. We present our results to date on two approaches, ZTEC Instruments ZT-410 digitizers, and a custom four-channel ADC analog front end board combined with National Instruments, Inc. digital I/O board. These two systems use PCI cards in a standard PC running Windows® XP. Our primary points of comparison include measured position resolution, phase resolution, phase linearity, minimum cycle rate and approximate cost for these portions of a BPPM system.

## INTRODUCTION

As in our previous designs, such as those for the Spallation Neutron Source, we are planning to add phase measuring BPPMs to the LANSCE linac [2-4]. Rather than analog downconversion, we plan to use direct down conversion, and we want to use COTS hardware where practical.

In this paper we compare the performance of a pair of ZTEC Instruments ZT-410 oscilloscope cards (two channel, 250 MHz BW, 14-bit, 500 MSPS PCI) with a custom designed (four-channel 700 MHz, 16-bit, 130 MSPS) analog front end (AFE) mated to a pair of National Instruments NI PCI-6542 digital I/O cards. Each of these solutions represents $11k-$12k in hardware costs.

Both systems were evaluated using the same PC running Windows XP and a BPPM application written in LabVIEW®. The BPPM application contains all of the functionality needed for correctly calibrating, calculating and displaying the beam position and phase. Additional gain and analog calibration circuits will be required on the real system and these will be a custom design.

## TEST CONFIGURATIONS

The computer PCI cards and their interfaces are shown in Figure 1. The ZTEC cards have BNC inputs that we use for top, bottom, right and left signals. The clock and trigger signals are routed in parallel to each card in both the ZTEC and the NI system

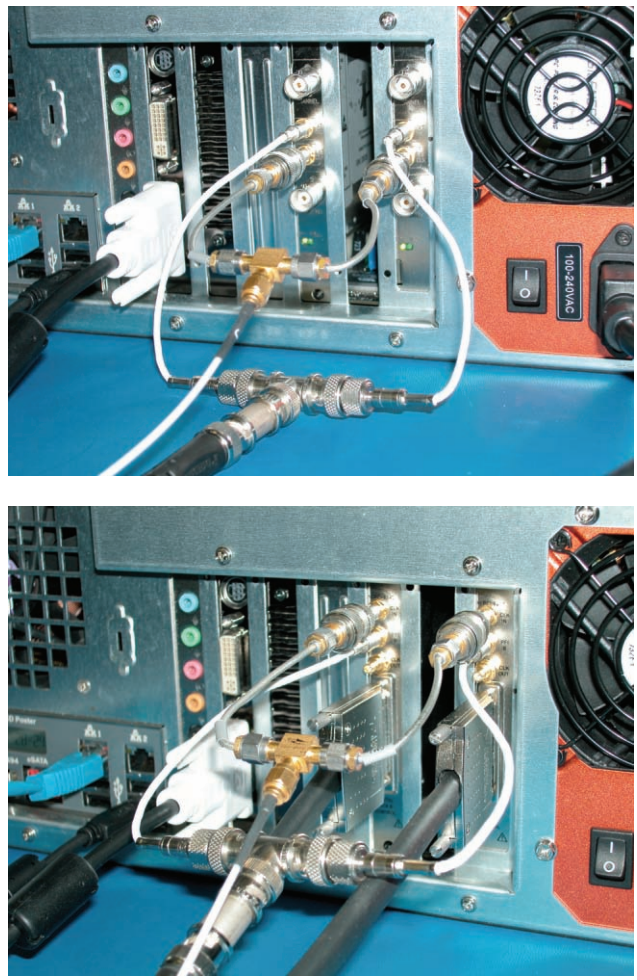

Figure 1: BPPM computer interfaces showing the ZTEC cards (top) and the NI/custom AFE (bottom).

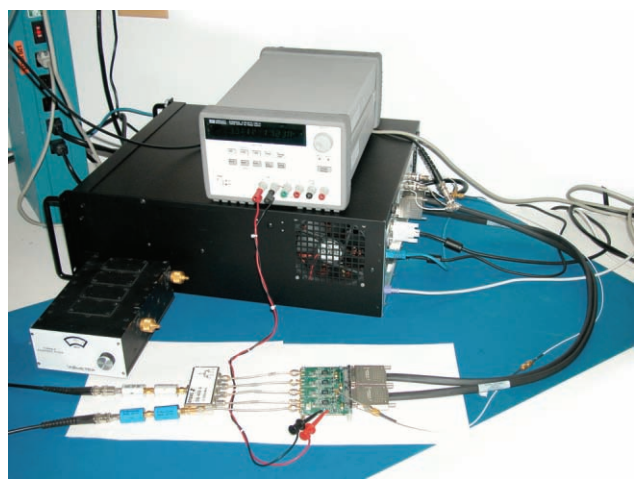

Figure 2: The custom AFE connected to the NI digital I/O cards. The filters and splitter are used to test both systems.

*Work supported by the U.S. Dept. of Energy

# HIGH RESOLUTION UPGRADE OF THE ATF DAMPING RING BPM SYSTEM*

N. Terunuma, J. Urakawa, KEK, Tsukuba, Japan
J. Frisch, J. May, D. McCormick, J. Nelson, A. Seryi,
T. Smith, M. Woodley, SLAC, Menlo Park, CA 94025, U.S.A.
C. Briegel, R. Dysert, N. Eddy, B. Fellenz, E. Gianfelice, W. Haynes, D. Nicklaus
P. Prieto#, R. Rechenmacher, D. Slimmer, D. Voy, M. Wendt, Fermilab, Batavia, IL 60510, U.S.A.

*Abstract*

A *beam position monitor* (BPM) upgrade at the KEK *Accelerator Test Facility* (ATF) damping ring has been accomplished in its first stage, carried out by a KEK/FNAL/SLAC collaboration under the umbrella of the global ILC R&D effort. The upgrade consists of a high resolution, high reproducibility read-out system, based on analog and digital donwconversion techniques, digital signal processing, and also tests a new automatic gain error correction schema. The technical concept and realization, as well as preliminary results of beam studies are presented.

## MOTIVATION

To achieve a high luminosity in the next generation, linear acceleration-based $e^+/e^-$ *high energy physics* (HEP) collider, low-emittance beam generation and preservation are mandatory. In frame of the *International Linear Collider* (ILC) R&D program, the goal of the beam studies at the KEK ATF damping ring[1] is to generate and extract a beam with an ultra-low vertical emittance < 2 pm [2]. This requires various optimization methods to steer the beam along an optimum ("golden") orbit with minimum disturbance of non-linear field effects. A high resolution BPM system is one of the important tools to achieve this goal, which requires a resolution in the 100 nm range in a "narrowband" mode.

The "ATF DR BPM Upgrade Project" is a KEK/SLAC/Fermilab collaboration that addresses the problem by installing and commissioning of new hard-, firm- and software for the signal processing to read-out the button type BPM pickups in the ATF damping ring:

- 714MHz-to-15MHz downmix and calibration module (located in the ATF tunnel).
- VME-based digital signal processing and timing electronics, based on the commercial *Echotek* digital receiver.
- Various FPGA-firmware, control and diagnostics drivers and software (C++, LabVIEW, VxWorks, Linux) and an EPICS interface to the ATF control system.

As proof of principle, 20 (out of 96) installed button BPMs are currently equipped with the new read-out system. To minimize the expenses, the experiment is based on available spare units, rather than implementing the latest generation of digital signal processing technology.

*This work supported by a high energy physics research program of Japan-USA cooperation, and by the Fermi National Accelerator laboratory, operated by Fermi Research Alliance LLC, under contract No. DE-AC02-07CH11359 with the US Department of Energy.
#prieto@fnal.gov

## THE ATF DAMPING RING

Figure 1 shows the KEK Accelerator Test Facility with S-Band linac, damping ring and extraction line, as of year 2008. Indicated is the staged upgrade process of BPM stations.

Table 1: ATD DR machine and beam parameters

| | | |
|---|---|---|
| beam energy E | = | 1.28 GeV |
| beam intensity, single bunch | ≈ | ~1.6 nC ≡ $10^{10}$ $e^-$ (≡ $I_{bunch}$ ≈ 3.46 mA) |
| beam intensity, multibunch (20) | ≈ | ~22.4 nC ≡ 20 x 0.7 $10^{10}$ $e^-$ (≡ $I_{beam}$ ≈ 48.5 mA) |
| $f_{RF}$ | = | 714 MHz (≡ $t_{RF}$ ≈ 1.4 ns) |
| $f_{rev}$ | = | $f_{RF}$/330 ≈ 2.16 MHz (≡ $t_{rev}$ ≈ 462 ns) |
| bunch spacing $t_{bunch}$ | = | 2/ $f_{RF}$ ≈ 2.8 ns |
| batch spacing | = | $t_{rev}$/3 = 154 ns |
| repetition freq. $f_{rep}$ | = | 1.56 Hz (≡ $t_{rep}$ = 640 ms) |
| beam time $t_{beam}$ | = | 460.41 ms (≡ 996170 turns) |
| vert. damping time τ | ≈ | 30 ms |
| hor. betaron tune (typ.) | ≈ | 15.204 (≡ $f_h$ ≈ 441 kHz) |
| vert. betaron tune (typ.) | ≈ | 8.462 (≡ $f_v$ ≈ 1 MHz) |
| synchrotron tune | ≈ | 0.0045 (≡ $f_s$ = 9.7 kHz) |

Table 1 lists some relevant machine and beam parameters of the ATF damping ring. In standard operation a single bunch in injected on axes from the S-Band linac. After ~200 ms all injection oscillations are fully damped, and the beam stays for another 400 ms in the ring, before being extracted. Optional multi-batch/multi-bunch operation can be set up on a cycle-by-cycle basis (no extraction), with up to three equally spaced batches, each containing 1…20 bunches, spaced by 2.8 ns.

## THE ATF DR BPM UPGRADE

A 10-20 μm RMS resolution, measured on the currently installed BPM read-out system, does not meet the

# DEVELOPMENT OF BUTTON ELECTRODE WITH IMPROVED TIME RESPONSE

M. Tobiyama*, J. W. Flanagan, KEK Accelerator Laboratory, 1-1 Oho, Tsukuba 305-0801, Japan
T. Obina, M. Tadano, KEK-PF, 1-1 Oho, Tsukuba 305-0801, Japan

*Abstract*

Good time response in a button electrode is essential to realize the bunch-by-bunch feedback / diagnostic systems for future short-bunch spacing accelerators such as an energy recovery linac (ERL) or super B-factory. The impedance matching and the time-domain response of the electrodes especially around the vacuum seal have been studied using 3-D electromagnetic codes (HFSS, MAFIA and GdfidL). Several candidates have been fabricated to examine the tolerances of mechanical pressures and heat stress due to the welding process. The real beam response from a short linac bunch has also been studied using a test beam line at the KEK-PF beam transport section.

## INTRODUCTION

The requirements on the bunch-by-bunch beam position diagnostics systems for future short-bunch spacing accelerators, such as energy recovery linac (ERL) or super particle factories such as SuperKEKB, are much harder than those of present accelerators because the systems play a major role in operating the accelerators or to realize the fairly difficult specifications. Since the signal inputs of the system which couples to the beam (head) limit the absolute performance of the system, it is necessary to design good electrodes such as button-type electrodes or stripline electrodes including feedthrough which fulfill the requirements.

The requirements on the front-end parts of bunch-by-bunch diagnostic systems might be summarized as follows:

- Good impulse response without long trailing signals, such as ringing from the bunch signal. It is also necessary to be free from trapped modes which not only make the response worse but easily damage vacuum sealing in high beam current conditions.
- High enough output voltage to keep good signal to noise ratio on succeeding detection circuits.
- Mechanically tough structure with respect to both signal induced heating and possible impacts such as mechanical pressure coming from fastening and unfastening the RF connectors or cable stress. Note it is also necessary to be strong enough in the construction process such as welding them to vacuum chamber.

For the KEKB bunch-by-bunch feedback systems, we designed and fabricated modified-SMA type button electrodes about 10 years ago[1]. We have done 3-D EM simulations such as MAFIA310 or HP-HFSS ver.3 using fairly poor computing power compared those available to now. The installed BPMs have been working excellently under tough conditions, with a maximum beam current of 2A, minimum bunch spacing of around 4ns (about 15nC / bunch), and a bunch length of about 7mm in standard deviation, without any troubles. Good frequency response of the electrodes also helps to investigate beam characteristics such as beam-beam effects or unknown beam instabilities. For an accelerator with a much shorter bunch length, say about 3mm, or with much shorter bunch spacing, however, the electrode might not be suitable.

Since the large permittivity of alumina-ceramics ($e_r$~9.7) used to seal vacuum makes impedance matching difficult, we have employed a glass of low permittivity ($\varepsilon_r$~4) as vacuum seal of the feedthrough and examined the frequency and time response using current 3D-electromagnetic field simulation codes (GdfidL, HFSS) [2, 3]. Several candidates have been fabricated to examine the frequency response, and tolerance to mechanical and heat pressures. The time response of the electrodes has been studied using the very short linac bunch using the test-beam line at KEK-PF beam transport section. The target specification of the electrodes for SuperKEKB and the ERL test facility proposed in KEK are shown in Table.1.

| **Specification** | | **unit** | |
|---|---|---|---|
| Bunch length | 3<br><0.9 | mm<br>mm | SuperKEKB<br>ERL |
| Bunch charge | 20<br>7.7 | nC<br>pC | SuperKEKB<br>ERL |
| Time response | <0.5<br><0.3 | ns<br>ns | SuperKEKB<br>ERL |

Table 1 Design target of new button electrodes.

## BUTTON ELECTRODE FOR KEKB FEEDBACK SYSTEMS

The structure of the present button electrode used in the KEKB feedback systems is shown in Fig. 1.For support

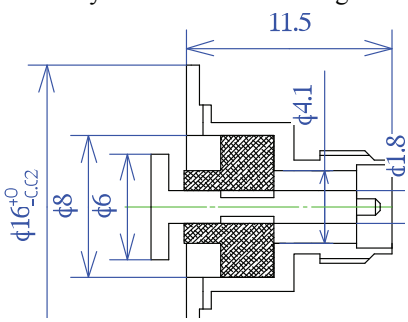


Fig.1 Button electrode for KEKB feedback systems.

*mailto:makoto.tobiyama@kek.jp

# BEAM QUALITY MEASUREMENTS AT THE SYNCHROTRON AND HEBT OF THE HEIDELBERG ION THERAPY CENTER

T. Hoffmann[1], D. Ondreka[1], A. Peters[2], A. Reiter[1], M. Schwickert[1]

[1]Gesellschaft für Schwerionenforschung (GSI), Darmstadt, Germany
[2]Heidelberg Ion Therapy Center (HIT), Heidelberg, Germany

*Abstract*

The Heidelberg Ion Therapy Center (HIT) for tumor treatment is presently being commissioned using the beam diagnostic devices designed and produced by the GSI beam diagnostic department. To fulfil the requirements for hadron therapy a high-resolution analysis of the particle distribution within the slowly extracted beam is necessary. We present spill-structure measurements for carbon ion beams at energies from 88 MeV up to 430 MeV, also with respect to the spill-pause and abort functionality of the rf-knock-out extraction method. The spill-structure, as measured by internal intercepting ionization chambers (IC) is compared to data recorded with external beam loss monitors (BLM). The high-resolution data acquisition system with sampling rates up to 10 kSa/s and the connected detectors are described and the achievements during the commissioning phase are discussed.

## INTRODUCTION

The Heidelberg Ion Therapy center (HIT) is a new dedicated hadron accelerator facility for medical treatment of tumor patients. The advantage of using hadrons in cancer therapy is their characteristic energy loss profile in irradiated materials. When applied to tumor tissue this leads to a DNA destructive maximum at the Bragg peak immediately before the particles come to rest. To reach penetration depths of 20-300 mm in water, which is almost comparable with human tissue, ion energies of 50-430 MeV for carbon ions are required. The tumor is irradiated in sliced fractions (iso-energy-layers) by means of cycle-to-cycle energy variation. Within such a layer the intensity controlled raster-scan method applies a pencil beam which is moved from voxel to voxel (3D-pixel) by two fast scanner-magnets. Due to this technique some accelerator characteristics have to be taken into account to assure the fulfilment of the manifold requirements of medical radiotherapy.

In this contribution the spill-pause and abort functionality are analyzed. During raster-scan operation within a synchrotron cycle the spill-pause functionality spares healthy tissue in cases where irradiation areas are spatially separated. Secondly the spill-pause is an important tool to optimize treatment planning, and machine efficiency. The qualities of the rising and falling edges and the intensity of the residual particles within the pause, and after the spill-abort have to be investigated. To gain a homogeneous irradiation per fraction the spill-structure has to be optimized as spike effects and small interrupts increase the failure rate. The spill-structure is influenced by many factors such as the rf-knock-out extraction (KO) method, the power supplies, and the beam bunching parameters.

## HIT ACCELERATOR COMPLEX

Presently HIT is in the final phase of its commissioning. All treatment areas can be served with carbon ion beam in the designed energies range from 88 MeV up to 440 MeV. As shown in Fig.1, the complex consists of two ECR ion sources, a 7 MeV RFQ/IH Linac (A), a Synchrotron (B) with magnetic rigidity of Bρ=0.38-6.5 Tm, two horizontal

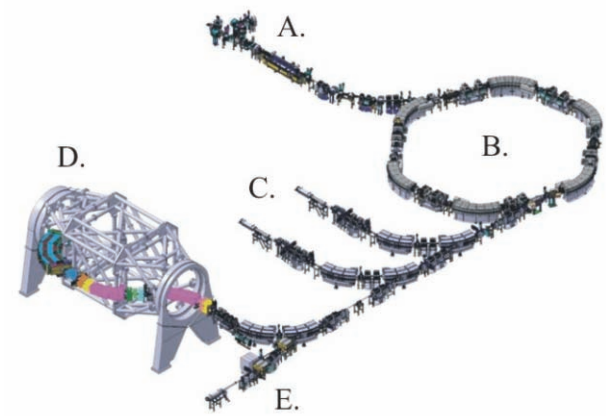


Figure 1: Isometric drawing of the HIT accelerator complex.

treatment places (C), a 360º patient irradiation gantry (D), and a quality assurance section (E). A more detailed description of the facility and its diagnostics is given in [1] and [2].

## BEAM DIAGNOSTICS AND DATA ACQUISITION

The complete beam instrumentation, from layout and production to the final installation including the final proof of operability with beam, was managed by the GSI beam diagnostics group. All beam diagnostic devices were categorized into separate device classes on the base of the detected beam parameter such as current, energy, beam profile, position, phase and others. One of these device classes is the “event counting” class, which is from its functional point of view a down-sized reproduction of the GSI ABLASS system [3]. It combines all particle

# CREATING A PSEUDO SINGLE BUNCH AT THE ALS — FIRST RESULTS*

G. Portmann, S. Kwiatkowski, J. Julian, M. Hertlein, D. Plate, R. Low, K. Baptiste, W. Barry, D. Robin, Lawrence Berkeley National Laboratory (LBNL), Berkeley, CA 94720 U.S.A.

*Abstract*

Typically storage ring light sources operate with the maximum number of bunches as possible with a gap for ion clearing. The Advanced Light Source (ALS) has 2 nanoseconds between bunches and typically operates with 276 bunches out of a possible 328. For experimenters doing timing experiment this bunch separation is too small and would prefer to see only one or two bunches in the ring. In order to provide more flexible operations and substantially increase the amount of operating time for time-of-flight experimenters, it is being proposed to kick one bunch on a different vertical closed orbit. By spatially separating the light from this bunch from the main bunch train in the beamline, one could potentially have single bunch operation all year round. By putting this bunch in the middle of the ion clearing gap the required bandwidth of the kicker magnets is reduced. To test this new method of operation on the beamlines one kicker magnet running at the ring repetition rate (1.52 MHz) has been installed at the ALS. This paper will show some first results running the kicker at 1.52 and 1.52/5 MHz.

## INTRODUCTION

The concept of using a camshaft bunch started many years ago and originated out of the needs of time-of-flight experimenters. Some time ago, NSLS at Brookhaven experimented kicking one bunch in the train at low repetition rates, [1]. This will introduce relatively long transient oscillations until the synchrotron radiation damps the bunch back to the closed orbit. To our knowledge no accelerator in the world has taken the next step to kick the camshaft bunch on a different closed-orbit to create a pseudo single bunch mode. Accelerators like the APS and ESRF can achieve similar functionality by installing choppers in the beamlines. However, even with state-of-the-art choppers this solution requires relatively large gaps in the bunch train, so it's presently only feasible on large accelerators. It also requires each beamline to purchase a relatively expensive and often difficult to use and maintain chopper. At the ALS the largest gap in the bunch train is presently 104 nanoseconds, which is out of reach for x-ray choppers.

There are a number of beamlines at the ALS interested in exploring a pseudo single bunch operational mode. A major reason is so that experiments using the camshaft bunch will not have to use gated detectors. The ability to use integrating detectors increases the variety and quality of the experiments that can be done. For instance, the combination of the pseudo single bunch mode and a chopper with an open time of just more than one turn allows for an effective single bunch operation at 1-10 kHz.

## A POSSIBLE NEW OPERATIONAL MODE

By kicking the camshaft bunch on a different closed-orbit, it may be possible to create a pseudo single bunch operation during a multi-bunch user run. There are a number of different ways the orbit of the camshaft bunch can be shaped depending on the number and location of the fast kicker magnets. The easiest thing to do is install one kicker magnet and place the camshaft bunch on a different global closed-orbit. This may not be optimal for all single bunch or multi-bunch users, but it would be a relatively easy thing to do to experiment with the method. Another obvious thing to do is locally bump the camshaft bunch in one part of the ring. This would isolate the disturbance to a relatively small section of the ring. A third option is to install kicker magnets all around the ring and profile the orbit much like global orbit correction. This paper will show results for the one kicker scenario. A more detailed explanation of the entire system can be found in [2][3]. Details of the kicker magnet and pulser design can be found in [4].

## GLOBAL ORBIT DISTORTIONS

The ALS is a 12 sector, triple bend achromat with 4.5 meter straight sections for insertion devices. A convenient location to install an experimental kicker happens to be in the straight section 2.

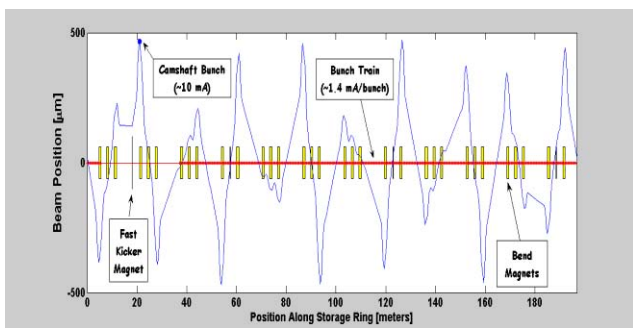


Fig. 1: Orbit Change for a One Kicker Magnet.

Using one fast kicker magnet running at the revolution rate (1.52 MHz) the camshaft bunch can be permanently put on a different closed orbit. Fig. 1 shows the change in

* This work was supported U.S. Department of Energy under Contract No. DE-AC03-76SF00098 and DE-AC03-76SF00515.

# ELECTRON BEAM DIVERGENCE MEASUREMENTS AT LOW ENERGIES USING A NOVEL OPTICAL DIFFRACTION RADIATION TRANSMISSION INTERFEROMETER

A.G. Shkvarunets, R.B. Fiorito, P. G. O'Shea, IREAP, University of Maryland, College Park, MD 20742, USA
J.G. Power, M.E. Conde and Wei Gai, ANL, Argonne, IL 60439, USA

*Abstract*

We have used an optical diffraction-transition radiation interferometer (ODTRI) in a transmission mode to measure the divergence of the low energy 8 MeV ANL-AWA electron beam. The interferometer employs a metallic micromesh first foil, which is used to overcome the inherent limitation due to scattering in the solid first foil of a conventional OTR interferometer, and an optically transparent dielectric foil. The interferences of forward directed ODR from the mesh and radiation from the dielectric foil is observed in transmission. This geometry allows a small gap between the foils (0.9 mm), which is required to observe fringes from two foils at low beam energies. The measured beam divergence is in a good agreement with that obtained using simulation code calculations. ODTRI measurements indicate that a single Gaussian distribution is insufficient to describe the angular distribution of the measured beam and that a second Gaussian beam faction or halo beam component is required to fit the data.

## INTRODUCTION

Conventional OTRI cannot be used for low emittance beams because scattering in the first foil of the OTR interferometer dominates and obscures the beam divergence (1μm of Aluminium scatters 8 MeV electrons by RMS θ ~ 5mrad). To overcome this problem we have devised a perforated foil (mesh) – solid mirror foil reflection interferometer [1, 2] which is useful at moderate beam energies (E > 50 MeV).

For low energy beams the inter foil spacing ($L \sim \gamma^2\lambda$) is too small to observe the interferences of forward ODR from the mesh and backward OTR from the mirror in a standard reflection geometry. For example, at beam energy E = 8 MeV and $\lambda$ = 632nm, L < 1 mm. To overcome this problem, we have developed a transmission interferometer [3, 4]. This interferometer uses a transparent dielectric foil as a second foil. The forward ODR produced by the mesh passes through the dielectric foil and interferes with forward radiation produced by the dielectric itself. A transport mirror is used to redirect the interfering radiations into the optical measurement system.

The radiation from the mesh is produced by two beam fractions: 1) unscattered electrons passing through the holes and 2) electrons heavily scattered in the mesh wires. Each component produces diffraction radiation ODR. Since no analytic theory for diffraction radiation from a matrix of holes in a metallic foil exists, we devised a simulation code (BEAMDR) to calculate the ODR from the two beam fractions.

A second code (CONVD) is then used to convolve the interferences of the ODR and OTR from the dielectric foil DOR with a given distribution of particle trajectory angles (typically a Gaussian distribution) and optical filter function. The latter is needed to produce distinct visible fringes for a given range of divergence. The essential part of code CONVD is the fitting procedure which varies the beam and interferometer parameters, and calculates the RMS deviation between the calculated and measured intensity distributions within some angular interval. The goal is to find a set of parameters which produces the minimum deviation. Beam divergence is one of the fitted parameters. A complete description of these codes is given in [2].

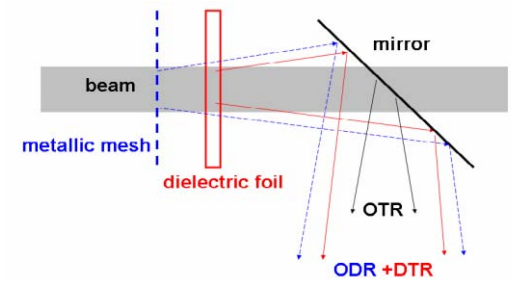


Figure 1: Mesh-dielectric foil interferometer.

There is a challenge in using dielectric foil in the interferometer, namely is to correctly prescribe the properties of optical dielectric optical radiation (DOR). In this work we use an additional measurement of OTR from metallic foil in order to "calibrate", the DOR from the kapton foil used in our interferometer and thus determine the parameters of the kapton foil.

## EXPERIMENTAL SETUP

An ODR-DOR interferometer was designed and used to measure the electron beam divergence of the Argonne National Lab's Advanced Wakefield Accelerator

# OVERVIEW OF BEAM INSTRUMENTATION AND DIAGNOSTICS FOR THE NSLS-II PROJECT*

Om Singh#` and Igor Pinayev, NSLS-II Project, BNL, Upton, NY 11973, U.S.A.

*Abstract*

A new, ultra-bright 3rd generation light source, the NSLS-II Project, is planned to be built at Brookhaven National Laboratory. The light source being developed will have unprecedently small beam horizontal emittance and will provide the radiation sources with a brightness of $3\times10^{21}$ photons/sec/0.1%BW/mm$^2$/mrad$^2$. In this paper we present the detailed specifications and a comprehensive description of the planned beam instrumentation system and the first results of the ongoing instrumentation R&D activities on beyond state-of-the-art subsystems.

## INTRODUCTION

The NSLS-II project will be a state-of-the-art synchrotron radiation facility [1,2] featuring ultra-high photon brightness with extremely low emittance. It consists of a 170–270 MeV S-band linac, 0.2–3 GeV ramping booster, transport lines and 3 GeV storage ring [3,4,5] with the latest available beam instrumentation and diagnostics systems. The storage ring consists of 15 identical superperiods, each consisting of two mirror symmetric DBA cells. There are alternating ID straights of 8.6-m long with high horizontal β for injection, RF, damping wigglers (DW), and high flux user ID's; and 6.6-m long with low β for narrow gap ID's for high brightness X-ray beams. Top-off injection once per minute will be necessary to maintain the stored beam current at 500 ± 5 mA. The main beam diagnostics related parameters for the storage ring are shown below in Table 1.

Table 1: NSLS-II Storage Ring Parameters

| Parameter | Nominal Value |
|---|---|
| Energy | 3.0 GeV |
| Circumference | 792 m |
| RF frequency | 499.68 MHz |
| Harmonic number | 1320 |
| Revolution period, $T_0$ | 2.642 μs |
| Number of bunches filled | 1056 (~80%) |
| Tunes - $Q_x$, $Q_y$ | 32.42, 15.15 |
| Emittance Bare Lattice $\varepsilon_0$ (H/V) | 2.05/0.01 nm-rad |
| Emittance with 8-DWs ε (H/V) | 0.51/0.008 nm-rad |
| Bunch length, rms natural | 2.9 mm; 10 ps |
| β-function at 8.6m ID ($\beta_x$, $\beta_y$) | 20/3.0 m |
| β-function at 6.6m ID ($\beta_x$, $\beta_y$) | 2.0/1.3 m |
| X,Y,E Damping times at 3 GeV | 5.4/5.1/2.5 ms |
| Synchrotron frequency, $f_s$ | 3.0-3.6 kHz |

*Work supported by the U.S. DOE under contract No DE-AC02-98CH10886
#singh@bnl.gov

To realize the benefits of the high brightness and small sizes of NSLS-II sources, photon beams must be exceedingly stable both in position and angle to the level of better than 10% of beam sizes and divergence. Table 2 provides the electron beam sizes and angular divergences for selected NSLS-II sources.

Table 2: The Electron Beam Sizes and Divergence

| Types of source | 8.6m ID | 6.6m ID | Bend magnet | 1-T 3-Pole wiggler |
|---|---|---|---|---|
| $\sigma_x$ (μm) | 108 | 29.6 | 44.2 | 175 |
| $\sigma_{x'}$ (μrad) | 4.6 | 16.9 | 63.1 | 14 |
| $\sigma_y$ (μm) | 4.8 | 3.1 | 15.7 | 12.4 |
| $\sigma_{y'}$ (μrad) | 1.7 | 2.6 | 0.63 | 0.62 |

The most stringent beam measurement and stability requirement will be for the vertical position at the short ID source ($\sigma_y$=3.1 μm); this will require special consideration for measuring both electron and photon beams. Instrumentation requirements for measurements are further discussed in the storage ring section.

## INJECTION DIAGNOSTICS

The diagnostics for the injection system will be procured with the subsystems with exception of beam transfer lines. The specifications for the required instrumentation will be provided for vendors by NSLS-II project team.

### *Linac*

The linac beam instrumentation comprises two integrating current transformers for monitoring total bunch train charge and one fast current transformer (FCT) to monitor the distribution of charge. In routine operations, the beam trajectory will be monitored with three monopulse beam position monitors. Fluorescent screens will complement beam position monitoring during studies periods and for measuring beam emittance and energy spread at the linac exit. Wall current monitors formed by equally spaced broadband ceramic resistors mounted on a flexible circuit board, wrapped around a short ceramic break, will also give information on beam charge as well as longitudinal profiles of electron bunches. Linac diagnostics are summarized in Table 3.

### *Booster*

The following booster beam parameters will be monitored:

- orbit,
- working point (tunes),
- circulating current and filling pattern,
- emittances for both planes,
- bunch length.

# LOW ENERGY BEAM DIAGNOSTICS AT THE VENUS ECR ION SOURCE*

D.S. Todd#, D. Leitner, and M. Strohmeier, LBNL, Berkeley, CA 94720, U.S.A.

*Abstract*

A dedicated effort to accurately simulate beam extraction and transport from the superconducting electron cyclotron resonance (ECR) ion source VENUS (Versatile ECR for NUclear Science) using particle-in-cell methods has been underway at Lawrence Berkeley National Laboratory (LBNL). The wide range of beam diagnostics used along the VENUS transport system has been essential in benchmarking simulation against experiment. Measurements with some of these devices are presented and are compared with simulation.

## INTRODUCTION

The fully-superconducting electron cyclotron resonance (ECR) ion source VENUS at LBNL serves as the prototype injector for the future radioactive ion beam accelerator in the United States [1]. Additionally, a dedicated effort at LBNL has been underway to develop a highly-adaptable, particle-in-cell simulation code to serve as a design tool for future sources and accelerators [2]. Benchmarking simulations against experiment plays a crucial role in model development, and for this reason the transport system for the VENUS ion source has been outfitted with a wide range of diagnostic devices.

Plasma confinement in an ECR ion source is provided through the superposition of solenoidal and sextupolar magnetic fields. Solenoids at each end of the source and a surrounding sextupole produce a confining magnetic field whose magnitude increases in all directions from the source center. This source-centered minimum is surrounded by a series of closed surfaces of constant magnetic field magnitude, and by supplying microwave heating at a frequency matching the electron cyclotron frequency on one or more of these surfaces electrons can be resonantly heated to produce and maintain a plasma through step-wise ionization.

Though the field geometry in ECR ion sources has proven very effective for producing high-current, multiple-charged ion beams, there are inherent characteristics of these sources which make difficult both analysis and simulation of extracted beams including:

- Superposed magnetic field confinement produces asymmetric plasma distributions at extraction
- Plasma is maintained through step-wise ionization, therefore extracted heavy ion beams are typically composed of thirty or more ion species
- Positional distribution of different ion species at the plasma extracting face is unknown
- Beams are extracted at a peak solenoidal magnetic field of up to 3 tesla which falls to zero over the first half-meter of travel giving each extracted ion species a different dynamical behavior
- Beam space charge self fields must be taken into account

From the outset, beam diagnostics have played an important role in the improvement of VENUS ion beam models. As an example, initial simulations of ion distributions at the plasma aperture indicated that while the plasma distribution had a triangular cross section, as expected, this distribution was much larger than the 8-mm diameter beam extraction aperture, was homogenously filled, and should have resulted in an axially-symmetric extracted beam. However, as can be seen in figure 1, imaging of a single species ion beam ($He^+$) on a 0.25-mm thick tantalum sheet just after extraction shows a triangular cross-section, making it clear that the initial conditions used for the simulation were invalid. As the initial ion beam distribution at the source extraction aperture is unknown and cannot be directly measured or computed, we are using various ion beam diagnostics to refine our simulation model as described in the following sections.

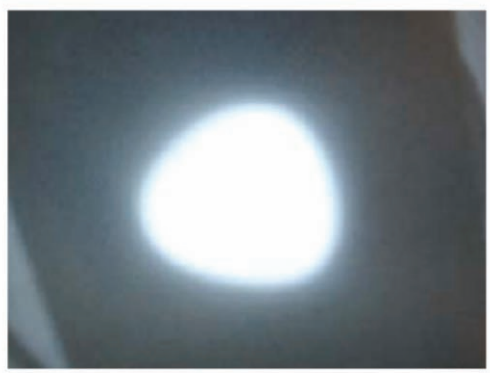

Figure 1: Beam imaging of a $He^+$ beam with the tantalum sheet, left, shows triangular beam structure 80 cm after extraction.

## PARTICLE-IN-CELL SIMULATION OF VENUS EXTRACTION AND TRANSPORT

The layout of VENUS and its accompanying beam transport system are shown in figure 2. Beams are extracted across potentials of up to 30 kV, and the shape of the extracting surface of the plasma can be optimized by a movable accel-decel extraction system. A solenoid lens and a mass analyzing dipole magnet serve as the only two optical elements after the source when used for ion

* Work supported by the Director, Office of Energy Research, Office of High Energy & Nuclear Physics, Nuclear Physics Division of the U.S. Department of Energy under Contract DE AC03-76SF00098
#dstodd@lbl.gov

# PHASE MEASUREMENTS FOR GANIL AND LANL

B. Baricevic, T. Karcnik, Instrumentation Technologies, Solkan, Slovenia

*Abstract*

Libera Brilliance has proved successful in the field of beam diagnostics. High performance, system reliability and its high level of integration into accelerator control systems makes Libera a very accurate, robust and powerful measuring system. Although Libera Brilliance has been developed mainly for applications involving frequency domain processing, the flexibility makes it a good time domain measuring system for single pass applications. Moreover, there are other applications dealing with pulses, where a modified version of Libera Brilliance can be used. This is the case of beam phase and position measurements in accelerators, like Spiral2 (Ganil) and LANSCE (Los Alamos), dealing with heavy particles (protons, deuterons and heavy ions). The phase information extracted by the measurement in such systems is used to control the acceleration process of such heavy particles. This paper shows the approach adopted in processing the signals produced by such bunch trains. A modified Libera Brilliance unit, configured for the LANSCE bunch trains, has been tested by means of extensive laboratory measurements. Performance has been evaluated by applying different digital signal processing.

## INTRODUCTION

Libera Brilliance is a very accurate beam position measuring system. Although its performance was improved for applications in circular electron machines, the Libera Brilliance processing structure is flexible enough to fulfil the requirements of applications requiring an accurate signal measurement in time domain too.

The scope of the phase measurement is to control the acceleration processes of heavy particles. Two applications with similar requirements for the beam position and phase measuring system were taken as reference.

The first application is the LANSCE linac, where bunches of $H^+$ and $H^-$ are accelerated. The bunches in the fundamental scheme have a repetition frequency of 201.25 MHz and are grouped in 0.625 ms long "macropulses" at the repetition rate of 30 Hz that results in a duty factor of 1.875%.

The second application is the Spiral2 linac (Ganil), where the deuteron or ion bunches are accelerated with bunching frequency of 88.0505 MHz, and are organized in "macropulses" with minimum duration of 100 us and repetition rate between 1 and 10 Hz. The minimum duty factor is in this case 0.01 %.

Table 1 compares the mentioned parameters for the two applications. The very low duty factors indicate that the signals produced by such beam signals need a time domain processing scheme, since the power is spread between the "macropulse" repetition rate harmonics.

Table 1: Macroplulse structure comparison

| | **LANSCE linac** | **Spiral 2 linac** |
|---|---|---|
| Bunch rep. rate | 201.25 MHz | 88.0505 MHz |
| Macropulse length | 0.625 ms | >0.1 ms |
| Macropulse rep. rate | 30 Hz | 1÷10 Hz |
| Duty factor | 1.875 % | >0.01 % |

The particles with the specified time structures cross stripline BPM pickups and excite bipolar pulses on four coaxial lines. The bunch repetition rate defines the main frequency component. Since the BPM pickup is time-invariant, the beam longitudinal shifts with respect to the RF reference are linearly transformed into a phase deviation of the main frequency component from the RF reference and therefore a phase measurement of the fundamental frequency can be used to adjust the set points of the LLRF system that controls the acceleration process.

## MEASURING SYSTEM REQUIREMENTS

An amplitude and phase measurement is performed on the main bunch frequency component, at the bunch repetition rate. The phase is measured with respect to an RF reference signal, provided by the accelerator timing system, at the same frequency of the bunch repetition rate. Table 2 shows the main requirements relevant to the measurement.

Table 2: Measurement requirements and additional parameters

| **Parameter** | **LANSCE linac** | **Spiral 2 linac** |
|---|---|---|
| Bunch rep. rate | 201.25 MHz | 88.0505 MHz |
| Input power range | 50 dB | 40 dB |
| Position repeatability | 100 um | ±10/±100 um |
| Phase repeatability | 0.25 deg | ±0.5 deg |
| Pickup position sensitivity | 1.26 dB/mm | 2.5 dB/mm |

The signal level varies inside the specified input range depending on the particles' charge. The pickup position sensitivity is a geometrical parameter defined by the pickup dimensions. The phase repeatability is expressed

# Beam Induced Fluorescence (BIF) Monitor for Intense Heavy Ion Beams *

F. Becker[1†], C. Andre[1], F. M. Bieniosek[3], P. Forck[1], P. A. Ni[3], D.H.H. Hoffmann[2]
[1]GSI, Darmstadt, Germany; [2]TUD, Darmstadt, Germany; [3]LBNL, Berkeley, USA

*Abstract*

Non-intercepting **B**eam **I**nduced **F**luorescence (**BIF**) monitors measure transversal beam profiles by observation of fluorescence light originating from excited residual gas molecules. Thus they are an alternative to conventional intercepting devices. Single photon counting is performed using an image intensified digital CCD camera. We investigated the BIF process in the energy range of 7.7 keV/u to 750 MeV/u in residual nitrogen. Experiments at low beam energies were performed at a Marx-accelerator (NDCX) at Berkeley Lab [1] whereas mid and high energy experiments were carried out at GSI accelerators [2, 3]. Especially in the vicinity of targets the neutron-generated radiation level limits the monitor's signal to background ratio. Therefore the radiation background was investigated for different ion species and particle energies. Background simulations using a Monte Carlo transport code are compared to experimental data taken with scintillators, thermo luminescence detectors and the BIF monitor. Alternative image intensifier techniques are presented as well as shielding concepts. Furthermore the dynamics of ionized nitrogen molecules in the electric field of intense ion beams is discussed.

## THE BIF METHOD AND APPLICATION

When beam ions collide with residual gas molecules, some molecules are ionized remaining in an excited state with a certain probability. In a $N_2$-dominated residual gas composition, a strong fluorescence at 390 nm $< \lambda <$ 470 nm (blue), of about 60 ns lifetime, is generated by a transition band to the $N_2^+$ electronic ground state ($B^2\Sigma_u^+(v') \rightarrow X^2\Sigma_g^+(v'')+\gamma$, for vibrational levels $v$) [4]. 'Single-photon counting' was performed with a commercial image intensifier [5], equipped with a double Micro-Channel Plate (MCP) for up to $10^6$-fold photo-electron amplification. Green light from a P46 phosphor screen of 300 ns decay time is taper-coupled to a digital CCD camera with a IEEE-1394a interface [6]. The device is mounted on a fused silica viewport at a distance of 20 cm from the beam axis. Remote controlled CCTV lenses with focal distances of 8 to 25 mm, lead to typical resolutions of 100-500 $\mu$m/pixel. Beam profiles were recorded on a single shot basis. To select specific transitions, 10 nm narrow band interference filters were installed in the optical path. A more detailed description of the experimental setup can be found in [7, 8, 9, 11].

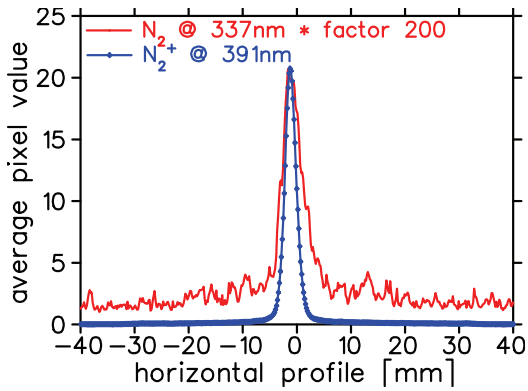


Figure 1: Beam profiles of a 10$\mu$A 5.4 MeV/u $Ni^{6+}$ beam in $10^{-3}$mbar nitrogen, recorded with spectral filters [9]. The $N_2^+$ profile @ 391nm shows a $\sigma$ of 1.1mm whereas $N_2$ profile @ 337nm has a $\sigma$ of 2mm.

This paper will focus on issues related to the challenging beam parameters of the FAIR-facility [3] like energies well above 100 MeV/u in considerable loss induced radiation environments and E-field induced profile falsifications for intense and strongly focused beams. During the last years the BIF method was applied successfully at the GSI heavy ion LINAC for various ion species and energies between 5 and 11.4 MeV/u [7, 8, 9]. An additional setup was installed behind the heavy ion synchrotron SIS-18 in a high energy beam transfer line (HEBT) close to a dump. Due to the beam energy between 60 and 750 MeV/u this location allowed to determine the radiation impact on the detector performance. In addition this part of the beam pipe was separated by vacuum windows so that residual gas densities from base-pressure $10^{-8}$ mbar up to atmospheric pressure could be applied. Systematic investigation of profile falsifications have shown that beam profile width remains constant up to nitrogen pressures of about 1 mbar and also, that $N_2$ transitions lead to increased profile width $\geq$40% compared to ionic $N_2^+$ transitions [9], see Fig.1. Cross sections for heavy ion induced transitions in $N_2^+$ are predominant compared to electron induced transitions. Unlike transitions in neutral working gases ($N_2$) which show enlarged beam profiles due to the secondary electron halo [10]. Although the contribution of $N_2$ transitions is $\leq$ 20% and in the near UV, it should be suppressed by optical filters and discriminated against the desirable $N_2^+$ transitions at (391, 428, 470nm) [9]. For typical beam parameters at GSI LINAC and high energy beam transfer lines, profiles recorded with the BIF-monitor complied with SEM-grid (Secondary Electron Monitor) measurements within 10% [11], see Fig.2.

* Work supported by EU, project FP6-CARE-HIPPI
† Frank.Becker@gsi.de

# A SOFTWARE UPGRADE FOR THE SNS WIRE-SCANNER*

W. Blokland, C. Long, ORNL, Oak Ridge, TN 37831, U.S.A.

*Abstract*

The SNS Beam Instrumentation Group has designed new software for all wire scanners at SNS. The original wire-scanner software was written by one of the Spallation Neutron Source (SNS) partners, Los Alamos National Laboratory. This software was designed for the types of wire-scanners initially planned and their usage at that time. New variations in the wire-scanner hardware added gearing, different position read-back methods, and a timing card. The new software handles these hardware variations in a flexible manner through configuration control files. The software upgrade allows the user to synchronize the stepping of the fork with external applications, such as with loss monitors to calibrate energy dependence of the beam losses caused by the wire. Another new functionality allows physicists to select what part of the beam pulse is used to determine the transverse profile after the data has been taken. This avoids time-consuming rescans in case the timing was not initially correct. The new software, also a LabVIEW program, is structured around a state-machine with sequence capabilities to manage the complexities of stepping through a scan and interacting with the user. This paper discusses the new software features, the implementation, and the obtained results of field tests.

## INTRODUCTION

Wire-scanners are used in the warm linac and the transfer lines to determine the transverse profiles of the accelerated particle beam. During a scan a fork holding three wires, one horizontal, one vertical, and one diagonal wire is stepped through the beam. As the beam hits each wire, it deposits on or strips charge from the wire. The resulting signal is low-pass filtered (30kHz) to reduce noise and sampled by a digitizer (up to 1Mhz). The sum of the trace at each step is plotted versus the wire position to create the transverse profiles.

The SNS accelerator was built in phases with different labs designing and supplying the wire-scanner hardware.

The software for these scanners was implemented by LANL and tested with the first wire-scanners at Berkeley, [1]. This software has now been successfully used for over 5 years. However, due to several factors it was decided that the software needed to be upgraded.

One factor was that new wire-scanner actuators, see Figure 1, has been developed that uses different motors, gearing, and position read-back methods. The old software has trouble handing these new variations leading to incomplete scans. Its code would have to be modified for each new style resulting in different versions, or a significant rewrite of the old code would have to be done.

Another factor is that the old software uses the ActiveX interface to Channel Access. This was the only available LabVIEW to Channel Access interface available to us at the time. Now most SNS diagnostic instruments use the Shared Memory IOC, which has faster processing and has a quicker response than the ActiveX interface.

Another motivation is the need for additional features. One important feature is the synchronization of the scan, the stepping through the beam, with an external application such as the Loss Monitor. By giving the loss monitor program control over the stepping of the wire-scanner, we can determine the energy dependency of the loss monitors.

Taking a scan from single wire-scanner can take several minutes. Often a scan has to be redone because the timing was not quite right. During studies the beam parameters are often adjusted, for example from a chopped beam to an unchopped beam. This change in the beam also requires a change in the setup parameters of the wire scan. To get these scan parameters just right can take several scans. At several minutes per scan this can become quite time-consuming.

All these factors combined lead us to the decision to rewrite the program.

Figure 1. Photo of a new CCL wire-scanner actuator.

* ORNL/SNS is managed by UT-Battelle, LLC, for the U.S. Department of Energy under contract DE-AC05-00OR22725

# CLOSED LOOP WIRE SCANNER ACTUATOR CONTROL FOR LANSCE ACCELERATOR BEAM PROFILE MEASUREMENTS*

Stanley Cohen, Sandeep Babel (BiRa, Albuquerque, New Mexico),

J. Douglas Gilpatrick, James D. Sedillo (LANL, Los Alamos, New Mexico),

David A. Bonal, Murali M. Ravindran (National Instruments, Austin)

*Abstract*

The design and test of a new beam-profile wire-scanner actuator for the LANSCE (Los Alamos Neutron Science Center) 800-MeV proton linear accelerator is described. Previous actuator implementations use open-loop stepper-motor control for position indexing. A fixed-frequency, fixed-duration pulse train is sent to the stepper motor driving the linear actuator. This has lead to either uncertainties in position due to mechanical resonances and electrical noise or slowing down actuator operation..

A real-time, closed loop control system is being developed and tested for more repeatable and accurate positioning of beam sense wires. The use of real-time controller allows one to generate a velocity profile for precise, resonance-free wire position indexing. High radiation levels in the beam tunnel, dictate the use of an electro-magnetic resolver, typically, used in servo applications, as the position feedback element. Since the resolver is an inherently analog device, sophisticated digital signal processing is required to generate and interpret the waveforms that the feedback mechanism needs for positioning. All of the electronic and computational duties are handled in one the National Instruments compact RIO real-time chassis with a Field-Programmable Gate Array (FPGA)

## DESIGN CONTRAINTS

### *Timing and Physical Environment*

Beam-profile wire scanners present a number of electrical and mechanical challenges for designers.. Achieving accurate, repeatable and rapid wire positioning is a key function that must be addressed to obtain reliable beam-intensity data in a timely manner. The high beam intensity, itself, limits the parameter space of what kinds of electronics and materials can be used in the wire-scanner design.

This report is focused on controlling wire-scanner position using the National Instruments cRIO system and getting the actuator movement in the FPGA of cRIO under close-loop conditions., For this first set of tests we are using a wire scanner assembly from the decommissioned LEDA project[1,2]. Operating the wire scanner with closed-loop control is one of the essential requirements for the beam diagnostics refurbishment of the 30-year-old LANSCE proton linear accelerator at Los Alamos [3, 4].

* Supported by LANL Contract SBA 030608

Incorporating closed-loop motion control for the positioning the wire will provide a more accurate picture of the proton beam profile than practice of using open-loop stepper-motor positioning.

Motion control in this design demands that the position for each intensity measurement be achieved during the 8ms between beam macropulses. That is the mechanism must move and settle, between beam pulses, before there is request to measure the beam intensity at that location.

## ACHIEVING CLOSED-LOOP MOTION WITH A STEPPER MOTOR

### *Mechanically Quantized Motion*

Using a stepper motor within a closed-loop motion control context introduces quantized motion into the system. The rotational motion of the motor cannot be moved to an arbitrary rotational angle. This can be mitigated somewhat, by microstepping the motor, but this slows down its rotational speed, hence the maximum linear velocity of the wire housing. Motion is, ultimatedly controlled by a computer. This has implications for the motor-control algorithm, since all I/O must be digitized. The wire cannot be positioned with arbitrary accuracy, using an analog to digital converter, (ADC) in conjunction with a linear encoder, may further limit the position accuracy. This limitation and the former quantization effects means that the wire can be positioned to the commanded position within, ±ε, a small error. This will determine the convergence criterion for reaching a position setpont.

### *Wire Scanner Physical Environment and Constraints*

Why use a stepper motor, at all, since servo motors are available? A stepper has the advantage of having detent torque or “holding torque”, when it’s stopped. This keeps the wire stationary without an explicit program for the stopped motion. It is assumed that the detent torque is great enough to overcome competing mechanical forces on the wire assembly. The stepper motor comes to a complete stop, when command signals are inhibited. This is advantageous for keeping the beam-sense wire steady for sensing the particle beam charge.

### *Linear Position Feedback Elements*

The choice of feedback elements for the LANSCE-accelerator is limited, since radiation levels are high

# ELECTRON BEAM TIMING JITTER AND ENERGY MODULATION MEASUREMENTS AT THE JLAB ERL*

P. Evtushenko#, D. Sexton, Jefferson Lab, Newport News, VA USA

*Abstract*

When operating JLab high current ERL a strong reduction of the FEL efficiency was observed with the increase of the average current of the electron beam. Investigating the FEL efficiency drop-off with the electron beam average current we have measured the electron beam phase noise and the fast energy modulations. The phase noise is a variation of the time arrival of the electron bunches to the wiggler. It could be a very effective way of reducing the FEL efficiency especially when the driver accelerator for the FEL is operated with the RMS bunch length of about 150 fs. Under a fast energy modulation we denote a modulation which can not be followed by the FEL due to its time constant, defined by the net FEL gain. Such a modulation also could be a possible cause of the efficiency drop-off. Making the measurements we could rule out the FEL efficiency drop-off due either the fast energy modulation or the phase modulation. We also have learned a lot about instrumentation and techniques necessary for this kind of beam study.

## ELECTRON BEAM PHASE NOISE MEASUREMENTS

Investigating the FEL efficiency drop-off with the electron beam average current we have measured the electron beam phase noise and the fast energy modulations. The so-called phase noise is essentially a variation of the time arrival of the electron bunches to the wiggler. That could be a very effective way of reducing the FEL efficiency if one takes in to account that the accelerator is routinely operated with the RMS bunch length of about 150 fs [1]. Under a fast energy modulation we denote a modulation which can not be followed by the FEL due to its time constant, defined by the net FEL gain. Such a modulation also could be a possible cause of the efficiency drop-off. The two effects are strongly connected in the FEL driver accelerator due to the longitudinal phase space transformation, i.e., longitudinal bunch compression. The simplified view of the longitudinal phase space transformation is a rotation of a long and low energy spread beam at the injector by ~90 degrees in the longitudinal phase space so that the bunch length minimum is located in the wiggler [2]. Under such a transformation an energy modulation in the injector would get transferred in to a phase modulation at the wiggler and a phase modulation in the injector would gets transferred in to an energy modulation at the wiggler.

The technique we use for the phase noise characterization of the electron beam was originally

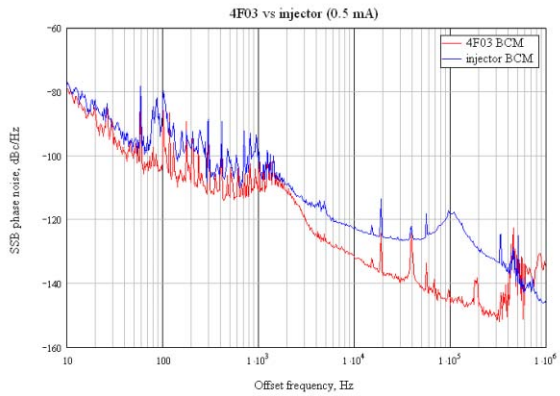


Figure 1 a: Single sideband spectrum measured at 0.5 mA

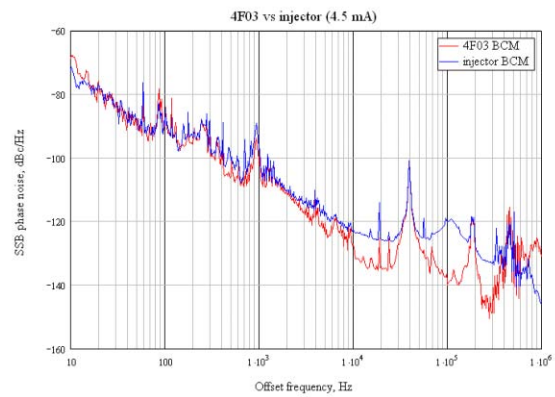


Figure 1 b: Single sideband spectrum measured at 4.5 mA

developed for noise characterization of ultra fast lasers [3]. It was shown that both phase noise and amplitude noise information can be extracted from the power spectrum measurements of the electron beam intensity. The power spectrum of the electron beam is a comb with spectral lines separated by the frequency of the bunch repetition rate. The envelope of the spectrum is determined by the longitudinal profile of a single bunch. Both the amplitude AM and phase modulation PM (or noise) of the beam intensity manifest themselves in the power spectrum as the sideband modulations of the spectral lines of the comb spectrum. It was shown in [3] that amplitude of the sideband modulations seen relative to the carrier amplitude changes differently with the harmonic number for AM and PM. The relative amplitude of the sidebands due to the amplitude noise does not change with the harmonic number, whereas the relative amplitude of the phase noise increase as $\mu^2$, where $\mu$ is the harmonic number. Thus measurements of sideband

* Work supported by the U.S. DOE contract # DE-AC05-06OR23177
# Pavel.Evtushenko@jlab.org

# COUPLING CORRECTION IN NSLS X-RAY RING

M. Fedurin#, I. Pinayev, BNL, Upton, NY, 11973, U.S.A.

*Abstract*

In this paper we present an algorithm for coupling correction in storage ring based on monitoring the vertical size of a stored beam, while varying skew quadrupoles. The details of the algorithm are realized as a Matlab script and experimental results of its application are presented.

## CORRECTION METHOD

There are 17 skew quadrupoles (Table 1) distributed around the X-ray ring, as well as beam profile, could be measured on pin-hole camera monitor (Fig.1). All this is enough to try to find the optimal skew quad configuration to minimize vertical beam size.

Varying one skew quad setting in defined range will affect the beam size change. So, one iteration cycle has this sequence: 1) find optimal quadrupole setting for minimal vertical beam size; 2) set it up and then turn to vary next quads; 3) make one pass for all quadrupoles; and 4) correct beam displacement after each pass or keep beam position feedback on all the time.

### *Optimal skew quadrupole setting*

The quadrupole variation range was made small, to avoid disturbing beam position too much or reaching the trim-current saturation limit if orbit feedback is running all the time. The skew quadrupole current was varied in 5 equal steps and beam size was measured by pin-hole camera beam profile monitors at every step. Then a polynomial curve fit on measured data was used to find the local extremum. Three possible types of extrema could be found in that way (Fig. 2): 1) extremum located on one of the edges of the range; 2) inside range; and 3) value corresponding to maximim, not minimum, beam size—in this case, sign check of second derivative always followed finding the value .

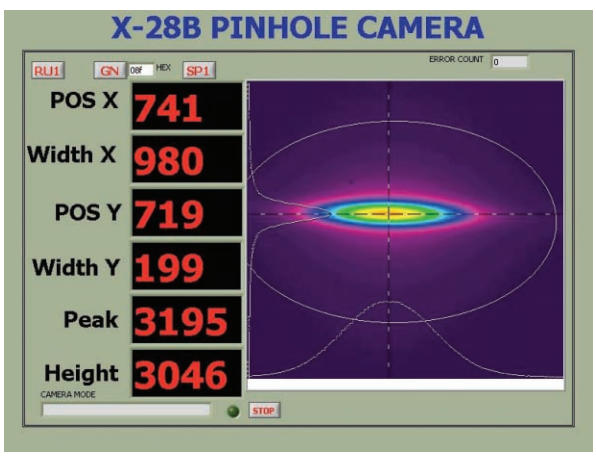


Figure 1: Pin-hole camera monitor located at X28 beamline used for beam profile measurements.

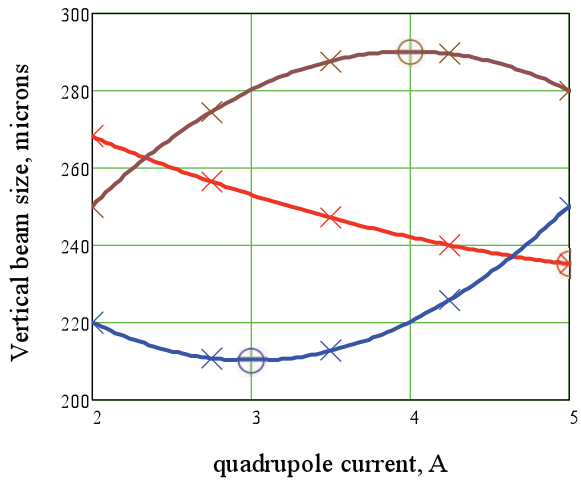


Figure 2: Three different types of local extremum: extremum located on one of the edges of the range (red curve), inside range (blue curve), and extremum value correspond maximum beam size (brown curve)

## CORRECTION SCANS

Before starting the correction process, all skew quadrupoles are set to zero. After the first pass, skew quadrupole settings bring vertical beam size down from 570 μm to 425 μm. Each other iteration step changes size value down, and after 9 passes goes below 300 μm. Every beam profile measurement is averaged over 10 seconds, so each quadrupole scan takes about 1 minute, and a whole pass about 20 minutes.

Skew quadrupole scan history is presented in Fig. 3 and vertical beam size changes in Fig. 4. It is noticeable that some quadrupoles reach saturation when making big steps in iterations. During the scan all three types of local extrema were observed but logic in the script code makes it choose the correct value.

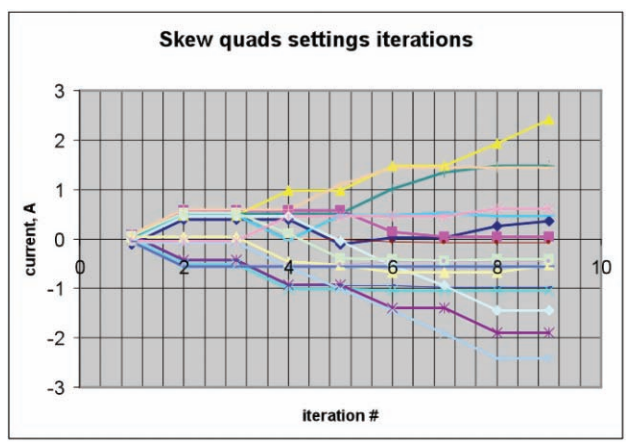


Figure 3: History of skew quadrupole current settings.

# CONSIDERATIONS ON ODR BEAM-SIZE MONITORING FOR GAMMA = 1000 BEAMS*

A.H. Lumpkin, Fermilab, Batavia, IL, U.S.A. 60510
C.-Y. Yao, Argonne National Laboratory, Argonne, IL U.S.A. 60439
E.Chiadroni, M. Castellano, LNF-INFN, Frascati, Italy, A. Cianchi, Univ. of Rome Tor Vergata

*Abstract*

We discuss the feasibility of monitoring the beam size of γ=1000 beams with 3000 times more charge in a video frame time and with a more sensitive 12- to 16-bit camera than were used in the previous electron beam studies at 7 GeV at the Advanced Photon Source. Such a beam would be generated at Fermilab in a new facility in the coming years. Numerical integrations of our base model show beam size sensitivity for ± 20% level changes at 200- and 400-μm base beam sizes. We also evaluated impact parameters of 5 $\sigma_y$ and 12 $\sigma_y$ for both 800-nm and 10-μm observation wavelengths. The latter examples are related to a proposal to apply the technique to an ~ 0.98 TeV proton beam, and this study shows there are trades on photon intensity and beam size sensitivity to be considered at such gammas. In addition, we report on first results at γ=1800 on a superconducting rf linac.

## INTRODUCTION

Characterization of the high-power electron beams of the superconducting rf (SCRF) accelerator to be installed in the New Muon Laboratory (NML) building at Fermilab will be an important aspect of the project [1]. Beam size, position, divergence, emittance, and bunch length measurements are all of interest. Due to the projected high beam power with 3000 micropulses of up to 3 nC each in a macropulse at 5 Hz at eventually up to 1800 MeV, the need for nonintercepting (NI) diagnostics is obvious. Although position is readily addressed with standard rf beam position monitors (BPMs), the transverse size, and hence emittance, are less easily monitored noninterceptively in a linear transport system. Besides an expensive laser-wire system, one of the few viable solutions appears to be the use of optical diffraction radiation (ODR) [2-8] which is emitted when a charged-particle beam passes near a metal-vacuum interface. Appreciable radiation is emitted when the distance of the beam to the screen edge (impact parameter) $b \sim \gamma\lambda/2\pi$, where γ is the Lorentz factor and λ is the observation wavelength. Previous near-field imaging experiments at the Advanced Photon Source (APS) with 7-GeV beams used an impact parameter of 1.25 mm from a single edge of a plane as compared to the scaling factor of ~1.4 mm (with an assumed operating wavelength of 0.628 μm) [7]. The near-field images were obtained with a single, 3-nC micropulse using a standard CCD camera. Since for the NML case, with its much lower gamma, the fields are reduced exponentially as $e^{-2\pi b/\gamma\lambda}$. We either have to use the longer wavelengths in the NIR or FIR or have more charge integrated in the image and a more sensitive camera. The NML design-goal beam intensity gives a factor of 3000, and the intensified or low-noise camera should give another factor of 1000. These two factors combined should allow visible to IR near-field imaging of a beam that is up to 10 to15 times lower in gamma than the APS case, if similar impact parameters can be used.

We considered focus-at-the-object or near-field imaging optics and established that the perpendicular polarization component of ODR has the beam-size sensitivity that would be needed for a transport line with 400- to 1000-μm rms sizes in the x-plane. These parameters are compatible with the proposed test-area location in the lattice after the SCRF linac [1] as shown in Fig. 1. In addition, we evaluated the possible extension of the technique to a very high intensity hadron beam with γ~1000 as would be found in the Fermilab Tevatron [2,10]. In the latter application, we also consider a larger impact parameter constraint and the possible compensation of the consequently reduced signal by going to much longer wavelengths. We show there are trades to be considered in this paradigm.

## ANALYTICAL BACKGROUND

The basic strategy is to convert the particle–beam information into optical radiation and to take advantage of the power of imaging technology to provide two-dimensional displays of intensity information. These images can be processed for beam size information. Possible radiation sources are optical transition radiation (OTR), ODR, and optical synchrotron radiation (OSR). For completeness, the near-field ODR model as described in Ref. 6 is provided here.

As stated before, ODR is produced when an electron beam passes near a region where different dielectric materials are present. This is generally a vacuum-to-metal interface, and the theory [3-6] is usually for the *far-field* diffraction pattern produced by a beam passing through apertures or slits in conducting planes. In the present case, we effectively integrate over angle and frequency since our optical system is focused on the ODR source itself, i.e. the *near-field* image on the screen. Therefore we proposed a simplified model of the

*Work supported by U.S. Department of Energy, Office of Science, Office of High Energy Physics, under Contract No. DE-AC02-06CH11357.

# INITIAL SYNCHROSCAN STREAK CAMERA IMAGING AT THE A0 PHOTOINJECTOR*

A.H. Lumpkin and J. Ruan, Fermilab, Batavia, IL U.S.A. 60510

*Abstract*

At the Fermilab A0 photoinjector facility, bunch-length measurements of the laser micropulse and the e-beam micropulse have been done in the past with a single-sweep module of the Hamamatsu C5680 streak camera with an intrinsic shot-to-shot trigger jitter of 10 to 20 ps. We have upgraded the camera system with the synchroscan module tuned to 81.25 MHz to provide synchronous summing capability with less than 1.5-ps FWHM trigger jitter and a phase-locked delay box to provide phase stability of ~1 ps over 10s of minutes. This allowed us to measure both the UV laser pulse train at 244 nm and the e-beam via optical transition radiation (OTR). Due to the low electron beam energies and OTR signals, we typically summed over 50 micropulses with 1 nC per micropulse. We also did electron beam bunch length vs. micropulse charge measurements to identify a significant e-beam micropulse elongation from 10 to 30 ps (FWHM) for charges from 1 to 4.6 nC. This effect is attributed to space-charge effects in the PC gun as reproduced by ASTRA calculations. Chromatic temporal dispersion effects in the optics were also characterized and will be reported.

## INTRODUCTION

The opportunity for a new series of streak camera experiments at the Fermilab A0 photoinjector was recognized in the last year. The enabling upgrade was adding the synchroscan option to the existing C5680 Hamamatsu streak camera mainframe. By locking this module to the 81.25 MHz subharmonic of the rf system, the synchronous summing of micropulses could be done with trigger jitter of <1.5 ps (FWHM) for both the UV drive laser component at 244 nm and the e-beam via optical transition radiation (OTR) measurements [1,2]. The synchronous summing of the low OTR signal from the 15-MeV electron beam micropulses allowed the needed bandpass filters to be utilized to reduce the chromatic temporal dispersion effects inherent to the broadband OTR source and the transmissive optics components. In addition, the C6768 delay module with phase feedback was also acquired, and this stabilized the streak camera sweep relative to the master oscillator so that camera phase drift was much reduced to the ps level over 10s of minutes. This latter feature allowed a series of experiments to be done on the bandwidth effects and transit time effects in the respective transport lines. After characterizing the UV laser bunch length, a series of e-beam experiments on the A0 beamlines was performed. We have measured a significant bunch-length elongation versus micropulse charge for the present conditions and show that this is consistent with ASTRA calculations. We also observed a micropulse slice emittance effect for charges of 4 nC per micropulse. In the course of our experiments, we have done a series of tests on the chromatic temporal dispersion effects for this particular input optics barrel with UV transmitting optics and our optical transport lines. We show our effects our less than that reported at SSRL at PAC07 with optical synchrotron radiation (OSR) [3], but ours still have to be characterized carefully to allow accurate bunch-length measurements using the OTR in our case. Finally, we report measurements of the bunch compression in a double-dogleg transport line as a function of the upstream 9-cell accelerator rf phase.

*Work supported by U.S. Department of Energy, Office of Science, Office of High Energy Physics, under Contract No. DE-AC02-07CH1135.

## EXPERIMENTAL BACKGROUND

The tests were performed at the Fermilab A0 photoinjector facility which includes an L-band photocathode (PC) rf gun and a 9-cell SC rf accelerating structure which combine to generate up to 16-MeV electron beams [4]. The drive laser operates at 81.25 MHz although the micropulse structure is usually counted down to 9 MHz. Previous bunch length measurements of the drive laser and e-beam [2] were done with the fast single-sweep module of the Hamamatsu C5680 streak camera with an inherent shot-to-shot trigger jitter of 10 to 20 ps. Such jitter precluded synchronous summing of the short pulses. We have upgraded the camera by acquiring the M5676 synchroscan module tuned to 81.25 MHz with a trigger jitter of less than 1.5 ps (FWHM) and the C6878 phase-locked delay unit which stabilizes the camera phase over 10s of minutes. Due to the low, electron-beam energies and OTR signals, we typically synchronously summed over 50 micropulses with 1 nC per micropulse. The tests were performed in the straight-ahead line where energizing a dipole sends the beam into a final beam dump. The setup includes the upstream corrector magnets, quadrupoles, rf BPM, the YAG:Ce/OTR imaging stations, and the beam dump as schematically shown in Fig. 1. The initial sampling station was chosen at Cross #9, and an optical transport system using flat mirrors and a parabolic mirror brought the light to the streak camera. A short focal length quartz lens was used to focus the beam image more tightly onto the streak camera entrance slit. The quartz-based UV-Vis input optics barrel transferred the slit image to the Hamamatsu C5680 streak camera's photocathode.

Alternatively, the 4-dipoles of the emittance exchange line could be powered and experiments done at an OTR station, Cross #24, after the fourth dipole.

# OBSERVATIONS OF ENHANCED OTR SIGNALS FROM A COMPRESSED ELECTRON BEAM*

A.H. Lumpkin, Fermilab, Batavia, IL U.S.A. 60510
N.S. Sereno, M. Borland, Y. Li, K. Nemeth, and S. Pasky,
Argonne National Laboratory, Argonne, IL U.S.A. 60439

*Abstract*

The Advanced Photon Source (APS) injector complex includes an option for photocathode (PC) gun beam injection into the 450-MeV S-band linac. At the 150-MeV point, a 4-dipole chicane was used to compress the micropulse bunch length from a few ps to sub 0.5 ps (FWHM). Noticeable enhancements of the optical transition radiation (OTR) signal sampled after the APS chicane were then observed as has been reported in LCLS injector commissioning. A FIR CTR detector and interferometer were used to monitor the bunch compression process and correlate the appearance of localized spikes of OTR signal (5 to 10 times brighter than adjacent areas) within the beam image footprint. We have done spectral dependency measurements at 375 MeV with a series of band pass filters centered in 50-nm increments from 400 to 700 nm and observed a broadband enhancement in these spikes. Discussions of the possible mechanisms will be presented.

## INTRODUCTION

During the commissioning of the LCLS injector in 2007, unexpected enhancements of the signals in the visible light optical transition radiation (OTR) monitors occurred after compression in a chicane bunch compressor [1]. These signals were attributed to a microbunching effect of some kind and the generation of coherent OTR (COTR). Since the Advanced Photon Source (APS) injector complex includes a flexible chicane bunch compressor that is similar to that at LCLS, we have an option to use an rf photocathode (PC) gun, and we had experience with SASE-induced microbunching [2], a series of experiments was performed to explore the phenomena. We initially performed studies on OTR measured at three screens located after the bunch compressor. We used focus-at-the-object or near-field imaging optics and established that there were clear enhancements of the OTR signals at maximum bunch compression. The compression was also monitored with a FIR CTR monitor and interferometer. The shortest bunches generally generate the strongest FIR signals, and the appearance of the enhanced OTR was strongly correlated with the maximum FIR signal, although there appeared to be a slight phase shift between the two maxima. We also accelerated the compressed beam to the end of the linac and evaluated the enhancements at 375 MeV. The localized spikes in the beam distribution were still visible at this energy. At this latter station we have the light transported outside of the tunnel to a small optics lab that allowed us to perform additional spectral dependency measurements. Moreover, the use of a thermionic cathode gun pulse train with only 40 pC per micropulse did not show the OTR enhancements when the bunch length was compressed comparably to that of the PC gun beam. Discussions of the possible mechanisms will be presented for the APS case which is similar, but not identical to that of LCLS.

*Work supported by U.S. Department of Energy, Office of Science, Office of High Energy Physics, under Contract No. DE-AC02-06CH11357.

## EXPERIMENTAL BACKGROUND

The tests were performed at the APS facility which includes an injector complex with two rf thermionic cathode (TC) guns for injecting an S-band linac that typically accelerates the beam to 325 MeV, the particle accumulator ring (PAR), the booster synchrotron that ramps the energy from 0.325 to 7 GeV in 220 ms, a booster-to-storage-ring transport line (BTS), and the 7-GeV storage ring (SR). In addition, there is an rf photocathode (PC) gun that can also be used to inject into the linac as shown schematically in Fig. 1. An extensive diagnostics suite is available in the chicane and after the chicane area as also shown in Fig. 1. The tests were performed in the linac at the three imaging stations (indicated by a flag symbol) after the chicane bunch compressor and at the end of the linac where another beam imaging station is located. A FIR coherent transition radiation (CTR) detector (Golay cell) and Michelson interferometer [3] are located between the three-screen emittance stations. A vertical bend dipole and diagnostics screens in this short beamline allow the monitoring of tranverse x-beam size and energy following compression.

The CTR converter is an Al-coated mirror with an 18 mm diameter clear aperture on a zerodur substrate, and it is mounted with its surface normal at 45 degrees to the beam direction on a pneumatic actuator assembly. A synthetic quartz lens at the port of the cross collimates the beam into the interferometer box. A remotely controlled translation stage steps the position of one arm of the interferometer for the autocorrelation tests. An EPICS interface allows the acquisition of the autocorrelation data. The YAG:Ce and OTR were directed by turning mirrors and relay optics to a Pulnix CCD camera located 0.5 m from the source. These Chicane stations also have options for low- and high-resolution imaging of the beam spot by selecting one of two lens configurations [4].

# BEAM TRANSVERSE PROFILE MONITOR FOR IFMIF-EVEDA ACCELERATOR

P. Abbon, É. Delagnes, F. Jeanneau, J. Marroncle, J.-P. Mols, J. Pancin,

CEA Saclay, DSM/IRFU, France

*Abstract*

In the framework of the IFMIF-EVEDA project, a high deuteron beam intensity (125 mA - 9 MeV) prototype accelerator will be built and tested at Rokkasho (Japan). CEA-Saclay group and Ciemat-Madrid (Spain) are responsible of the beam instrumentation from the ion source to the beam dump. One of the most challenging diagnostic is the Beam Transverse Profile Monitor (BTPM). CEA-Saclay group investigates such a monitor based on residual gas ionization. This monitor uses a high electric field to drive the products (electrons and ions) of ionization to micro-strips. A priori, no primary amplification is required due to the high beam intensity. Nevertheless, in order to study the feasibility, a prototype will be tested in a proton beam.

## INTRODUCTION

This paper is devoted to the description of a non-destructive profiler prototype for the IFMIF-EVEDA project. In a first part, the context of this project will be briefly given. The second part will present the prototype, its principle, the expected counting rates, the design and some issues addressed to a future preliminary test.

## CONTEXT

The International Fusion Materials Irradiation facility (IFMIF) aims at producing an intense flux of 14 MeV neutrons, in order to characterize materials envisaged for future fusion reactors. The primary mission of IFMIF is to provide a materials irradiation database for the design, construction, licensing and safe operation of the Fusion Demonstration Reactor (DEMO) [1]. In such a reactor, high neutron fluxes may generate up to 30 dpa/fpy (displacements per atom / full power year). IFMIF facility is based on two high power cw drivers (175 MHz) delivering 125 mA deuteron beams at 40 MeV each, colliding a liquid lithium target.

In the framework of the "Broader Approach", the IFMIF-EVEDA (Engineering Validation and Engineering Design Activities) project includes the construction of an accelerator prototype with the same characteristics as IFMIF, except 9 MeV instead of 40 MeV for the incident deuteron energy. Most of the components of the accelerator are developed by France, Italy and Spain. Commissioning of this accelerator at Rokkasho is foreseen for 2013.

France (CEA-Saclay) and Spain (Ciemat-Madrid) are responsible of the beam instrumentation from the RFQ to the beam dump.

One of the relevant IFMIF issues is to avoid lithium boiling at beam-target crossing (5×20 $cm^2$), thus placing stringent conditions on the beam spot. In particular, beam intensity fluctuations must be kept below ±5 %. Consequently, non-destructive beam profile monitors have to be designed to drive safely the beam in a very hard radiation background of neutrons and γ, and to precisely monitor the transverse beam profile and intensity fluctuations, especially just upstream the target. CEA-Saclay has decided to investigate such a monitor based on residual gas ionization.

## BEAM TRANSVERSE PROFILE MONITOR (BTPM) PROTOTYPE

The BTPM prototype is based on the ionizations, induced by the beam particles, of the residual gas contains in the beam pipe of the accelerator. It will be first tested with a proton beam.

### *Accelerator parameters*

Below are listed the parameters of the IFMIF accelerator:

- Deuteron cw linear beam (175 MHz ≡ 5.7 ns).
- Energy range: 5 to 9 MeV (40 MeV for IFMIF).
- Beam intensity: 125 mA which represents 4.5 $10^9$ deuterons/burst (250 mA close to IFMIF target).
- Vacuum pipe: $10^{-5}$ mb (target region) and $10^{-7}$ elsewhere.

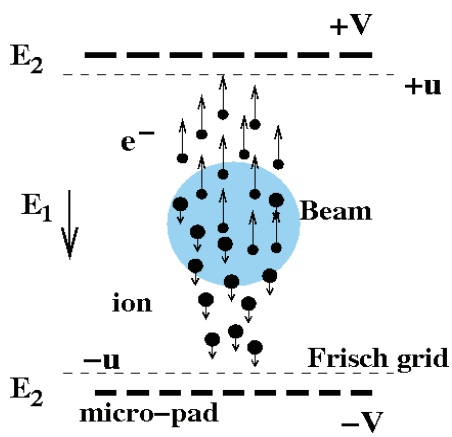


Figure 1: Transverse cross-section of a BTPM. Ionized pairs are sketched in the electric field.

# EVALUATION OF PINHOLE CAMERA RESOLUTION FOR NSLS-II STORAGE RING *

I. Pinayev #, NSLS-II Project, BNL, Upton, NY 11973, U.S.A.

*Abstract*

The NSLS-II Storage Ring will provide ultrabright radiation sources with extra-small sizes of the circulating electron beam. The beam dimensions will be monitored with a pinhole camera. In this paper we discuss the possible design and ultimate achievable resolution of the system. Modeling is based on the SRW code as well as numerical calculations using MATLAB.

## INTRODUCTION

The pinhole camera has been a workhorse for measuring electron beam size on the storage ring-based light sources since it was first utilized at ESRF [1]. The NSLS-II storage ring will utilize an electron beam with diffraction limited source size in the vertical plane [2] in order to achieve unprecedented brightness. The goal of the study described in this paper is to define parameters that most affect resolution of the imaging system and optimize beamline design.

## BEAMLINE LAYOUT

The expected layout of the pinhole camera beamline is shown in Fig. 1. The bending dipoles of the storage ring have low magnetic field of 0.4 T in order to reach small horizontal emittance [2]. Therefore the expected critical energy of the dipole synchrotron radiation is rather low, namely 2.4 keV. To improve resolution by utilizing a shorter wavelength we will employ a three-pole wiggler as a source. The field of the central pole is 1.14 T, the critical photon energy is 6 keV, and the useful synchrotron radiation spectrum extends to 50 keV. The electron beam parameters at the location of the three-pole wiggler are $\eta_x$=0.17 m, $\beta_x$=4.1 m, and $\beta_y$=19.3 m. Taking emittances $\varepsilon_x$=1 nm and $\varepsilon_y$=8 pm and relative energy spread $\sigma_E/E$=0.1% one can easily find the transverse dimensions of the source: $\sigma_x$=180 microns (defined mostly by energy spread) and $\sigma_y$=12.4 microns.

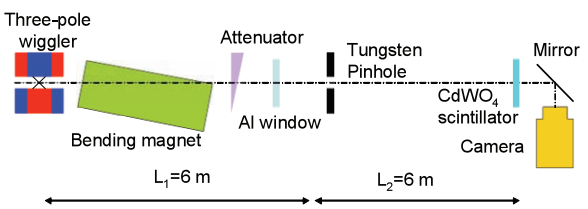


Fig.1 Layout of the pinhole camera beamline.

The first element of the pinhole camera beamline is a variable filter/attenuator. It constitutes a wedge, mounted on a linear actuator to set desirable transmission level. The filter serves two functions: the first is to bring intensity down to an acceptable level. The second function is to suppress long-wavelength radiation, in order to improve resolution. The filter is followed by an aluminum window so synchrotron radiation can exit to the atmosphere. Usually the material of the wedge is copper but we found it unsuitable due to substantial transmission of low-energy photons (Fig. 2).

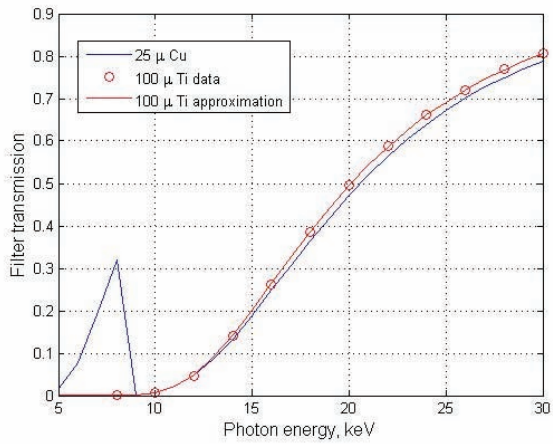


Fig. 2. Transmission curves for 25 microns of copper and 100 microns of titanium. Data from [4].

For our design we plan to use titanium, which does not have absorption lines in the spectral range of interest and has excellent vacuum compatibility. The Ti filter transmission curve also is shown in Fig. 2. Fig. 3 shows on-axis brightness of a three-pole wiggler source after being filtered by 50 microns of titanium.

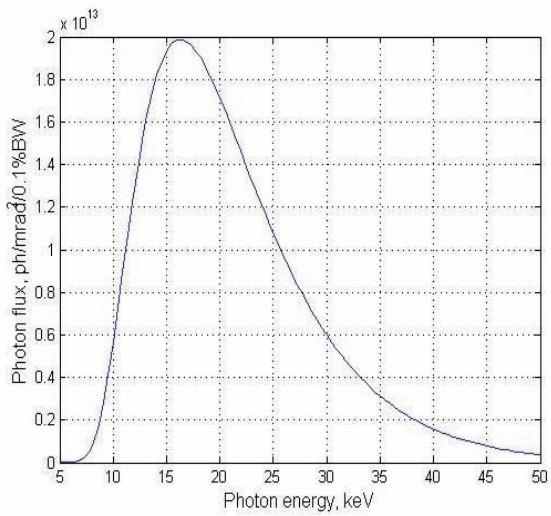


Fig. 3. Spectral brightness of the three-pole wiggler source after a 50 micron Ti filter.

*Work supported by the U.S. Department of Energy with Contract No. DE-AC02-98CH10886

#pinayev@bnl.gov

# OPERATIONAL LIMITS OF WIRE SCANNER ON LHC BEAM

M. Sapinski*, Tom Kroyer, CERN, Geneva, Switzerland

*Abstract*

A heat flow equation with beam-induced heating and various cooling processes for a carbon wire passing through a particle beam is solved. Due to the equation nonlinearity a numerical approach based on discretization of the wire movement is used. An estimation of the wire sublimation rate is made. Heating of the wire due to the beam-induced electromagnetic field is taken into account. The model is tested on SPS data. Results are discussed and conclusions about limits of Wire Scanner operation on LHC beams are drawn.

## INTRODUCTION

Wire Scanners [1] are devices widely used in accelerators to measure the beam profile. They provide direct and accurate measurement with resolution down to $1\ \mu\mathrm{m}$ and they are considered as a reference for calibration of other instruments.

During the scan, the wire is moved through the beam. It is heated by the RF-coupling to the beam. When it enters into the beam it is irradiated, heated up and cooled down by heat transport along the wire, by thermal radiation and by thermionic emission. In high temperatures it sublimates and it might melt if the pression due to thermal stress is high.

The wire breakage has been observed many times with different beams. The cross-section of the broken wire has been photographed and analysed [2, 3]. These photographs indicate different breakage mechanism depending on beam conditions.

The mechanisms leading to the wire damage during the scan can be: brittle failure, plastic failure, sublimation, melting and thermal fatigue. In case of normal operation, when the wire breaks after thousands of scans, a combination of the above factors is relevant. For instance, as seen in some photographs in [2], the wire has significantly sublimated before breaking. The sublimation removes the external part of the wire which contributes the most to its total strength, as it contains crystals which are more oriented then the ones in the core [5]. In case of LHC beams the heating is slower than the sound speed therefore the thermal shock does not develop.

The LHC beam poses very demanding conditions for the wire. If scanning of the full beam would be possible the total energy deposited by the direct beam interaction during a scan would be about 0.1 J in a time of $900\ \mu\mathrm{s}$, in $1\mu\mathrm{g}$ of fiber. No material can withstand such conditions.

* mariusz.sapinski@cern.ch

In this paper the modeling of the wire temperature during the scan is presented. Separate models describe RF-heating and beam heating as they apply to different length scales along the wire. Conclusions about operational limits of Wire Scanners on LHC beams are drawn.

## INDUCTIVE HEATING FROM BEAM

The wire heating due to RF-coupling to the beam field has been observed even when the scanner was in the parking position [6], with the wire hidden in a cavity. After this experience RF-absorbing ferrites have been fixed in the parking cavity what cured the wire breaking problem. In this paper the wire heating during the scan is calculated.

Ansoft HFSS was used for the simulation of the beam power loss on the wire [4]. The model parameters are summarized in the Table 1.

Table 1: Parameters used in the simulation.

| parameter | unit | value |
|---|---|---|
| beam pipe side length | mm | 60 |
| structure length | mm | 40 |
| RMS beam size | mm | 1 |
| wire radius | $\mu$m | 15 |
| wire conductivity | S/m | $4 \cdot 10^4$ |
| relative permittivity | | 1 |

The losses on the wire scale with the square of the beam current density. They increase with the distance from the beam pipe center and with frequency as shown in Figure 1. Due to symmetry no current is generated in the wire center therefore there are no losses in the place which later is heated by direct interaction with the beam.

For a given beam the power deposited in the wire can be calculated by weighting the relative losses from Figure 1 with the beam spectrum. The field power in the 40 MHz harmonics of the nominal LHC beam at top energy is depicted in Figure 2.

The power deposition has been used in the wire model which contains thermal conductivity. Other cooling processes are not adequate for the temperatures reached by the wire. The thermal conductivity gives relatively small effect due to weak thermal conductivity of the wire. In Figure 3 the temperature evolution along the wire during the scan is presented. The characteristic pattern with large losses on the sides of the wire and almost no heating in the wire center, observed in LEP wire scanners [7], is confirmed.

The temperature of the wire center, in case of scan of 25% of LHC injection beam, increases only by a few de-

# FAST PINHOLE CAMERA FOR OPTIMISATION OF TOP UP INJECTION

C.A. Thomas, G. Rehm, Diamond Light Source, Oxfordshire, U.K.

*Abstract*

Top up is increasingly becoming a standard mode of operation for synchrotron light sources. Although it brings a very stable source in terms of intensity and position, the regular injections potentially perturb the beam. In order to investigate the perturbation of the beam from imperfections of the injection kickers (i.e. non-closure of the bump), we use an X-ray pinhole camera equipped with a fast CMOS-sensor giving a rate of up to 3200 frames per second to monitor the image of the beam. The analysis of the observed beam size as well as position allows quantifying the perturbation from the kickers that can be seen on beamlines. In addition we compare the observed motion to bunch-by-bunch position data recorded in both vertical and horizontal planes, which reveals to be very complementary.

## INTRODUCTION

In almost all third generation synchrotron light source like Diamond there are plans to operate the machine in top up mode [1, 2, 3, 4, 5, 6, 7]. This operational mode presents many advantages for the machine and for the users. However, it implies injecting a small amount of charge regularly to compensate for the losses. By doing that, there is a necessity to take into account the perturbation of the stored beam by the injection kickers and their consequences on beamlines activities. In this paper we present a method to measure the perturbation of the stored beam by the kickers from the view point of a beamline. This method consists of using a fast camera, operating from 200 to 3200 frame per second (FPS), in a X-ray pinhole camera setup. We firstly present the system and its performance. Then we show some results obtained at Diamond to finally discuss the potential use of such a system and give some concluding remarks.

## INSTRUMENTATION AND PERFORMANCE

The system we use is the X-ray pinhole camera setup that is currently used to measure the beam size, and thus calculate the emittance, the relative energy spread and the coupling emittance of the electron beam [8]. But instead of using our standard CCD camera, we use the Pulnix TM-6740GE from JAI[1]. This camera achieves 200 FPS with full frames of the 640 by 480 CMOS sensor and transmits the image data through Gbit Ethernet. The pinhole has a $25 \times 25$ $\mu$m$^2$ aperture, and the system pinhole screen camera provides a good resolution for the measurement we intend to do, i.e. measuring the centroid and the beam size vs. time. The resolution has been evaluated to $\Delta \approx 16\mu$m when using a 0.5 mm thick $CdWO_4$ screen [9]. The other important parameter of the measurement is the flux reaching the camera in order to have a low noise floor on the images. To this end we used the flux from a stored beam with our nominal two third fill at 125 mA. In this case, the average number of photons on the scintillator screen is of the order of $10^{11}$ $s^{-1}$ [8].

The camera software provided by JAI is extremely basic but sufficient to allow us to acquire all the frames desired. We setup the camera to 1200 FPS by selecting a small region of interest, 224 by 160 pixels. Higher rates can be obtained by bining the pixels up to 4x4, which provides rates up to 3200 FPS on the whole sensor size but with 4 times less resolution.

## MEASUREMENT OF THE KICKED BEAM

Top up mode requires regular injections of a small amount of charge, either after a fixed period of when the stored current drops below a certain threshold. During injections, the stored beam is kicked through a theoretically closed bumped. In practice, a residual angular kick resulting from the four kicks not adding up to precisely zero, or from leakage field from the septum, will perturb the beam. As the residual kick typically originates from a mismatch in the shapes of the kicker pulses, it shows fast changes within the duration of the pulse. This leads to different kicks seen by individual bunches along the bunch train and causes a damped oscillating motion of varying amplitude along the bunch train. As a result of this, using a beam position monitor with turn by turn acquisition (which averages the position of the beam over one turn) to judge when the bunch motion is minimised is fundamentally flawed, as opposite motion of the head and tail can cancel out.

Recording the position bunch by bunch (see figure 1) will reveal the full extent of the residual kick on the first turns after the injection, but it cannot correctly record the full temporal evolution of the damped oscillation. Decoherence of the electrons inside each bunch leads to the oscillation appearing to damp faster as a beam position monitor is only able to record the centre of mass motion.

The disturbance of the stored beam can best be investigated with our fast pinhole camera setup as it records the beam as seen from a beamline and the perturbation can be quantified. We have been acquiring images at 1200 FPS while kicking the electron beam and followed this with an image by image analysis of the horizontal and vertical centroid, the image beam size and the intensity across a given aperture. The beam size is measured by fitting each image

[1] www.JAI.com

# COMPLEMENTARY METHODS OF TRANSVERSE EMITTANCE MEASUREMENT*

James Zagel, Martin Hu, Andreas Jansson, Randy Thurman-Keup, Ming-Jen Yang (Fermilab, Batavia, Illinois, USA 60510)

*Abstract*

Several complementary transverse emittance monitors have been developed and used at the Fermilab accelerator complex. These include Ionization Profile Monitors (IPM), Flying Wires, Schottky detectors and a Synchrotron Light Monitor (Synchlite). Mechanical scrapers have also been used for calibration purposes. This paper describes the various measurement devices by examining their basic features, calibration requirements, systematic uncertainties, and applications to collider operation. A comparison of results from different kinds of measurements is also presented.

## SYSTEMS IN USE

Several emittance measuring systems exist across the Fermilab accelerator complex. Booster has both IPM's and Crawling Wires. Main Injector has IPM's, Flying Wires, and Multiwires. Recycler has Flying Wires and Schottky detectors. Tevatron has IPM's, Flying Wires, Schottky detectors, Synchrotron Light Monitors, and Optical Transition Radiation (OTR) [1] instruments. We will discuss the comparative measurements from only those instruments used in the normal course of stacking and storing, protons and antiprotons (pbars). Crawling Wires, Multiwires (secondary emission monitors,) and OTR are used for studies of injection and tolerate only a few turns of beam.

## MAIN INJECTOR

Three types of instrumentation devices are installed in the MI10 straight section of Main Injector Ring for transverse emittance measurements; a horizontal and vertical Flying Wire, horizontal and vertical IPM[2], and one magnetic electron IPM[3]. The straight section, being of zero dispersion function by design, ensures that measurements are free from effects of longitudinal beam motion.

For collider operation, beam emittances of both horizontal and vertical plane are measured using the Flying Wire system and logged for every pbar transfer from Accumulator to Recycler Ring, Recycler Ring to Tevatron, and each proton transfer from Booster to Tevatron. In Main Injector, these measurements are taken at 8 GeV/C injection and at 150 GeV/C flat-top, before transfering beam to Tevatron.

The Flying Wire system measures beam loss profiles as a 33um carbon filament flies through the beam. Flying at 6 meters/second the wire takes about 5 milliseconds, or 450 revolutions, to traverse the entire width of beam. Quasi-stationary beam is a necessary condition for measurement to make any sense. . Unlike the flying wire system, the ion profile monitor records a complete profile from each successive turn of beam

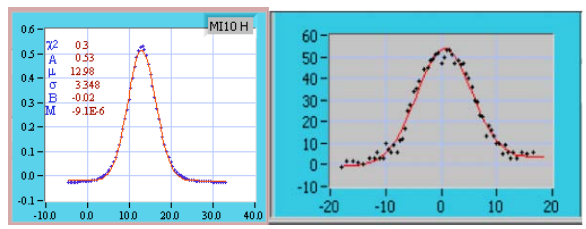


Figure 1. Main Injector Flying Wire And IPM Profile.

The IPM's are placed directly next to the flying wire system, of corresponding plane, to make comparisons more straight forward. Only one magnetic electron IPM for the horizontal plane is installed. A second unit is anticipated for the vertical plane in the near future. This is expected to be an improvement over the ion IPM for measurements at or above 120 GeV.

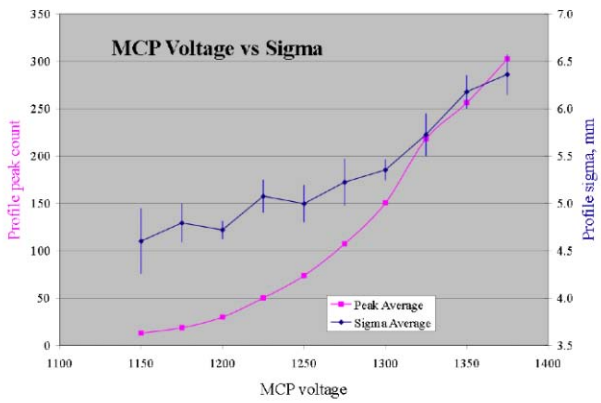


Figure 2. Sigma and peak count vs MCP Voltage

The full characterization of IPM response has so far not been completed. Figure 2 shows a measurement of beam profile sigma with varying high voltage to the Micro Channel Plate. While the increase in peak count is expected the dependency of sigma on high voltage is of concern. The best setting allows for good signal to noise measurement without saturation, or sag, at the peak of the profile. Two straight forward comparisons have been made. A simultaneous measurement of sigmas on both systems with increasing intensity and, in a separate measurement, a position bump was implemented through

*Operated by Fermi Research Alliance, LLC under Contract No. DE-AC02-07CH11359 with the United States Department of Energy

# ADVANCED LIGHT SOURCE FGPA-BASED BUNCH CLEANING*

M. J. Chin, J. M.Weber, F. Sannibale, W. M. Barry, LBNL, Berkeley, CA 94720, U.S.A.

*Abstract*

At the Advanced Light Source (ALS), imperfections in the injection system plus electron diffusion result in storage ring RF bucket contamination. A Virtex-4 FPGA is used to generate a Direct-Digital Synthesized (DDS) sinewave waveform at the vertical betatron tune frequency, which is synchronously gated on or off at the 1.6MHz ring orbit frequency. Any pattern on/off/invert in 328 buckets by 2ns at the ring orbit frequency can be set. An embedded Power-PC core in the FPGA provides TCP access for control and monitoring via a remote PC running LabVIEW.

## INTRODUCTION

The ALS has several fill patterns (camshaft, 2-bunch) that require a filled bucket be surrounded by empty buckets. This requires actively "cleaning" by selectively exciting the empty buckets at the vertical tune [1]. The major components of such a system include transverse kickers, kicker amplifiers and a signal source.

The ALS signal source uses a Xilinx FPGA demo board, the ML403 [2] together with a custom add-on board that has a 12-bit 500MHz DAC. By clocking the FPGA and DAC at the 500MHz master oscillator rate $f_{RF}$, any of the 328 bunches can be set to an independent value. Bunches to be cleaned are then selectively kicked at the tune frequency, while the isolated filled bunch is left un-stimulated. Additionally, due to tune shift, the kick frequency is swept in a few KHz bandwidth.

## BUNCHCLEANER HARDWARE

The BunchCleaner board in Figure 1 was designed to investigate the LTC 2242-12 ADC (12-bits, 250MHz clock speed, 1.2GHz bandwidth) and the MAX5886 DAC (12-bits, 500MHz clock speed, 450Mhz bandwidth, 375ps rise/fall times) using the ML403 for FPGA interfacing and system design. Both ADC and DACs use LVDS digital I/Os. The DAC takes advantage of the double-data rate I/Os of the Virtex-4 to allow full speed updates at 500MHz while allowing the gate array internal clock to run at 250MHz.

For BunchCleaning, only the DAC is used, but the ADC was also successfully tested for transverse feedback.

### *ML403 Interfacing*

There are two DIN-style connectors intended for user expansion that connect to FPGA pins and provide power. These connectors are not impedance controlled, and not specified for any maximum speed. Nevertheless, there are nearly 1 ground pin per 2 signal pins, and acceptable signal distortion was measured when used in 100ohm LVDS (the lower trace of Figure 2).

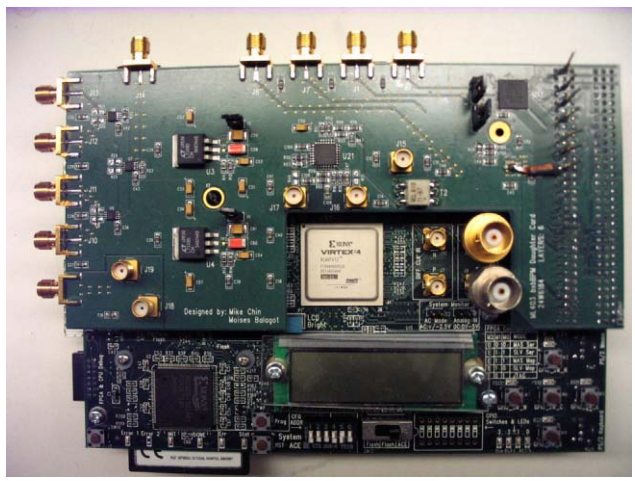

Figure 1: BunchCleaner mounted to ML403

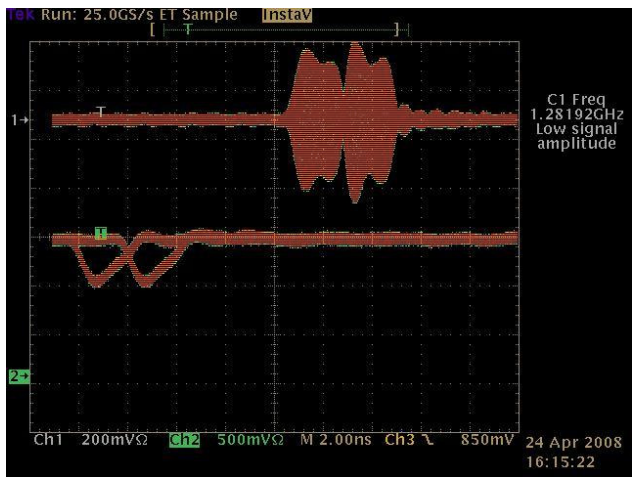


Figure 2: Top trace is DAC Output, lower trace is LVDS to DAC. Pattern is 1,-1 (rest are 0's)

500MHz is brought into the ML403 on two of its onboard SMAs, which are hooked up to an LVDS clock input of the FPGA. An RF transformer is used for a single-ended to differntial converison

## FPGA DESIGN – BUNCHCLEANER

The main goal of the bunch cleaning is to generate a gated-sinewave where the stimulus is only on for bunches to be kicked out. Due to the 250MHz bandwidth of the Amplifier Research kicker amplifiers, a simple on-off approach does not work, because they cannot turn fully on

*This work was supported by the Director, Office of Science, Office of Basic Energy Sciences, of the U.S. Department of Energy under Contract No. DE-AC02-05CH11231

# A SOLID-STATE PINGER TUNE MEASUREMENT SYSTEM FOR THE INTENSE PULSED NEUTRON SOURCE (IPNS) RAPID CYCLING SYNCHROTRON (RCS)*

J. C. Dooling†, L. Donley, M. K. Lien, and C. Y. Yao
Argonne National Laboratory, Argonne, IL 60439, U.S.A.

*Abstract*

A cw tune measurement system for the IPNS RCS is described. The pinger magnets are energized by a solid-state, transformer-coupled power supply operating at 30 Hz. In its present configuration, the power supply provides a 160-A pulse to a pair of series-connected, single-turn ferrite magnets. The magnet pair separately drive x- and y-plane orbit bumps in the h=1 beam. The dipole oscillations generated in the beam are sensed with pairs of split-can, pie electrodes. Raw signals from the H and V electrodes are carried on matched coax cables to 0/180-degree combiners. The output difference signals are recorded with gated spectrum analyzers. Bunch circulation frequency varies from 2.21 MHz at injection to 5.14 MHz at extraction. With a fixed frequency span of 24 MHz, between four and ten bunch harmonics and sidebands (SBs) are present in the difference spectra. Software has been developed to use the multi-harmonic SBs present over the span to improve the accuracy of the tune measurements. The software first identifies and then fits the multiple SBs to determine the tune. Sweeping the beam across the momentum aperture provides a method for measuring the chromaticity.

## RCS PINGER DIAGNOSTIC

The IPNS RCS operated for almost 25 years without a dedicated tune diagnostic system [1]. Finally in February 2006, a ferrite pinger magnet set was added [2]. The horizontal and vertical magnets were initially driven by a thyratron-switched transmission line, essentially using 1/4 of the extraction kicker system. Assisted by an AC septum and a combined-function, horizontally defocusing singlet, the kicker provides 24 mrad of deflection, sufficient to extract the 450-MeV proton beam in a single turn. By contrast, the pinger supply need only provide a beam deflection on the order of 0.1-0.5 mrad. Therefore one of the goals of this work is to build a lower power, lower maintenance supply relative to the thyratron-based system. Another goal is to develop a diagnostic that can determine tune and chromaticity values more quickly than the single-shot measurements previously described [2]. In that case, pie-electrode data are recorded on a fast, deep memory oscilloscope. An optimized spectrum is then generated off-line; this process tends to be CPU intensive. In the present study, spectral data are recorded directly using two Agilent E4402B spectrum analyzers (SAs). Signals are first collected in each plane from a pair of split-can pie electrodes [3]. Each signal pair is fed on matched transmission lines to 0/180-degree combiners producing an A-B output. The x- and y-difference signals are recorded on the gated SAs.

*Work supported by U.S. DOE, Office of Science, Office of Basic Energy Sciences, under contract number DE-AC02-06CH11357.
†jcdooling@anl.gov

### *Pinger Power Supply*

The power supply combines the properties of SCR-Marx and transformer step-up circuits. The amp-turns of four Marx circuit outputs are summed through a transformer to provide the final output to the pinger magnet load as shown in Figure 1. In addition to the series-connected horizontal and vertical magnet pair, the pinger load includes a 6.2-Ω resistor in parallel with 0.040-μF of ceramic disk capacitance. The terminating load is shown in Figure 2 prior to installation. To roughly match the terminating load impedance, eight 50-Ω, RG-217 coaxial cables are run in parallel from the pinger supply to the terminating load. Each cable is 7.6-m (25-ft) in length. To provide current protection for the 2N6405 SCRs, a 1.4-Ω series resistor is placed between each Marx stage. Initial testing of the pinger was conducted with two turns on each primary side winding and four turns on the secondary output side. The terminating impedance was connected in series to a single horizontal test magnet.

Several different values of capacitance in parallel with load resistance were tried to see if rise time could be reduced. In Figure 3, pinger output current waveforms are presented for terminating capacitances of 5 and 40 nF. The risetime is seen to improve from 186 to 174 ns as capacitance is raised between these two capacitance values; however, greater oscillations in output voltage and current also occur as the load impedance drops below a matched condition. To reduce hysteresis in the output transformer ferrite, each core is gapped to 0.38 mm (15 mils), lowering the energy per cycle lost in the NiZn core

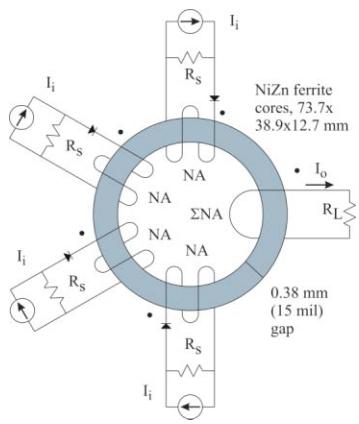


Figure 1: Output transformer schematic.

# AN OVERVIEW OF THE LHC TRANSVERSE DIAGNOSTICS SYSTEMS

M. Gasior, A. Boccardi, R. Jones, R.J. Steinhagen, CERN, Geneva, Switzerland

*Abstract*

The unprecedented intensity and energy of the LHC proton beams will require an excellent control of the transverse beam dynamics in order to limit particle loss in the superconducting systems. Due to restricted tolerances of the machine protection system and a tight beam emittance blow-up budget only small beam excitation is allowed, making precise measurements of the transverse beam parameters very challenging. This overview outlines the systems measuring the tune, chromaticity and betatron coupling of the LHC beams, referred to in the paper as the transverse diagnostic systems. As manual correction of the parameters may reach its limit with respect to required precision and expected time scales, the LHC is the first proton collider that can be safely and reliably operated only with automatic feedback systems for controlling transverse beam dynamics. An outline of these feedback systems is also presented.

## INTRODUCTION

During nominal operation the LHC has a stored beam energy of about 350 MJ per beam circulating inside a cryogenic environment, which tolerates energy depositions in the order of only a few mJ/cm³. This requires an excellent control of particle loss, which for the LHC is provided by its Machine Protection and Beam Cleaning System [1-3]. The function of these systems depends critically on the stability of orbit, energy, tune ($Q$), chromaticity ($Q'$) and betatron coupling ($C^-$), and imposes significant constraints on the maximum allowed beam excursions, traditionally required to measure $Q$ and $Q'$. The transverse oscillation 'budget', which at nominal is below a few tens of μm, must be shared between several accelerator systems, such as the orbit and energy feedback, the $Q$ phase-locked loop (PLL) and the bunch-by-bunch transverse damper feedback. As a result, the amplitudes of the explicit beam oscillations used by the transverse diagnostic systems for nominal beam operation are limited to a few μm. The non-zero dispersion at the collimator locations and available RF power relates this to an effective limit in the order of $10^{-5}$ on the maximum allowed momentum modulation Δp/p, with a maximum modulation frequency of about 5 Hz.

Due to persistent currents, the related decay and snap-back phenomena (inherent to superconducting magnets) and other perturbation sources, the induced changes in $Q$, $Q'$ and $C^-$ will exceed LHC beam stability requirements by orders of magnitude, as summarized in Table 1. Assuming that a large part of these perturbations are reproducible from fill-to-fill, these effects may be partially compensated by feed-forward systems. However, due to the intrinsic uncertainties related to the mentioned processes and the tight tolerances requested on $Q$, $Q'$ and $C^-$, beam-based measurements and their exploitation in automated feedback systems will be mandatory for a safe and reliable LHC operation.

The nominal requirements of the LHC transverse diagnostic systems can be summarized as follows:

- sensitivity, allowing operation with excitation amplitudes in the 1 μm range for the rms beam sizes about 0.2-1 mm;
- resolution and measurement speed;
- robustness, required to reliably operate automatic feedback systems under varying beam conditions.

This overview focuses on the measurement and control of $Q$, as both $Q'$ and $C^-$ are usually derived from it. While $C^-$ can be calculated using cross-amplitude terms of the tune eigenmode oscillations [4, 5], the base-line LHC $Q'$ measurement employs the classic method, based on tracking the $Q'$ dependent tune changes $\Delta Q$ as a function of momentum modulation Δp/p. The underlying relation, also defining the unit of $Q'$, is given by

$$\Delta Q = Q' \frac{\Delta p}{p}$$

Table 1. Parameters and requirements of the LHC transverse diagnostic systems [6].

| Parameter | Tune [$f_{rev}$] | Chromaticity [$Q'$] | Coupling [$C^-$] |
|---|---|---|---|
| Nominal value | 0.31, 0.32 | 2 | < 0.001 |
| Nominal stability | < 0.001 | ±1 | < 0.001 |
| Perturbations | 0.14 | 70 | 0.01 |
| Worst-case perturb. | 0.18 | 300 | 0.1 |
| Max drift per sec. | < 0.001 | 1.3 | – |

## TUNE MEASUREMENT

The biggest challenge in measuring tunes of high intensity beams is the dynamic range of the processed signals, as the small signal related to transverse beam oscillations is carried by large, short pulses. For example, the nominal 1 ns long LHC bunches induce some 50 V on the 40 cm electrodes of the $Q$ measurement stripline pick-ups. For the 80 mm pick-up diameter and 1 μm beam oscillation amplitudes the modulation of the pick-up output pulses is in the order of $10^{-5}$, i.e. a few mV. An efficient way to filter out the betatron modulation signal from its inconvenient carrier is to use the Direct Diode Detection (3D) [7, 8]. The principle of this technique is shown in Fig. 1, with the simplified signal waveforms sketched above the corresponding circuit paths.

The pick-up electrode signals are processed by diode peak detectors, which can be considered as fast sample-and-hold circuits, with the sampling self-triggered at the bunch maxima and 'held' by the parallel capacitors. The purpose of the parallel resistors is to slightly discharge the capacitors so that the next bunch with a potentially smaller amplitude also contributes to the detector output signal.

# PROGRESS WITH THE DIGITAL TUNE MONITOR AT THE TEVATRON*

V. Kamerdzhiev#, V. Lebedev, A. Semenov, FNAL, Batavia, IL 60510, USA

*Abstract*

Monitoring the betatron tunes of individual proton and antiproton bunches is crucial to understanding and mitigating the beam-beam effects in the Tevatron collider. To obtain a snapshot of the evolving bunch-by-bunch tune distribution a simultaneous treatment of all the bunches is needed. The digital tune monitor (DTM) was designed to fulfill these requirements. It uses the standard BPM plates as a pickup. The vertical proton monitor is installed and allows us to gain valuable operational experience. A major upgrade is underway to implement an automatic bunch-by-bunch gain and offset adjustment to maintain the highest possible sensitivity under real operational conditions. We present the concept of the DTM along with its technical realization as well as the latest experimental results. Major challenges from the design and operation point of view are discussed.

## INTRODUCTION

In the TEVATRON 36 proton bunches collide with 36 anti-proton bunches at the center of mass energy of 1.96 TeV. The bunches of each species are arranged in 3 trains of 12 bunches circulating around the ring with the revolution frequency $f_{rev}$ = 47.7 kHz. The bunch spacing within a train is 396 ns corresponding to 21 RF buckets (53.1 MHz). The bunch trains are separated by 2.6 $\mu$s abort gaps corresponding to 139 RF buckets. The betatron tunes of individual bunches are affected, among other phenomena, by the head on and long range beam-beam interaction [1]. These mechanisms limit the performance of modern colliders. In order to be able to mitigate the beam-beam effects, the knowledge of the bunch-by-bunch tune distribution is crucial. Three transverse tune monitors are presently available at the Tevatron: the 21.4 MHz Schottky, the 1.7 GHz Schottky and the Direct Diode Detection Base Band Tune (3D-BBQ) detector [2]. The 21.4 MHz Schottky is used to measure the horizontal and vertical tunes of the 36 proton bunches without the possibility of gating on individual bunches. The 1.7 GHz Schottky is capable of measuring the horizontal and vertical tunes of a single proton and anti-proton bunch but needs a few minutes of averaging time to get the precision of $10^{-4}$. Furthermore, the significant width of the betatron sidebands at high frequency and the presence of transverse coupling in the machine result in additional uncertainty of the reported tune values. The 3D-BBQ detector is under development and allows to gate on proton and anti-proton bunches. This monitor showed promising results (individual proton and anti-proton tunes have been observed without additional beam excitation) and is presently used to cross-check the tunes measured by the two other monitors. The Digital Tune Monitor (DTM) [3], the subject of this paper, has the potential to report the horizontal and vertical tunes of each proton and anti-proton bunch, at a repetition rate of 1 Hz.

## EXPERIENCE WITH THE DTM

The DTM was successfully used to acquire proton vertical spectra in numerous HEP stores [4]. The theoretical estimates show that detecting the betatron oscillation of individual bunches without additional beam excitation might be possible. However, under real operating conditions the ultimate achievable sensitivity and the dynamic range are limited by the orbit drifts (Fig.1), low frequency beam motion (Fig.2) and the bunch to bunch intensity and position variation.

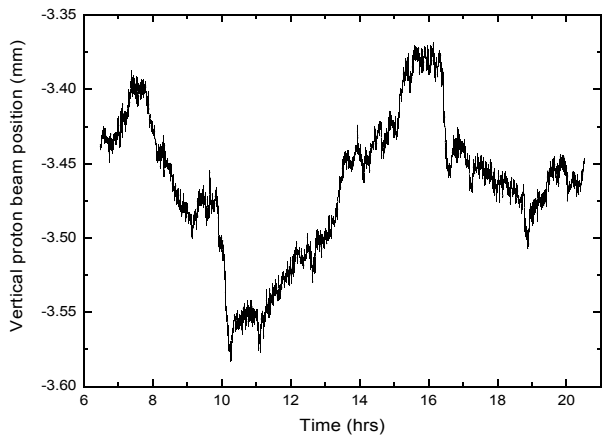


Figure 1. Vertical proton beam position reported by the Tevatron BPM over the course of a store.

The present DTM design makes use of a linear discriminator in a feedback loop in the difference channel. This technique allows for compensation of the slow beam motion (based on the average position measured over several turns).

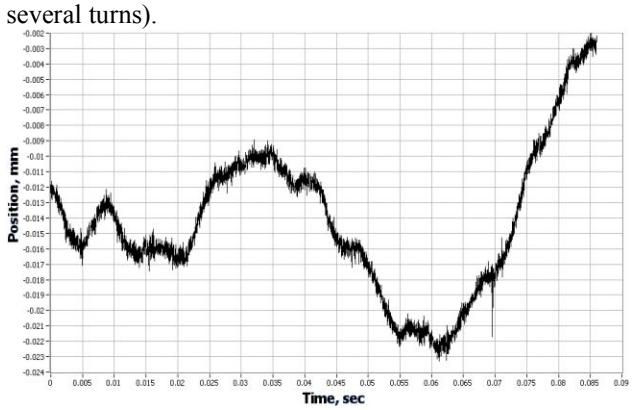


Figure 2. An example of the vertical proton beam position as seen by the DTM. Full scale is 22 μm, ~4000 turns.

*Work supported by the U.S. Department of Energy under contract No. DE-AC02-07CH11359

#vsevolod@fnal.gov

# AN FPGA-BASED TUNE MEASUREMENT SYSTEM FOR THE APS BOOSTER SYNCHROTRON*

C.-Y. Yao#, W. E. Norum, Ju Wang
Advanced Photon Source, ANL, Argonne, IL 60439, U.S.A.

*Abstract*

The Advanced Photon Source (APS) injection booster is a 7-GeV electron synchrotron with a ramping time of 226 ms and a repetition rate of 2 Hz. A real-time tune measurement system is needed in order to monitor and correct tune drift during the 226-ms energy ramp. Such a drift occurs during user beam operations, especially during continuous top-up operations, and results in shot-to-shot efficiency fluctuations. We designed and developed an FPGA-based system that pings the beam at variable intervals and measures tunes. An operational system has been built and commissioned. It has achieved a time resolution of better than 2 ms and a tune resolution of better than 0.001. This report describes the system design and main parameters, and results from our preliminary commissioning. We also briefly discuss the application of such a system in ramping correction and ring diagnostics.

## INTRODUCTION

A real-time tune measurement system is needed for the APS booster synchrotron in order to monitor the tune drift during the 226-ms energy ramp. Such drift may occur during user beam operations and results in inconsistent performance of the booster synchrotron. We designed and developed an FPGA-based tune measurement system that can measure booster tune using a pulsed pinger and an FPGA processor. The system is operational, and its performance is better than the VSA-based configuration we used previously in terms of speed, cost, and the ability to continuously monitor tunes.

## PEAK DETECTION MECHANISM

The Numerical Analysis of Fundamental Frequency (NAFF) method [1,2] has been widely used to analyze frequency components of various objects. Transverse betatron oscillations of a bunch can be observed by kicking or chirping the bunch in the plane of observation. A turn-by-turn position signal is acquired from a beam position monitor (BPM). The instantaneous tune is obtained by maximizing the absolute value of the correlation term

$$I(\nu_m)=\sum_{n=1}^{N} x_n[\cos(2n\nu_m)+j\sin(2n\nu_m)]w(n),$$

where N is total number of turns from which the tune is measured and W(n) is a window function. Typically several iterations are necessary to reach the desired accuracy.

*Work supported by U.S. Department of Energty, Offices of Science, Office of Basic Energy Sciences, under contract No. DE-AC02-06CH11357.
#cyao@aps.anl.gov

Another frequency analysis method was reported by Gasior et al. [3] This method first performs fast Fourier transform (FFT) with N data points, and then interpolates the result with a parabolic or Gaussian function. The frequency peaks are then derived from the fitted curve. This method improves the FFT resolution and not only produces the peak frequency but also generates a full spectrum, which is useful for diagnostics purposes. It is easier to implement, very efficient, and more appropriate for our application. We adopted the latter method in the current version of the FPGA firmware.

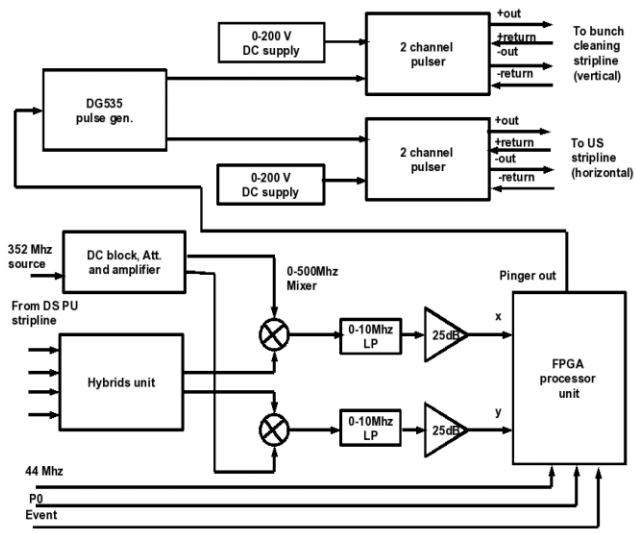


Figure 1: Block diagram of booster tune measurement system.

## SYSTEM DESCRIPTION

Figure 1 shows a diagram of the booster tune measurement system. The booster is a ramped accelerator in which beam energy ramps from 325 MeV to 7 GeV in 226 ms. We use two bipolar pulsed supplies to drive two sets of striplines, one in the vertical plane and another in the horizontal plane. The output pulses are half sinusoid with a width of around 600 ns, half of the booster revolution period, and a repetition period of 1.5 ms to 10 ms. The time intervals between the pings can be programmed by writing an array to the FPGA.

The front-end electronics consists of a hybrids converter box that converts signals from four diagonal blades into x, y, and sum signals, a mixer that down-shifts the stripline signal into base-band; and a low-pass filter with a bandwidth of 23 MHz.

Signal acquisition and processing is performed by a Stratix II FPGA processor [4]. There are two separate channels, one each for the x and y planes. Figure 2 shows the block diagram of the FPGA processor firmware. FFT is performed after each pinging and the tune traces are

# ACCELERATOR VACUUM 101, MADE EASY???*

T. Anderson, FNAL, Batavia, IL 60510, U.S.A.

*Abstract*

This paper, FERMILAB-CONF-06-568-AD and MSDN – ME – 000069, has been formatted for presentation as background material for the BIW08 tutorial on vacuum issues. The original paper is used as a vacuum primer for engineers and technicians at Fermilab's Accelerator Division, Mechanical Support Department. This version is without the appendix, which has specific examples to illustrate how this material is used. The full document can be obtained from the Fermilab, AD/MS Department.

## INTRODUCTION

This paper presents a condensed, simplified, and practical discussion of the principles, procedures, and operating parameters of particle accelerator vacuum systems as practiced at Fermilab. It is intended to provide a basis for designers, builders, and operators of accelerator systems to communicate with each other about the needs and impact of the vacuum system. Rigorous analytical development of the equations and concepts are not given. It is assumed that the reader has some limited understanding of the subject. Practical examples of real world experiences are used to illustrate the concepts outlined. Examples of how to use this material is given in appendix 1 and references for further study are given in appendix 2. The following advice is given for people who design, build, or operate accelerator vacuum systems:

A) Keep it simple.
B) Keep it clean.
C) Establish guidelines and standard practices; then follow them.
D) Always stop and think about what the outcome will be before you do something to the system.
E) Test and certify everything you can before it goes in the system.
F) Despite the abundance of "hot air" around physics laboratories, air is not the only gas we need to think about.
G) There is no vacuum gauge on this planet that, in and of itself, gives you the real picture.

Vacuum can be a complicated subject, but on a base level it does not need to be. Some may view this discussion as over simplified, but they should realize others don't have their level of understanding. Others may find it complicated and they should realize that they need to have a base understanding in order to meet operational goals.

* Work supported by Fermi Research Alliance, LLC under Contract No. DE- AC02-07CH11359 with the U.S. Department of Energy.

All need to realize that they need to communicate with each other on some base level. Most of the problems that arise in vacuum practice are a result of a lack of knowledge or communication. Complicated technical issues can be addressed by physicists and experts. Practical issues are usually addressed by engineers and technicians. Having a base understanding by all involved is essential to ensure a successful outcome for the projects they work on.

### WHY VACUUM?

Most all vacuum texts start out with a discussion on the ideal gas law (PV = nRT). For this discussion it would be nice to avoid this, but it is simply too fundamental to ignore. In particle accelerators the purpose of the vacuum system is to remove gas molecules from the path of the beam. So, for accelerators it is more appropriate to think of the ideal gas law in terms of the number of moles in a volume. Pressure is nothing more than a measure of the number of molecules that can interfere or interact with the beam.

$$n = P\,V / R\,T \qquad (1)$$

Where: n = Number of Moles
P = Pressure (Torr)
V = Volume (L)
R = Universal Gas Constant (62.3632 Torr-L/K-mol) )
T = Temperature (K)

### THE VACUUM WORLD ACCELERATORS LIVE IN

Figure 1, below, is a graphic representation of the vacuum bounds associated with accelerator vacuum systems. The information depicted is intended to be a guide or a starting point when thinking about accelerator vacuum systems. Given a pressure range that a system needs to operate in, the chart gives a reasonable estimate of the out-gassing rate needed, the time scale that will be needed to achieve a given pressure, and the likely pump types that will be needed.

The chart shows $1(10)^{-3}$ Torr as the transition point between the viscous and molecular flow regimes. This is not strictly the case, though. Molecular flow can exist above $1(10)^{-3}$ Torr and there is the transition flow regime between viscous and molecular. For all practical purpose in accelerator vacuum systems $1(10)^{-3}$ Torr is a good place to start thinking about molecular flow.

For the systems encountered in accelerators the range between atmosphere and $1(10)^{-3}$ Torr is not of a lot of concern. The roughing pumps and turbo molecular

# TRANSITION, DIFFRACTION AND SMITH-PURCELL DIAGNOSTICS FOR CHARGED PARTICLE BEAMS*

R. B. Fiorito†, Institute for Research in Electronics and Applied Physics, University of Maryland, College Park, MD 20742, U.S.A.

*Abstract*

I review the state of the art of diagnostics based on transition, diffraction and Smith Purcell radiation in the optical to millimeter wave band, which are currently being used to measure the transverse and longitudinal parameters of charged particle beams. The properties and diagnostic capabilities of the incoherent and coherent forms of these radiations are described. Examples of TR, DR and SPR diagnostics for electron and proton beams are presented.

## INTRODUCTION

The spatial, angular and spectral distributions of radiation produced from a charged particle beam interacting with a material object or field, e.g. magnetic field, carries information about the beam properties. In this paper we review the state of the art in the diagnostic application of three important beam based radiations: transition, diffraction and spatially coherent diffraction from a grating, i.e. Smith Purcell radiation. These radiations, and indeed all radiation from charged particles, can be analysed using some fundamental concepts: 1) the radiation impact parameter; 2) the coherence length of radiation from a moving charge; 3) the resonance radiation condition for spatially coherent radiation from $N_r$ radiators; and 4) the bunch coherence of radiation from N charges.

The radiation impact parameter $\alpha = \gamma\lambda/2\pi$ is the distance where the radial field of the charge is significant and therefore provides a convenient scale length for significant interaction of the charged particle's field with a medium. This property is analogous to the usually defined impact parameter which is the distance where a moving charged particle interacts with another charge.

For relativistic particles, the parameter $\alpha$ is also the effective source size of a virtual photon of wavelength $\lambda$, which is associated with the field of the moving charge. If the size of the radiator $r >> \alpha$, the radiator can be considered to be infinite and the radiation is transition radiation whose spectral angular density is frequency independent. If, however, $\alpha >\sim r$, or if the radiator is an aperture whose size $r <\sim \alpha$, the radiation produced is diffraction radiation (DR) and the spectral angular density is dependent on frequency and on the ratio $r/\alpha$.

The radiation field of DR from a hole in an infinite radiator, TR from a complementary finite size solid radiator and TR from an infinite radiator are related by Babinet's principle[ 1] ,

$$E^{TR}_{\infty Screen} = E^{DR}_{Hole} + E^{TR}_{FiniteScreen}. \quad (1)$$

In this sense, TR from a finite screen can be considered to be a form of DR as Figure 1 suggests.

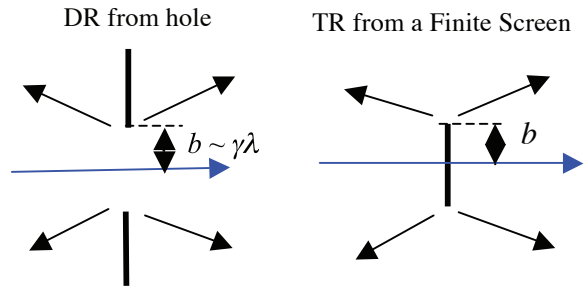


Figure 1. Diffraction and transition radiation from two complementary screens.

The coherence or "formation" length, as it is sometimes referred to in the literature, is the distance where the fields of the charge and the photon generated in the interaction defer in phase by $\pi$ radians [2]. There are two types of coherence lengths, i.e. the vacuum coherence length, $L_v = (\lambda/\pi)(\gamma^{-2} + \theta^2)^{-1}$, which applies to the radiation produced when a charge moves from a medium into vacuum or vice versa; and the material coherence length, $L_d$ which applies to a charge moving within a material with dielectric constant $\varepsilon$. Note that $L_v$ is a function of the Lorentz factor $\gamma$ for a relativistic charge while $L_d$ is independent of $\gamma$. The definition of $L_v$ indicates that for high energies and observation angle $\theta \sim 1/\gamma$ , the coherence of TR or DR fields and the field a co-moving charge is maintained over distances in proportion to the square of the Lorentz factor. The phenomenon of interference of TR/DR from two foils or apertures in the path of a relativistic particle is an example where the vacuum coherence length plays a major role.

When the charge interacts with a series of radiators spaced periodically, e.g. a stack of foils or the periods of a grating, the radiation can be resonant, i.e. in phase, for a particular observation angle or wavelength [3]. Examples of resonance radiation are TR from a stack of foils and Smith Purcell radiation.

The last concept of interest to us is the coherence of charges in a bunch radiating in or out or phase. The general expression for the spectral angular density of any type of beam base radiation can be written in the form:

* Work supported by ONR and the DOD Joint Technology Office
† rfiorito@umd.edu

# THE CLIC TEST FACILITY 3 INSTRUMENTATION

T. Lefèvre, CERN, Geneva, Switzerland

*Abstract*

Built at CERN by an international collaboration, the CLIC Test Facility 3 (CTF3) aims at demonstrating the feasibility of a high luminosity 3TeV $e^+$-$e^-$ collider by the year 2010. The CLIC project is based on the so called 'two-beam acceleration scheme' where the RF accelerating power is provided by a high current high frequency electron beam. The required performances put high demands on the diagnostic equipment and innovative monitors have been developed during the past years. This paper gives an overview of the instrumentation developed at CTF3 with a special emphasis on short bunch length measurements, nanometer beam position monitors, femtosecond synchronization technique and high dynamic range beam imaging system.

## INTRODUCTION

In the framework of the Compact Linear Collider (CLIC) project [1], a test facility named CTF3 [2] is constructed at CERN by an international collaboration. It shall demonstrate by 2010 the key technological challenges for the construction of a high luminosity 3TeV $e^+$-$e^-$ collider. The two main issues to be addressed on CTF3 are the development of 100MV/m 12GHz accelerating structures and the generation of the CLIC RF power source which is based on the production of a high frequency high current electron beam, called Drive Beam. The layout of the CTF3 machine is depicted in Figure 1.

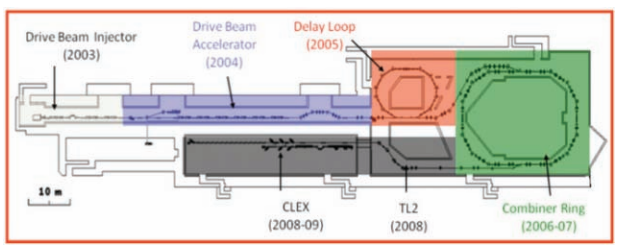


Figure 1: Overview of the CTF3 complex

In the present scheme, a long train of bunches with a bunch spacing of 20cm is converted into an eight times shorter train with a 2.5cm bunch spacing. The complex starts with a 3GHz linac (twice the bunch frequency) that produces a pulsed electron beam with a present maximum energy of 150MeV. By means of RF manipulation in the Delay Loop (DL), the beam is converted of four consecutive bunch trains, each of them having 7.5A average current and 10cm bunch spacing. The electrons are then injected into the Combiner Ring (CR) using a 3GHz RF deflector [3]. After the 4$^{th}$ turn, the bunch trains are combined into a single one with a current of 30A and a 2.5cm distance between bunches.

The beam is finally extracted and sent to the CLIC experimental area (CLEX) where several beam lines are under construction at the moment. A 'Test Beam Line' [4] will study the reliability and the stability of the Drive Beam decelerator which must operate with a low level of beam losses. A 'Two-Beam Test Stand' is devoted to the test of a relevant CLIC module [5] with Power Extraction and Transfer Structures (PETS) on the Drive Beam side and 12GHz accelerating structures on the Probe Beam side [6].

This paper presents an overview of the CLIC Test Facility 3 instrumentation. The first paragraph is dedicated to essential beam diagnostic to measure position, intensity and size. The second paragraph presents the beam diagnostics specifically developed for the need of CTF3. The third and final paragraph discusses some CLIC specific instruments which are currently tested on CTF3.

## ESSENTIAL INSTRUMENTS

### *Beam Position and Intensity Monitors*

Beam position and intensity monitors are the first instruments used when the accelerator is turned on. An overview of the different types of pick-up developed for CTF3 is shown in Figure 2.

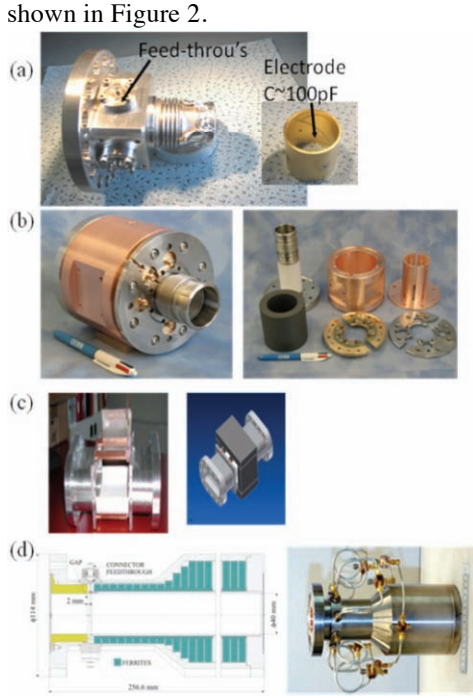


Figure 2: CTF3 Beam position and intensity monitors (a) BPE, (b) BPM, (c) BPI, (d) WCM

In the first part of the accelerator, electrostatic beam position and intensity monitors (BPE) have been installed. They present the advantage of functioning inside the

# NEAR-FIELD OPTICAL DIFFRACTION RADIATION MEASUREMENTS AT CEBAF*

P. Evtushenko#, A. P. Freyberger, C. Y. Liu, Jefferson Lab, Newport News, VA USA
A. Lumpkin, Fermilab, Batavia, IL USA

*Abstract*

An optical diffraction radiation (ODR) diagnostic station was recently designed and installed on a CEBAF transfer beam line. The purpose of the setup is to evaluate experimentally the applicability range for an ODR based non-intercepting beam size monitor as well as to collect data to benchmark numerical modeling of the ODR. An extensive set of measurements was made at an electron beam energy of 4.5 GeV. The ODR measurements were made for both pulsed and CW electron beam of up to 82 μA. The wavelength dependence and polarization components of the ODR were studied using a set of insertable bandpass filters (500 nm short and 500 nm long pass filter) and polarizers (horizontal and vertical). The typical transverse beam size during the measurements was ~150 microns. Complete ODR data, wavelength and polarization, were recorded for different beam sizes and intensities. The beam size was also measured with optical transition radiation (OTR) (using the surface of the ODR converter) as well as a wire scanner located next to the ODR station. In this contribution we describe the experimental setup and present the results of the measurements with the comparison to the numerical simulations.

## INTRODUCTION

Optical diffraction radiation is generated when a charged particle passes near a conductor at a distance comparable or smaller than $\gamma \cdot \lambda/2\pi$, where $\gamma$ is the relativistic Lorenz factor and $\lambda$ is the wavelength of the radiation. The theory of the diffraction radiation is well developed [1]. In the case of a highly relativistic particle beam with large $\gamma$, a conductor located at a distance bigger than the transverse beam size will generate a significant amount of diffraction radiation in the optical wavelength range. Several ODR based schemes were suggested for non-intercepting beam size measurements [2-6]. Some of them utilize the angular distribution of the ODR whereas others make use of imaging of the radiator surface, i.e., near-field measurements. The near-field ODR was observed experimentally previously [7, 8]. A common condition in such measurements was that the integrated charge used to generate the ODR was several nC.

The Continuous Electron Beam Accelerator Facility (CEBAF) is a multipass superconducting LINAC delivering CW electron beam with an energy up to 6 GeV and average current up to 100 μA for nuclear physics experiments on fixed targets [9]. A typical beam size in CEBAF at high energy is 100 μm. The total charge delivered by CEBAF within the time a standard video camera uses to integrate one field of a video signal (16.6 ms) and when running 100 μA beam is 1.66 μC. The combination of the these parameters, GeV range energy, 100 μm beam size and μC charge integrated within 16.6 ms, makes CEBAF an ideal facility to study develop and implement an ODR based non-intercepting beam size diagnostic, as was pointed out previously [10]. At the same time, from an operational point of view it is very desirable to have such a non-intercepting beam size monitor. It can be used to detect drifts leading to a change in the betatron match early and therefore can improve beam availability for the nuclear physics experiments. A set of such beam size monitors positioned properly along a transport beam line could also provide online emittance monitoring as well as emittance measurements virtually at any bunch charge when running CW beam. With such motivation in mind we have designed built and installed an ODR diagnostic station which would serve in a first place as an evaluation setup for the ODR, but also would be a prototype of such a diagnostic setup for CEBAF.

## EXPERIMENTAL SETUP

The most important part of the ODR diagnostic station is the ODR radiator. The optical transition radiation (OTR) was used for reference beam size measurements. Thus we have designed and built a radiator which could be used for both OTR and ODR measurements. The radiator is shown in Fig. 1. The ODR part of the radiator is a 300 μm thin silicon wafer optically polished and aluminized on one side. The thickness of the aluminum layer is about 600 nm. The wafer is mounted on an

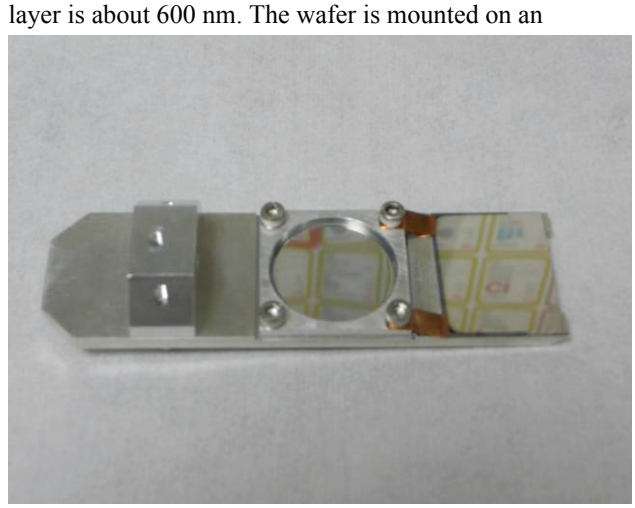

Figure 1: ODR-OTR radiator

* Work supported by the U.S. DOE contract # DE-AC05-06OR23177
# Pavel.Evtushenko@jlab.org

# COMMISSIONING OF SOLEIL FAST ORBIT FEEDBACK SYSTEM

N. Hubert, L. Cassinari, J-C. Denard, J-M. Filhol, N. Leclercq, A. Nadji, L. Nadolski, D. Pédeau;
Synchrotron SOLEIL, Gif-sur-Yvette, FRANCE

*Abstract*

The SOLEIL Fast Orbit Feedback system has been integrated in the BPM electronics, using the FPGA resources of the LIBERA modules. On top of their position measurement, the FPGAs compute the orbit correction and drive the power-supplies of the 48 dedicated air coil correctors. Position data are distributed all over the ring by a dedicated network connecting the 120 BPMs modules together. The correction rate is 10 kHz and is applied with low latency. Even if at almost all the source points, the high frequency stability specifications have already been achieved thanks to great care in the design of the machine, remaining vibrations are still observed in the 46-54 Hz band and during the changes in gap and phase of some insertion devices. Those perturbations can be efficiently damped by the Fast Orbit Feedback system. While the BPM system has been operational for some time, the Fast Orbit Feedback system is presently in its commissioning phase. The design and first results of the latter are reported.

## INTRODUCTION

The SOLEIL BPM system has been in operation from the start of the Storage Ring commissioning in May 2006 [1, 2]. There are 120 BPMs, 72 are located in the arcs and there is one at each end of the 24 straight sections. The electronic processing has been defined and designed by SOLEIL and Instrumentation Technologies, a company in Slovenia [3]. The BPM electronics consists of one crate per BPM called "LIBERA". It is plugged into the 50 Hz mains and the Ethernet control network. It has been designed from the start for supporting a Fast Orbit Feedback embedded into the BPM processing FPGA. The BPM digital electronics has subsequently equipped most of the new storage rings around the world.

The stability of the beamline at the source points are required to be better than $1/10^{th}$ the rms size and angular divergence of the photon beam.

| Photon Source | $\sigma_x/10$ µm | $\sigma'_x/10$ µrad | $\sigma_z/10$ µm | $\sigma'_z/10$ µrad |
|---|---|---|---|---|
| Bending magnets (≤ 35 keV) | N/A | N/A | 1.5 | 5.3 |
| Hard X-ray IDs (≤ 18 keV) | 39 | 1.5 | 0.55 | 0.51 |
| Soft X-ray IDs (≤ 1.6 keV) | 18.3 | 3.4 | 0.65 | 1.6 |
| UV IDs (≤ 0.04 keV) | 32 | 4.6 | 6 | 4.2 |

**Table 1: Beam stability requirements at source points with $\varepsilon_H$ = 3.75 nm.rad and K = 0.4%**

These parameters for the main beamline types depend on their location on the machine and on their maximum photon energy. They are shown in table 1.

## SLOW AND FAST ORBIT FEEDBACK

A Slow Orbit Feedback (SOFB) based on an SVD algorithm with the 120 BPMs and 56 correctors in each plane is operational since May 2007 [2].

Initially, the FOFB was mainly meant to suppress the residual vibrations at frequencies higher than 1 Hz; the slow drifts, below 0.01 Hz being corrected by the SOFB. The SOFB acts on 56 correctors built in the sextupoles. One of the technological innovations at SOLEIL is the extensive use of NEG coated aluminium vacuum chambers in the arcs and straight sections. It improves the vacuum pressure and beam lifetime without increasing the broadband wall impedance. However, the eddy currents in aluminium suppress the magnetic field over few Hz in the vacuum chamber.

In each plane the FOFB acts on 48 fast air correctors that are installed around stainless steel BPM bellows, at the ends of the 24 straight sections. The correctors can yield orbit kicks in the ±20 µrad range, which is much less than that of the slow correctors (±0.8 mrad in H and ±0.6 mrad in V, values necessary for the closed orbit distortion), but its cut-off frequency due to eddy currents is ≥ 2.5 kHz. The power-supplies can provide currents in the ±10A range within ±24V voltage limits.

The Slow and the Fast Orbit Feedback systems do not use the same set of correctors, which is not a problem if the two systems are kept well separated by functioning in different frequency ranges. Actually, we found that the FOFB is very efficient at suppressing two unexpected sources of orbit perturbation: i) use of the overhead cranes in the experimental hall during photon beam delivery ii) imperfections of the feedforward correction process during undulator gap changes. At the moment, the feedforward steerers correct the orbit very well before and after gap changes, but not well enough during the transitions. The cause of the problem is currently being addressed (better synchronization between the four feedforward correctors and smooth interpolation between consecutive points of the correction tables). It should be corrected by the end of the year, but in the mean time, the FOFB would greatly help.

The tests conducted so far were aimed at demonstrating that the FOFB can stabilize the beam position alone (without SOFB) for about 8 hours without saturating the air correctors.

## BEAM NOISE SPECTRUM

We identify three different ranges in the beam spectrum: i) the "high frequency" noise from 1 to 150 Hz, ii) the beam movements due to crane operation and

# BEAM DIAGNOSTICS AT DAΦNE WITH FAST UNCOOLED IR DETECTORS

A. Bocci, A. Clozza, A. Drago, A. Grilli, A. Marcelli, M. Piccinini, A. Raco, R. Sorchetti,
INFN/LNF, Frascati, Italy
Lisa Gambicorti, INOA, Firenze, Italy
A. De Sio, E. Pace, Università degli Studi di Firenze, Firenze, Italy
J. Piotrowski, Vigo System Sa, Warsaw, Poland

*Abstract*

Bunch-by-bunch longitudinal diagnostics is a key issue of modern accelerators. To face up this challenging demand, tests of mid-IR compact uncooled photo-conductive HgCdTe detectors have been recently performed at DAΦNE. Different devices were used to monitor the emission of $e^-$ bunches. The first experiments allowed recording of 2.7 ns long $e^-$ bunches with a FWHM of a single pulse of about 600 ps. These results address the possibility to improve diagnostics at DAΦNE and to this purpose an exit port on a bending magnet of the positron ring has been set-up. An HV chamber, hosting a gold-coated plane mirror that collects and deflects the radiation through a ZnSe window, is the front-end of this port. After the window, a simple optical layout in air allows focusing IR radiation on different detectors. The instrumentation will allow comparison in the sub-ns time domain between the two rings and to identify and characterize bunch instabilities. Moreover, to improve performances tests of new photovoltaic detectors with sub-ns response times are in progress. We will briefly summarize the actual status of the 3+L experiment and will discuss future applications of fast IR photovoltaic detectors and the development of fast IR array detectors.

## INTRODUCTION

Beam diagnostics is an essential component of a particle accelerator. All storage rings emit synchrotron light and different radiation energies can be used for beam diagnostics. Indeed, the synchrotron radiation emission covers a wide energy range from IR to X-ray energies with a pulsed structure that depends by the temporal characteristic of the stored beam. The radiation can be used to monitor the beam stability and to measure the longitudinal profiles of the accumulated particles. However, due to the time structure of the synchrotron radiation, to perform beam diagnostics fast detectors are required. At third generation synchrotron radiation sources useful devices for the diagnostics of accelerated particles need response times from the ns to the ps range while the future FEL sources need response time in the fs domain.

The main advantage of photon diagnostic is that it is a direct and non-destructive probe. Diagnostic based on synchrotron light is typically used for imaging and allows the measure of the beam cross section as well as the longitudinal structure such as the bunch length of stored particles. The determination of the bunch length is an important operational parameter of storage rings that allow monitoring the beam dynamics.

The main requirements of a beam diagnostic system could be: fast, at least in the sub-ns regime to guarantee the installation in all accelerators, compact and robust. However, it could be also easy to manage, possibly vacuum compatible and at low cost.

Standard beam diagnostic methods use a streak camera, an extremely fast photon detectors that takes an instantaneous image of the particles running along the orbit. Images of the temporal structure of a beam have resolution time of ~1 ps or below [1]. Streak cameras are powerful detectors whose principal drawback is the cost. Moreover, streak cameras are complex and fragile devices and usually are not used for permanent full-time beam diagnostics. As a consequence fast, cheaper and compact photon detectors may represent an important alternative for photon beam diagnostics. Photon devices are also easier to manage with respect to a streak camera. The availability of uncooled infrared devices optimized for the mid-IR range, based on HgCdTe alloy semiconductors, already now allow obtaining sub-ns response times [2]. These detectors can be used for fast detection of the intense synchrotron radiation IR sources and then for beam diagnostics. Preliminary measurements of the pulsed synchrotron light emission have been performed with uncooled IR photo-conductive detectors at DAΦNE, the $e^+$-$e^-$ collider of the LNF laboratory of the Istituto Nazionale di Fisica Nucleare (INFN), achieving a resolution time of about few hundred of picoseconds [3,4]. In this contribution we will present and discuss preliminary results obtained with such photo-conductive detector.

Experiments have been performed at SINBAD (Synchrotron Infrared Beamline At DAΦNE), the IR beamline operational at Frascati since 2001. Moreover, to improve the DA_NE diagnostics a new experiment, 3+L (*Time Resolved Positron Light Emission*), funded by INFN, started the installation at the exit of one of the bending magnet of the DAΦNE positron ring. The installation, when completed, will allow monitoring the positron bunch lengths at DAΦNE with the main aim to study and characterize the instabilities of the positron beam and in order to possibly increase the positron current and the collider luminosity.

A short description of the 3+L experiment, the optical simulations and the actual status of the experiment will be

# DIGITAL SIGNAL PROCESSING USING FIELD PROGRAMMABLE GATE ARRAYS

J. Serrano, CERN, Geneva, Switzerland

*Abstract*

This paper presents an introduction to digital hardware design using Field Programmable Gate Arrays (FPGAs). After a historical introduction and a quick overview of digital design, the internal structure of a generic FPGA is discussed. Then we describe the design flow, i.e. the steps needed to go from design idea to actual working hardware. Digital signal processing is an important area where FPGAs have found many applications in recent years. Therefore a complete chapter is devoted to this subject. The paper finishes with a discussion of important peripheral concepts which are essential for success in any project involving FPGAs.

## HISTORICAL INTRODUCTION

Digital electronics is concerned with circuits which represent information using a finite set of output states [1]. Most of the applications use in fact just two states, which are often labeled '0' and '1'. Behind this choice is the fact that the whole Boolean formalism becomes then available for the solution of logic problems, and also that arithmetic using binary representations of numbers is a very mature field.

Different mappings between the two states and the corresponding output voltages or currents define different logic families. For example, the Transistor-Transistor Logic (TTL) family defines an output as logic '1' if its voltage is above a certain threshold (typically 2.4 V). For the same family, if we set the input threshold for logic '1' as 2 V, we will have a margin of 0.4 V which will allow us to interconnect TTL chips inside a design without the risk of misinterpretation of logic states. This complete preservation of information even in the presence of moderate amounts of noise is what has driven a steady shift of paradigm from analogue to digital in many applications. Here we see as well another reason for the choice of binary logic: from a purely electrical point of view, having only two different values for the voltages or currents used to represent states is the safest choice in terms of design margins.

Historically, TTL chips from the 74 series fuelled an initial wave of digital system designs in the 1970s. From this seed, we will focus on the separate branches that evolved to satisfy the demand for programmability of different logic functions. By programmability, we mean the ability of a designer to affect the logic behavior of a chip after it has been produced in the factory.

A first improvement in the direction of programmability came with the introduction of Gate Arrays, which were nothing else than a chip filled with NAND gates that the designer could interconnect as needed to generate any logic function he desired. This interconnection had to happen at the chip design stage, i.e. before production, but it was already a convenient improvement over designing everything from scratch. We have to wait until the introduction of Programmable Logic Arrays (PLAs) in the 1980s to have a really programmable solution. These were two-level AND-OR structures with user-programmable connections. Programmable Array Logic (PAL) devices were an improvement in performance and cost over the PLA structure. Today, these devices are collectively called Programmable Logic Devices (PLDs).

The next stage in sophistication resulted in Complex PLDs (CPLDs), which were nothing else than a collection of multiple PLDs with programmable interconnections. FPGAs, in turn, contain a much larger number of simpler blocks with the attendant increase in interconnect logic, which in fact dominates the entire chip.

## BASICS OF DIGITAL DESIGN

A typical logic design inside an FPGA is made of combinatorial logic blocks sandwiched in between arrays of flip-flops, as depicted in Fig. 1. A combinatorial block is any digital sub-circuit in which the current state of the outputs only depends, within the electrical propagation time, on the current state of the inputs. To this group belong all the well known basic logic functions such as the two-input AND, OR and any combination of them. It should be noted, that logic functions of arbitrary complexity can be derived from these basic blocks. Multiplexers, encoders and decoders are all examples of combinatorial blocks. The input in Fig. 1 might be made of many bits. The circuit is also supplied with a clock, which is a simple square wave oscillating at a certain fixed frequency. The two flip-flops in the circuit, which might be flip-flop blocks in the case of a multi-bit input, are fed with the same clock and propagate the signals from their D inputs to their Q outputs every time there is a rising edge in the clock signal. Apart from that very specific instant in time, D is disconnected from Q.

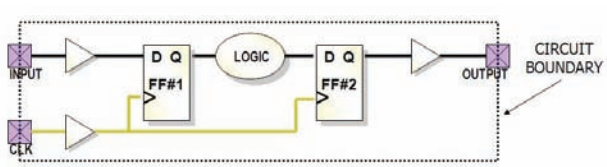


Fig. 1: A typical digital design

The structure of the circuit is thus very simple, and its application as a template covers the vast majority of digital design requirements in standard applications, such

# RECENT BEAM MEASUREMENTS AND NEW INSTRUMENTATION AT THE ADVANCED LIGHT SOURCE*

F. Sannibale[#1], K. Baptiste[1], W. Barry[1], M. Chin[1], D. Filippetto[2], L. Jaegerhofer[4], J. Julian[1], S. Kwiatkowski[1], R. Low[1], D. Plate[1], G. Portmann[1], D. Robin[1], T. Scarvie[1], G. Stupakov[3], J. Weber[1], M. Zolotorev[1],

[1]Lawrence Berkeley National Laboratory, Berkeley, CA 94720, U.S.A.
[2]Istituto Nazionale di Fisica Nucleare, Laboratori Nazionali di Frascati, 00044 Frascati, Italy
[3]Stanford Linear Accelerator Center, Stanford, CA 94309 U.S.A.
[4]Vienna University of Technology, 1040 Vienna, Austria

*Abstract*

The Advanced Light Source (ALS) in Berkeley was the first of the soft x-ray third generation light source ever built, and since 1993 has been in continuous and successful operation serving a large community of users in the VUV and soft x-ray community. During these years the storage ring underwent through several important upgrades that allowed maintaining the performance of this veteran facility at the forefront. The ALS beam diagnostics and instrumentation have followed a similar path of innovation and upgrade and nowadays include most of the modern and last generation devices and technologies that are commercially available and used in the recently constructed third generation light sources. In this paper we will not focus on such already widely known systems, but we will concentrate our effort in the description of some measurements techniques, instrumentation and diagnostic systems specifically developed at the ALS and used during the last few years.

## INTRODUCTION

The Advanced Light Source (ALS) at the Lawrence Berkeley National Laboratory (LBNL) was the first soft x-ray source built among the so-called third generation synchrotron light sources [1]. In this kind of storage rings, fully dedicated to and optimized for the production of synchrotron radiation, insertion devices in the straight sections allow for many order of magnitude increased brigthness respect to those of the previous generation light sources. After the ALS many other 3rd generation sources have been and are still being built around the world under the always increasing requests from users. Despite its age, the ALS performance as a storage ring as well as a light source compare well with those of the younger machines in the category. This is due to the fact that during these years the machine underwent to a number of upgrades of the lattice, of the ring and beamline components, and of the instrumentation and beam diagnostics systems.

In this paper, after a brief introduction of the ALS and its instrumentation, we focus on the description of three new systems developed at the ALS that improve the beam measurements capabilities and potentially allow for the operation of the ring in a new mode of operation.

* Work supported by the Director, Office of Science, of the U.S. Department of Energy under Contract DE-AC02-05CH11231.
# FSannibale@lbl.gov

## THE ADVANCED LIGHT SOURCE

Figure 1 shows the "clock diagram" of the ALS with its collection of beamlines. More than 40 beamlines with source points inside dipoles or insertion devices allow for more than 2000 users per year, using photons from the far-infrared to the hard x-rays. Figure 1 also shows the injector system composed by a 50 MeV linac and by a booster ring that ramps the beam energy up to 1.9 GeV before the injection into the storage ring.

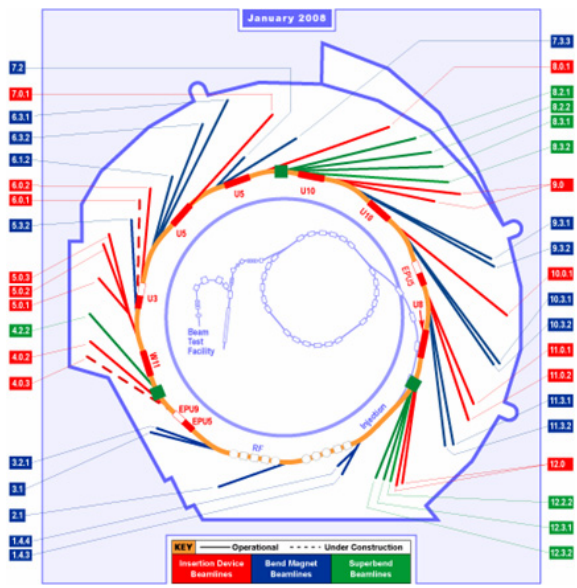


Figure 1: Clock diagram of the ALS showing the different beamlines now in operation.

Table 1 contains the main parameters of the storage ring. During standard user operation, 400 mA of electrons are stored in about 280 of the 328 available buckets. The 12 triple bend achromat cells distributed over a circumference of ~ 197 m allow for the small emittance value of 6.3 nm. A cost effective upgrade of the ALS is being proposed that will reduce the emittance by about a factor 3 by replacing four corrector magnets in each sector

# DEVELOPMENT OF BEYOND STATE-OF-THE-ART DIAGNOSTIC TECHNIQUES WITHIN THE EUROPEAN NETWORK DITANET

C.P. Welsch

*University of Heidelberg, GSI, Darmstadt and MPI-K, Heidelberg, Germany*
on behalf of the DITANET consortium

*Abstract*

The development of new particle accelerators with unprecedented beam characteristics has always driven the need for an intense R&D program in diagnostic techniques. The successful operation of these machines is finally only possible with an adequate set of beam instrumentation.

DITANET is a large European network between several research centers, Universities, and partners from industry that aims for the development of beyond-state-of-the-art diagnostic techniques for future accelerator facilities. This includes research projects focusing on beam profile, current, and position measurements, as well as on particle detection techniques and related electronics. A particular focus of the consortium is the training of young researchers in this multi-disciplinary field and to thus prepare them for their future careers in academia or industry.

This contribution will introduce the network participants, present the general structure of DITANET, and give an overview of its research and training activities.

## INTRODUCTION

Beam diagnostics is a rich field in which a great variety of physical effects are made use of and consequently provides a wide and solid base for the training of young researchers. Moreover, the principles that are used in any beam monitor or detector enter readily into industrial applications or the medical sector, which guarantees that training of young researchers in this field is of relevance far beyond the pure field of particle accelerators. Beam diagnostics systems are essential constituents of any particle accelerator; they reveal the properties of a beam and how it behaves in a machine. Without an appropriate set of diagnostic elements, it would simply be impossible to operate any accelerator complex let alone optimize its performance.

Future accelerator projects will require innovative approaches in particle detection and imaging techniques to provide a full set of information about the beam characteristics. Since a long time, Europe has played a major role in this field and the declared goal of this network is to pave the way for world-class research with particle accelerators. This will only be possible by a joint training effort, where knowledge and technology transfer are encouraged, where close collaboration with industry is an integral part of the network, and where leading research centers and major universities work closely together.

Marie Curie Initial Training Networks (ITN) are aimed at improving the career perspectives of researchers who are in the first five years of their career by offering structured training in well defined scientific and/or technological areas as well as providing complementary skills and exposing the researchers to other sectors including private companies.

DITANET - "**DI**agnostic **T**echniques for particle **A**ccelerators - an initial training **NET**work" - covers the development of advanced beam diagnostic methods for a wide range of existing or future accelerators, both for electrons and ions. The proposed developments in profile, current, and position measurement techniques clearly stretch beyond present technology and will mark the future state of the art.

The network comprises almost all of the European expertise in this field, either in the form of the network members themselves or as associate partners, having well-proven expertise in finding solutions to the technological challenges related to the development of cutting edge diagnostic techniques. This stimulates on one hand the search for the most advanced methods and technologies and ensures at the same time a comprehensive training of young researchers who will get the unique possibility to become experts not only in their main research field, but also in related techniques.

DITANET consists of the following network participants: University of Heidelberg (coordinator, Germany), CEA (France), CERN (Switzerland), DESY (Germany), GSI (Germany), HIT GmbH (Germany), IFIN-HH (Romania), Stockholm University (Sweden), Royal Holloway University of London (UK), and the University of Seville/Centro Nacional de Aceleradores (Spain).

It is complemented by twelve associated partners from all over the world: ESRF (France), idQuantique (Switzerland), INFN-LNF (Italy), Instrumentation Technologies (Slovenia), MPI for Nuclear Physics (MPI-K), PSI (Switzerland), THALES (France), Thermo Fisher